Design of a Novel Rear Cradle for Electrified Powertrains

by

Timothy Er

A thesis
presented to the University of Waterloo
in fulfillment of the
thesis requirement for the degree of
Master of Applied Science
in
Mechanical and Mechatronics Engineering

Waterloo, Ontario, Canada, 2021

Author's Declaration

I hereby declare that I am the sole author of this thesis. This is a true copy of the thesis, including any required final revisions, as accepted by my examiners.

I understand that my thesis may be made electronically available to the public.

Abstract

With the ever-increasing, stringent requirements of fuel economy, automotive manufacturers have cited reduction of vehicle weight as one of the most effective methods of decreasing fuel consumption and emissions. Due to the abundance of traditional combustion-engine vehicles on the road, it is not uncommon for independent research groups or shops to convert these vehicles to hybrid, or full electric. In doing so, major changes to key structural aspects of the vehicle are required. However, it is far too often found that changes are made without proper analysis and design of the component. As such, this thesis provides an outline on the processes and methods used to develop a prototype structural component; in this case a custom rear cradle was used as an example, which was redesigned to house an electric motor drive unit in an existing production vehicle.

Firstly, requirements such as structural strength, stiffness, and manufacturability were devised. In considering all these requirements, 6061-T6 aluminum was set as the new material for this component, given its high specific strength and stiffness, as well as ease of manufacturability and cost. Fatigue analysis was conducted to develop new structural requirements for this component, given its differing material properties from the previous design being made from steel.

Next, topology optimization was conducted to gain an idea of an optimized, lightweight structure that met requirements. Structural analysis utilizing beam theory allowed for rapid iteration of tube diameters and wall thicknesses, this was translated to analysis of full geometry once requirements were met.

All in all, the final design yielded a lighter component, while maintaining structural integrity. The new cradle design represents a weight savings of 57% over the 2019 cradle, while satisfying all the requirements set. It is expected that further weight reduction is possible, given future development in fatigue analysis and certain design aspects of the cradle. As such, the processes and methods outlined in this thesis can be applied to other structural components of similar nature for prototype vehicles.

Acknowledgements

First, I must acknowledge my advisor, Dr. Roydon Fraser, who provided me with the opportunity in working with the UWAFT EcoCAR team for my graduate studies and has supported the team in its perseverance in the face of the pandemic. I would also like to thank Asad Bhatti and Paul Boctor, we have been through so much together on the team and I couldn't have had better colleagues who are now great friends.

Second, I must thank those that directly supported this thesis. I would like to thank Hung Nguyen for serving as a mentor, this project would not have been possible without his direct support and guidance. I would also like to acknowledge my friend Daryn Huang, who provided assistance with debugging models when a roadblock was hit. I would also like to express my gratitude to Dr. Steve Lambert, Dr. William Melek, and my friend Serhat Unsal, for their input in reviewing this thesis.

Lastly, I would like to thank the rest of the UWAFT team as well as the AVTC organizers, mentors, and sponsors for making this entire competition possible. This program has had a tremendous impact on my development as an engineer, and for that I am sincerely grateful.

Dedication

To my mother and father, thank you so much for all the sacrifices you have made, which allowed me to pursue my passions in automotive; I would not be where I am today without them.

To the rest of my extended family, thank you for your unwavering support and for always being there for me.

Table of Contents

List of Figures

List of Tables

Chapter 1
Introduction

1.1 Motivation

In the past few years, development and sales of hybrid (HEV) and electric (EV) vehicles have been steadily increasing, as government regulations on fuel consumption and emissions are rigorously tightened year by year [1]. As consumer demand for fuel economy and performance increase, manufacturers are turning towards methods such as vehicle weight reduction coupled with innovations in electrified powertrain technology that continuously push the capabilities of these vehicles [2].

New advancements in powertrain technology are not just implemented in production vehicles through mass manufacturing, as HEV and EV conversion of older vehicles are becoming increasingly widespread [3]. The downside with converting a vehicle is that significant modification is required to structural aspects of the car to integrate new components such as electric motors, inverters, and high-voltage (HV) batteries [4], whereas these components are integrated throughout all stages of development for a production vehicle [5]. Additionally, the 'homemade' nature of these conversions often means that there is little consideration for insightful engineering of these modifications, which can result in a weight penalty and pose a potential hazard to the safety of the vehicle.

One such application of this is with the vehicle being built by the University of Waterloo EcoCAR Team (UWAFT). UWAFT is currently competing in the EcoCAR Mobility Challenge, which is a four-year collegiate design competition that challenges 13 teams from universities across North America to develop a hybrid-electric vehicle with improved fuel economy and reduced emissions [6]. Each team is provided with a 2019 Chevrolet Blazer, which serves as the basis for which the teams retrofit custom hybrid powertrains. UWAFT incorporated two discrete powertrains on each axle: combustion in the front and electric in the rear. The electric vehicle (EV) powertrain incorporated the use of an e-axle, which integrates the gearbox and motor in one sealed unit. This resulted in the need for a custom rear cradle to which the rear suspension and e-axle are mounted.

As the UWAFT Blazer is a unique, one-off vehicle built by students, large-scale manufacturing technologies commonly used for cradles found in production vehicles are not feasible. As such, this study will cover the analysis and design of a cradle, with an emphasis on limiting manufacturing to low-volume techniques commonly found in local machine shops.

1.2 Objective

The overall objective of this research is to provide a process that allows for re-engineering of structural components for unique vehicles with extremely limited production, with the aim of minimizing component weight while maintaining adequate structural integrity. This is achieved by utilizing multiple software tools, which allows designers to conduct structural analysis and quickly iterate on component design. Specific steps and procedures for these tools are defined throughout this thesis, allowing for this methodology to be replicated.

The methods and procedures outlined in this document are applicable towards projects such as small companies conducting HEV or EV conversions, research groups with prototype vehicles, or student teams such as UWAFT. Consequently, there are many limitations that are inherently imposed with projects of this nature, such as manufacturing restrictions – techniques commonly used with large-scale production such as forging or casting are not feasible, as costs are only reasonable through economies of scale [7].

Although manufacturing technologies may seem limited, the nature of low-volume prototyping opens the possibility of using certain niche processes. For example, the methods used to manufacture a tubular spaceframe require a significant amount of time due to the amount of manual labour and setup required [8]. However tube chassis have been around since the 1950s due its high strength, stiffness, and low weight [9]. As a result, while not suitable for large-scale production as it cannot be automated, it is a process that is widely used for low-volume production vehicles or kit cars, and thus suitable for the UWAFT Blazer.

As such, this thesis will use the custom rear cradle for UWAFT as an example for analysis and design of structural components for prototype vehicles.

1.3 Outline

Along with the introduction, this thesis spans 9 Chapters:

Chapter 2 provides background information. It starts off with an overview of the cradle for the reader to gain a basic understanding of the purpose and layout of this component. Information on general design considerations such as material selection, manufacturing methods, and geometry are also summarized. As the example project used has specific requirements and procedures, details pertaining to this example are also reviewed.

Chapter 3 provides further information on strength, and how fatigue analysis played the dominant role in this process. Once a material was selected, calculations were performed to estimate cycle count, which were then translated to stress targets that could not be exceeded.

Chapter 4 outlines design requirements specific to this project. For example, stiffness was also a concern with his project, therefore deflection requirements were defined in addition to strength. Geometrical and manufacturing requirements were also set, based on the available resources for this project.

Chapter 5 outlines topology optimization, the starting point of analysis. With the target of minimizing weight while not exceeding stress limits, optimization was conducted to gauge the form factor of the most ideal structure that met requirements.

Chapter 6 covers continuing structural analysis. From the topology optimization, two initial design concepts were investigated, each utilizing a specific manufacturing method within the confines of low-volume production. From this, further development of the structure was conducted, culminating in a semi-finalized layout of the structure utilizing a tubular spaceframe construction.

Chapter 7 covers detailed design, leading to the final product. The semi-finalized layout from Chapter 6 was used as a basis for the final structure, which required further adjustments after

more detailed structural analysis was conducted. All the requirements set in Chapter 4 were then verified towards the end of this section.

Chapter 8 provides a framework in the form of a flow chart, summarizing the entire component development process that was just completed. This section can serve as a quick-reference guide for small shops or research groups, should the need arise to develop a structural component critical for a prototype vehicle.

Chapters 9 and 10 outline the conclusion and recommendations for this project. Although a significant weight reduction was achieved, given the findings upon the completion of this project, it became apparent that there was potential for more.

Chapter 2
Literature Review and Background

This chapter provides background information that is pertinent to development of structural components for low-volume production in a general sense, as well as prerequisite knowledge specific to the development of the UWAFT cradle. General design requirements such as considerations with respect to clearance, strength, manufacturability, and materials are reviewed in detail. The current market of low-volume aftermarket parts is also examined, which revealed the need for proper engineering analysis and design of these components. Lastly, background on UWAFT, the competition, and the initial cradle that was integrated is also provided.

2.1 Introduction

Cars are one of the most widely used forms of transportation in the world, as there are approximately 1.4 billion vehicles on the road at present [10]. With the power of the latest computers, engineers are able to continuously push the boundaries of automotive engineering, leading to significant advances in fuel efficiency and performance [11]. Current trends in the automotive industry are pushing towards alternative methods of propulsion, and EVs are on the rise [12].

With these goals in mind, automotive manufacturers quickly realized that reducing the weight of a vehicle is the most effective method of maximizing vehicle efficiency [13]. The benefits of minimizing weight are independent of the energy source, as less energy overall is required to move a lighter vehicle [14]. Minimizing vehicle weight is especially important with new vehicles, as consumer needs have dictated higher safety standards along with added comfort and technology, all of which increase a vehicle's mass [15].

A key aspect of engineering a vehicle to be light is to use computer simulations to ensure that the vehicle can endure over 20 years of operation [16]. As a vehicle is driven, forces are exerted on various components of the car; as such, minimizing the weight of the vehicle can compromise structural integrity if insufficient analysis is performed. As a result, the importance of conducting

structural analyses in the development of major structural components of the vehicle cannot be understated, and it is the purpose of this document to outline a concrete glidepath to guide the reader in the development of a lightweight component while meeting design requirements. As previously mentioned, the component to be used as an example is the custom rear cradle developed for the UWAFT vehicle, so the next section will provide a general overview of this specific component.

2.2 The Cradle

The modern vehicle is a complicated machine composed of roughly 30,000 parts [17]. Ever since the advent of automotive mass production a hundred years ago, manufacturers have constantly been improving upon the large-scale manufacturing processes used to create and assemble all these components [18]. It is through these processes that the cradle was invented, as there are significant benefits with respect to production time and cost [19].

The cradle serves the purpose of being a central mounting point for various suspension and drivetrain components. Instead of having to assemble each individual part to the primary structure of the vehicle, the cradles allow manufacturers to create a subassembly of all these components separate from the body, as shown in Figure 1. Keeping these distinct steps separate greatly increases production efficiency as the body and cradle assemblies can be produced in parallel on two separate lines. Once both are complete, the body is lowered and mounted onto the cradle assembly. In production terms, this step is called the “marriage”, as the body and cradle assemblies are joined together, as shown in Figure 2 [20].

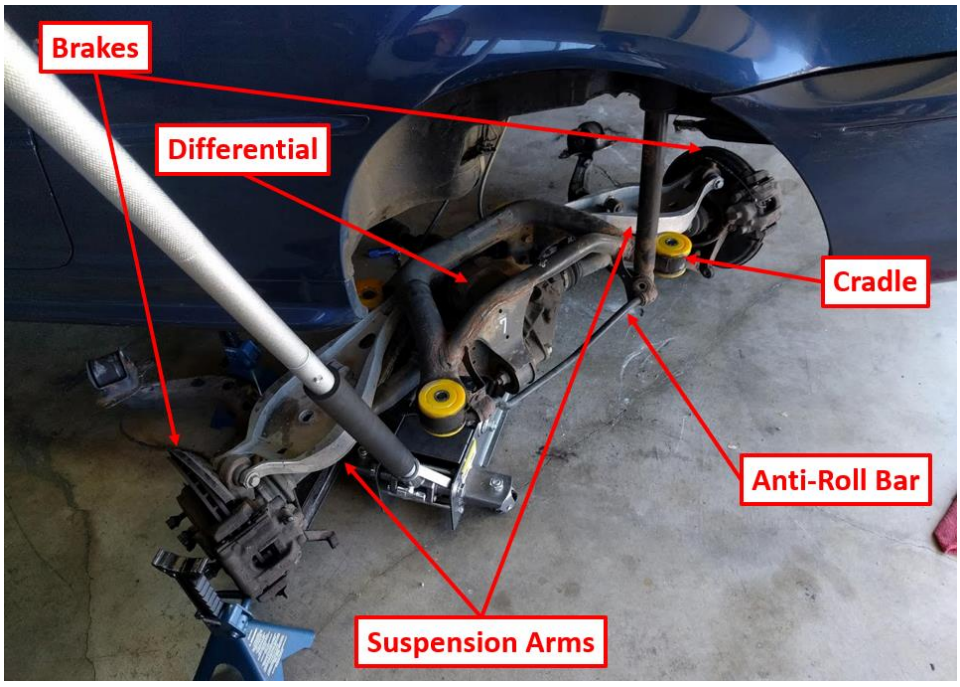

Figure 1: Close-up view of rear cradle assembly with associated components

Figure 2: Marriage of body and cradle assemblies during production [21]

Another benefit of the cradle is the ability to isolate vibrations and noise from the body. Irregularities in the road surface such as potholes or speedbumps transfer through the tires and suspension system to the body, which in turn results in a level of noise, vibration, and harshness (NVH) transmitted to the cabin. Additionally, driveline components such as the engine, transmission, and differential all generate some amount of NVH as an unwanted side effect during operation [22]. Suspension members and driveline components are typically fitted with rubber bushings, but there is an added layer of isolation by mounting the cradle itself to the body with rubber bushings which further isolates NVH from the cabin.

2.3 General Design Considerations

As major structural parts such as the cradle are key components of any modern vehicle, there are many aspects that must be considered throughout the development process. Matters such as geometry and packaging to ensure no interferences with surrounding components, strength and stiffness to meet input loads and compliance targets, material options and manufacturing methods used to build the part are all important concerns that are considered throughout the years that a manufacturer would take for the development of a major component of a vehicle.

2.3.1 Geometry and Integration

All major subsystems within a vehicle are kept tightly knit throughout the entire vehicle development process. This is especially important given the size and scope of the project as engineers are closely packaging thousands of parts within the confines of a car's body. Preliminary integration studies are conducted to plan out general packaging space between subsystems within the constraints of top-level design decisions such as interior space, ergonomics, and powertrain selection. Aside from these initial integration studies which involve major subsystems of the vehicle, detailed packaging studies are also conducted later in the development process [23].

In a general sense, these detailed studies must take into consideration matters that affect installation, serviceability, and full functionality of the component. With the modern vehicle being composed of thousands of parts and expected to last more than 20 years, regular

maintenance must be performed. As such, automotive engineers design vehicles in a way that repairs to the vehicle can be reasonably conducted. Consequently, these design considerations also aid in quicker production when the vehicle is built, which reduces manufacturing cost. These practices are known as Design for Assembly (DFA) and are vital to not only the design of a vehicle but to any mechanical assembly [24].

The concept of ensuring full functionality of a component from a geometrical standpoint is rather simple. There are many moving parts in a vehicle, as energy is transferred throughout the propulsion system to move the car forward, and the suspension system allows the wheels to move independently from the body. Given the tight clearances between various parts of the vehicle, it is crucial that there are no interferences between components that could impede on these movements. An example is shown in Figure 3, where there is interference between a control arm and the frame of a vehicle. As the suspension articulates, the components must be designed such that there is no possibility of unwanted contact throughout the designed travel of the system.

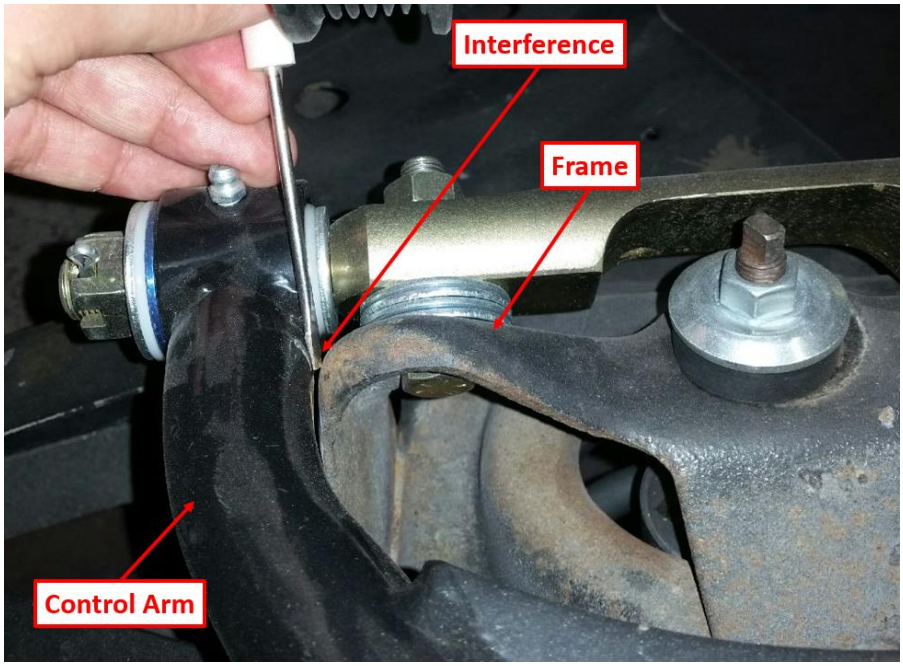

Figure 3: Example of interference between control arm and frame with articulation [25]

With respect to the cradle, DFA is applied to ensure that there is ease of access to all the fasteners holding the suspension and driveline components in place. For each fastener, adequate clearance for common tools such as a socket and ratchet must be considered, otherwise there will be difficulties with assembly and parts replacement. Ease of removal and installation is also important to facilitate quick and simple repairs. For example, many rear cradles in rear-wheel-drive (RWD) vehicles are provisioned to allow for removal of the differential without having to remove the cradle as well – which significantly reduces repair time and subsequently cost, as shown in Figure 4.

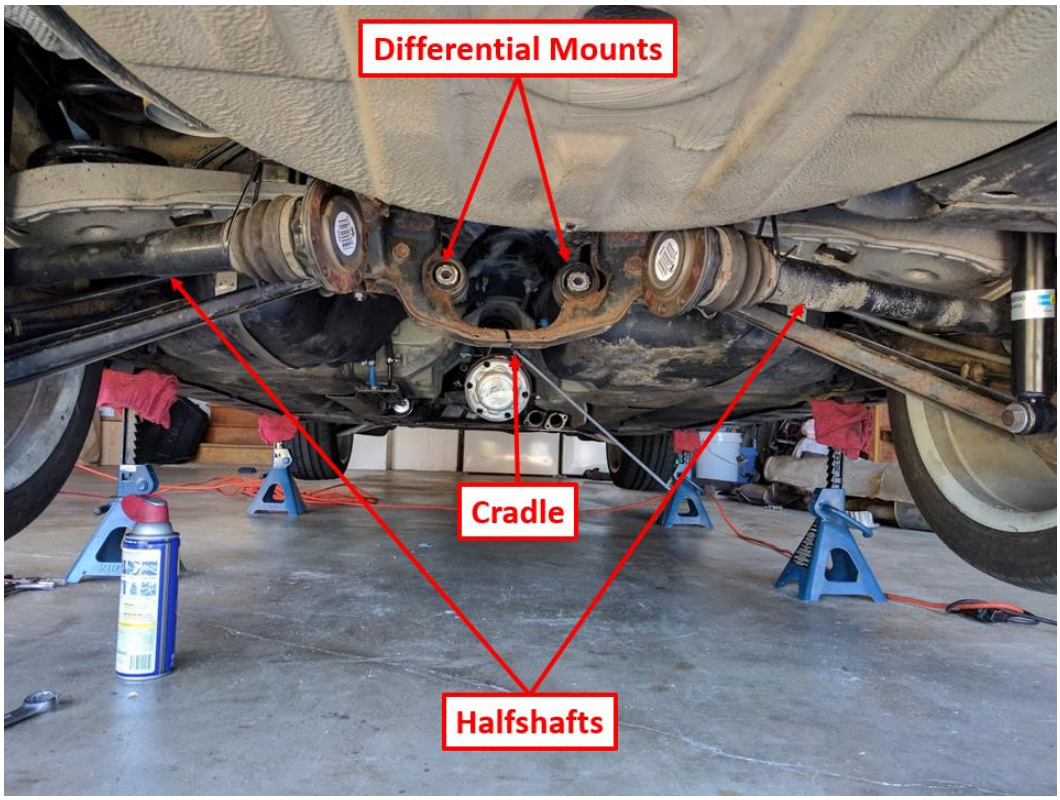

Figure 4: Example of differential removed from rear cradle assembly

With regards to interferences, the cradle mounts various suspension and driveline components to the body, thus it is important to ensure that it does not impede on these subsystems throughout normal vehicle operation. For example, as the wheel moves relative to the body and cradle, the suspension members at the cradle rotate to accommodate this. Therefore, it is important to

ensure that these members do not hit the cradle as the wheel travels through its full range of motion. Figure 5 is a depiction of how a potential interference could exist – an improperly designed cradle could prevent the toe link from rotating throughout its full travel.

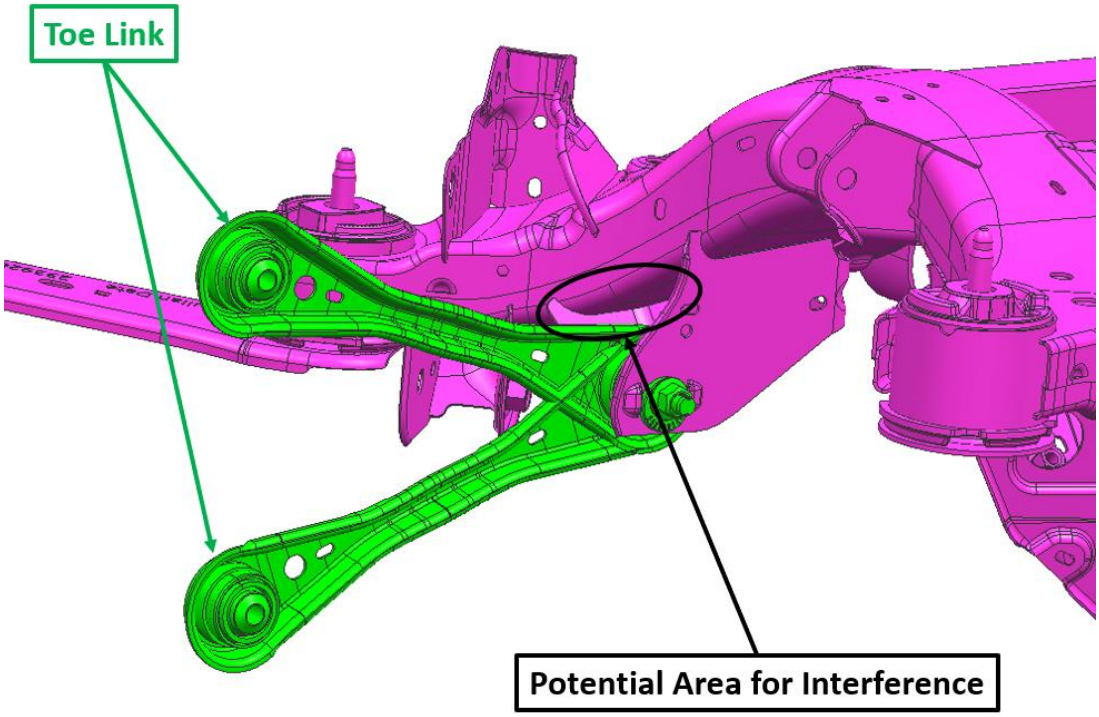

Figure 5: Example of potential interference area between cradle and toe link

Another important consideration is the relative position of a driveline component to the wheels. Many cradles have differentials or transaxles mounted, and power is transmitted to the wheels through a halfshaft. These halfshafts have CV joints that articulate such that power can still be transmitted with wheel travel. However, these CV joints have limits to the angles that they can safely articulate before premature wear or joint failure occurs. Additionally, higher articulation angles equate to higher friction, thus reducing efficiency [26] – a poor example of this is shown in Figure 6. As a result, it is important to consider halfshaft angles when dictating where to locate a driveline component mounted on a cradle relative to the wheels.

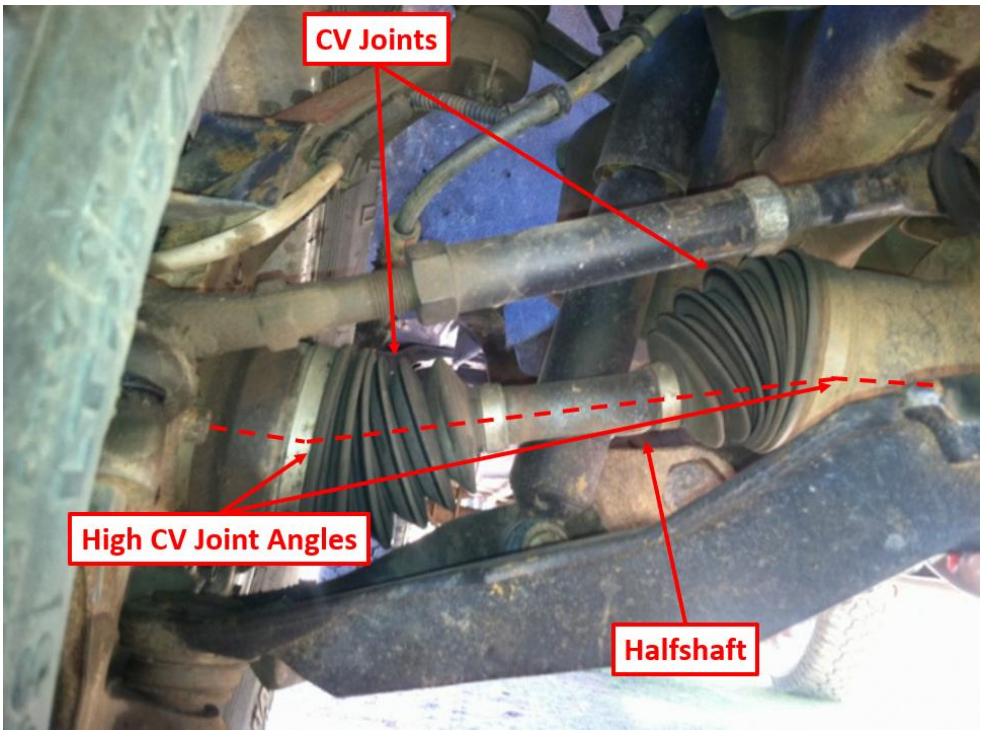

Figure 6: Example of extremely high CV joint angle, leading to increased wear and decreased efficiency [27]

2.3.2 Noise, Vibration, and Harshness (NVH)

With respect to major structural components, there are two primary sources of NVH – input from the road through the suspension and input from the propulsion system as an unwanted side effect of operation [22]. Generally, components that play a role within either of these subsystems are mounted through rubber bushings to mitigate the effect of NVH to the cabin. In essence, engineers conduct extensive frequency and acceleration analysis as part of the process to determine the desired bushing stiffness. Additionally, considerable vehicle testing is performed, with data to support and compare different bushing stiffnesses in the real world [28].

However, it is important to note that development of bushings is outside the scope of this project, as the engineering and manufacturing processes are outside the capabilities of small companies or shops. Generally, integration of custom suspension or driveline components involves using a

bushing that is easy to install, relatively inexpensive, with little consideration for NVH [29]. With an EV powertrain, it is especially important to ensure NVH is kept to a minimum; therefore, where possible, bushings native to their application are used [29].

2.3.3 Strength, Fatigue, and Stiffness

Strength and stiffness are one of the most critical considerations for load-bearing components such as the cradle. As most of the suspension and driveline of a vehicle are mounted to the cradles, it must subsequently be designed to react to all loads applied by these components. For example, power transmitted from the engine to the wheels goes through the differential, which will want to move as a result of the input forces from the transmission, and output forces to the wheels [30]. In a similar fashion, loads applied to suspension members are generated due to forces applied at the tire contact patch, such as reaction forces under braking, or the tire driving over a pothole [31], and are directly transferred to the mounting points on the cradle.

It is important to note that there is another factor that must be considered in addition to absolute strength. Vehicles are designed to last many years and hundreds of thousands of miles with proper maintenance [32]. As such, components within the vehicle are subject to frequent repetitive loads which generates microcracks within the material. As a result, it is possible for these components to break, even when peak stresses are well within the yield stress of a material [33]. This phenomenon is commonly known as fatigue, and extensive analysis on this subject must be conducted as the cradle is designed.

Stiffness of structural components is important as well. For example, engine and transmission mounts have deflection requirements, since those components are typically situated close to the body. As these want to move under operation, mounts that are insufficiently stiff can cause contact with the body and surrounding components, resulting in unwanted NVH and potential damage [34].

The stiffness of a cradle must be considered as loads from the suspension and driveline cause deflection. This is typically not an issue with most of the deflections arise from the bushings.

However, with an inadequately stiff cradle large enough deflections can compromise control of the vehicle as suspension geometry is affected [35]. For example, excessive rear toe compliance can cause the car to feel unstable, which compromises driver confidence in the vehicle [36]. Therefore, within the development of a cradle by a manufacturer, engineers in charge of the cradle's structural aspects work closely with those from the vehicle dynamics team to ensure the stiffness of the cradle is sufficient [37].

2.3.4 Material Options

Selecting a material to use is another critical consideration in the development of major structural components in a vehicle. For the most part, matters such as manufacturability, strength, stiffness, and fatigue, as well as other factors such as cost and time all play a role in this crucial decision. There are three primary categories of materials used in automotive structures – metals, plastics, and composites [38].

Metals are one of the oldest materials used in building, as copper was discovered as early as 9000 BC [39]. As of 2020, the typical automobile is composed of metal by over 50% by mass, and for good reason [38]. Steel is one of the oldest, most common metals used in the construction of vehicles, its widespread usage dating back to the early 1900s [40]. Steel has a low material cost relative to other metals, has relatively high strength, and is incredibly versatile in how it can be used to manufacture car parts [41]. In particular, steels are used extensively in automotive body structures due to their high capability to absorb impact energy from a crash [38].

Aluminum is another metal that is commonly used and offers some benefits over steel as it has approximately one-third the density and higher specific strength [38] while still being relatively easy to manufacture [42]. As such, with the recent trend of prioritizing lightweighting, the usage of aluminum in the automotive industry is becoming increasingly widespread [38].

Both titanium and magnesium are also used in the automotive industry, though somewhat more sparingly than steel or aluminum. Magnesium is about two-thirds the density of the already lightweight aluminum and, as a matter of fact, has even higher specific strength [43]. However, its

usage is limited due to disadvantages such as low high-temperature strength [44], relatively poor corrosion resistance, and high cost [45]. Titanium has approximately 1.5 times the density of aluminum, yet has lower yield, and thus significantly lower specific strength [46]. The primary advantage of titanium is its ability to maintain strength at high temperatures; however, as a result, it is also not as easy of a material to weld as steel or aluminum [47]. It is also a costly material, therefore its usage is limited to high-temperature areas within premium vehicles where lightweighting is important [48].

Plastics are another family of materials that are becoming more widespread in cars, as they also allow for additional lightweighting while being relatively inexpensive to produce [49]. Most plastics are molded, which allows for significant freedom in part geometry without the hassles of requiring finishing operations or the worry of corrosion [50]. However, the fact that expensive tooling is required for molding deems it unsuitable for prototyping due to high initial costs, which is only suitable for high-volume production through economies of scale. There is the possibility of 3D printing plastics, though this is usually relegated to small, superficial components that do not bear high loads [51]. Printing structural components is still possible, though this usually has to be outsourced, as it usually requires different printing techniques and special materials which significantly increases cost.

Lastly, composites are another set of revolutionary materials that are gaining widespread use in the automotive industry, as they also support vehicle lightweighting. The definition of a composite is a material made from two or more materials that combine to create one stronger than either of the materials used to create it [52]. Fibre reinforced polymers (FRPs) in automotive were first used in 1981 when McLaren built the first Formula 1 car with a Carbon Fibre (CFRP) monocoque [53]. In the years that followed, FRPs, along with other composite materials slowly trickled down to consumers and the mass market. The BMW i3 is a good example of this, as it is an EV that uses a CFRP monocoque to minimize weight, to maximize range [54].

Manufacturing composite parts is a relatively tedious process; however, it is one suitable for small volume production and thus within the capabilities of small shops or companies [55].

Unfortunately, development of structural composite parts is a rather non-trivial process. Unlike regular materials, the material properties of composites are highly dependent on the manufacturing method and quality, ply orientation and number, as well as the actual constituents used [56]. As such, significant amounts of material testing and research is required to develop a reliable material model [57], and it is likely that one would need to develop this in conjunction with an outside source.

2.3.5 Manufacturing Methods

Generally, selecting a manufacturing method is conducted simultaneously with material selection, as both categories highly influence one another. However, there are other considerations that need to be taken into account, such as available manufacturing tools, time, and cost.

Most metals are incredibly versatile in how they can be used in manufacturing – for example, they can be cast, forged, extruded, drawn, stamped, machined, and even 3D printed [58]. As a matter of fact, it is possible to manufacture the same part geometry using many different methods with the differences between each method being production cost based on the quantity required [59]. In spite of this, only a few of these methods make financial sense if one were to build a handful of cars. For example, forging a has high initial cost which is absorbed by production volume and material savings, thus it is not financially viable for prototyping [60]. In general, rapid prototyping methods for metals are restricted to 3D printing, casting, and various machining and fabrication methods commonly found in a machine shop [61].

The manufacture of plastic parts in prototyping, aside from traditional machining processes, is generally limited to 3D printing. There are various methods of 3D printing, such as Fused-Deposition Modelling (FDM), Stereolithography (SLA), and Selective Laser Sintering (SLS) [62]. FDM is the most widely used 3D printing technique, where a nozzle extrudes molten thermoplastic filament as it travels. Meanwhile, SLA and SLS use a laser to cure photopolymer resin or powder, respectively. In general, FDM printed components have lower part quality and strength compared to those made using SLA and SLS. As such, SLA and SLS printing methods would be more suitable for prototype structural components.

Early production methods for composite FRPs were tedious and slow, which was well suited for low-volume production, and are near identical to the methods used at present. It is only in recent years that advanced, mass-manufacturing techniques have been developed as FRPs have become more commonly used in automotive manufacturing [63]. The FRP manufacturing process is commonly known as the layup, as it consists of placing layers of fabrics onto the mold which defines the shape of the part. The polymer component in FRPs are resins that can either be pre-impregnated into the fabric or added during the layup process. The layup is then cured, which requires time and can require heat and pressure, depending on the resin. The part is then removed from the mold and post-processing steps such as trimming and bonding can then be performed to complete the part [64].

2.3.6 Material Joints

The last topic to cover is joining, and it is one of the most important considerations in manufacturing. Certain structural components like suspension links or arms can be manufactured in a single piece, but the cradle is such a large component that it typically made in multiple pieces and joined together. There are three major categories for joining two parts together – mechanical joining, welding, and bonding with adhesives [65].

Mechanical joining involves the use of rivets or fasteners to clamp two materials together. It is quite a versatile method that allows for ease of assembly and disassembly; however, it can lead to increased manufacturing complexity and cost, as bolted or rivetted connections require an interface integrated within the part. Additionally, these discrete joints create stress concentrations which can lead to fractures originating at rivet or bolt holes. Fastener count can be increased to mitigate this, but the part consequently becomes increasingly complex and heavier [66].

Welding is a process where two or more parts are fused together through the use of heat, and potentially pressure [67]. In essence, welding generally involves locally heating the joint area, which melts the parent material together. In most cases, filler material is also added, which adds to the amount of molten metal and thus increases joint strength with poor part fitment [68]. Welded joints are more efficient than mechanical joints, as the entire perimeter of the joint bears

the load. As such, welded structures can be made lighter, especially considering the elimination of extra fasteners and fastener interfaces. The downsides with welding are that the process of locally melting the parent material forms a heat-affected zone (HAZ) which is often of lower strength and brittle [69]. As such, the HAZ is an area where failures can occur. Furthermore, the use of heat can cause distortion that can result in a dimensionally inaccurate component. Lastly, dissimilar metals can be welded together, but this requires specialized welding processes not common to a standard machine shop [70].

There are processes similar to welding at lower temperatures, known as soldering or brazing, where only the filler material is melted [71]. These methods mitigate the side effects that create distortion and the HAZ, as well as allowing dissimilar metals to be joined. Unfortunately, these methods are unsuitable for structural components, as the joints are not nearly as strong as a weldment.

As more plastics and composites are used in vehicles for lightweighting, the usage of structural adhesives follows suit [72]. Structural adhesives are similar to welding without much of the drawbacks as there is minimal heat input. The usage of structural adhesives within automotive structures is increasing; however, there are still downsides, including joint design and preparation [73]. Adhesives are weakest under peel or cleavage, which are concentrated tensile stresses perpendicular to the bond line [74]. As such, joints should be designed such that stresses imparted on the adhesive are primarily in tension, compression, or shear across the entire bond face. Part tolerances are kept tight, in order to minimize and keep bond gaps consistent. Next, the surface must be prepared for bonding, so it must be kept clean. Bonding should be performed from one parent material to the next, therefore surface coatings such as oxidation, paint, or any other impurities should be removed [75]. Furthermore, surface roughness is also critical to allow the adhesive to effectively bond to the substrate. As the consistency of a bonded joint is highly dependent on all these factors, it is likely that physical testing would be required before it can be modeled accurately in software [76].

2.4 Aftermarket Parts

Ever since the car was first invented, many owners were customizing them, constantly tweaking various aspects of their personal vehicle to suit their needs and tastes [77]. There are practically countless amounts of aftermarket parts available for vehicles, and owners install them for the benefits of improved aesthetic and function. Many of these aftermarket parts replace structural components which are critical for vehicle durability and safety. An example of this are aftermarket lower control arms, which can offer performance benefits such as lower weight, reduced suspension compliance, and increased adjustment [78].

Figure 7: Example of stock and aftermarket control arms [79]

One thing to note is that vehicle modifications are not limited to simple replacement of parts. Owners have taken extreme measures to modify their vehicles with major modifications such as engine swaps or adjustments to suspension geometry. The extent of these changes frequently results in modification, or a complete redesign of the cradle, as it is an integral component to the suspension and driveline systems of a vehicle. Often, these changes are executed without proper

engineering input, resulting in an unoptimized structure with respect to weight, stiffness, and strength. An example of this is shown in Figure 8, where the front cradle for a Mazda Miata was cut and welded to package a larger engine.

Figure 8: Stock [80] versus modified [81] cradle for Mazda Miata

There are even complete aftermarket cradle assemblies available with quantitatively high quality of manufacture. However, it is often not stated how much engineering was conducted throughout the development of these parts.

Figure 9: Stock (left) versus aftermarket cradles (right) for Toyota Supra [82]

As a matter of fact, the lack of proper engineering of aftermarket parts is a huge issue. Automotive manufacturers spend years in vehicle development, and individual parts undergo a thorough engineering process that involves a significant amount of analyses, design, and validation through testing on a component or vehicle level basis [83]. There are many reputable companies that manufacture aftermarket parts using proper engineering tools and methodology [84] but many more that do not. The manufacturing of improperly engineered parts can lead to premature failure or constitute a danger to the vehicle operator and to the public in general [85]. With major structural components of the vehicle, the consequences can be disastrous, as shown in Figure 10, where fatigue failure occurred on an aftermarket control arm after only 6,000 miles of use [86].

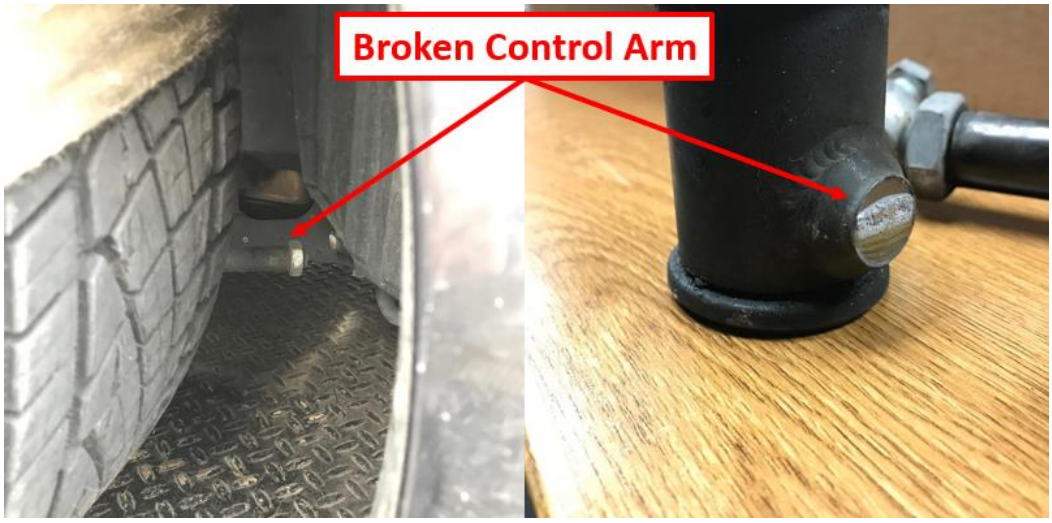

Figure 10: Example of aftermarket control arm failure [86]

2.5 EcoCAR and UWAFT

As this thesis is using the UWAFT rear cradle as an example to outline procedures for developing major structural components of a vehicle, some background on the team and its activities are required for context. UWAFT is a student team at the University of Waterloo that has been competing in Advanced Vehicle Technology Competitions (AVTC) since 1996 [87]. The AVTC series provides a unique opportunity that challenges students to accelerate the development and

demonstration of the latest automotive technologies to the US Department of Energy and the automotive industry [88].

The current competition from this series is called the EcoCAR Mobility Challenge, which spans four years and challenges 11 university teams to integrate new vehicle technologies to a 2019 Chevrolet Blazer. More specifically, teams are to implement advanced propulsion systems and components that will enable SAE Level 2 automation and innovations in vehicle connectivity for carsharing [89]. To meet the needs of the competition, UWAFT has implemented a custom hybrid powertrain, requiring the integration of many new components and significant modification to some components that were re-used. To facilitate this, General Motors (GM), as one of the largest sponsors of the competition, donated the vehicles and provided necessary engineering data and support for the conversion.

2.5.1 Vehicle and Rear Cradle Assembly

The powertrain architecture implemented on the Blazer is known as a parallel-through-the-road hybrid. This type of hybrid system involves two separate propulsion systems, a conventional internal combustion (IC) powertrain driving the front wheels and an electric (EV) powertrain driving the rear wheels [90], as shown in Figure 11. Through availability from competition, risk assessment, and modeling & simulation, UWAFT selected components that would make up these powertrains, one of which is the e-axle, which is an integrated motor and transmission [91]. This e-axle is known as the EDU4 and supplied by American Axle & Manufacturing Inc. (AAM), a company that supplies driveline solutions to automotive manufacturers [92]. As a matter of fact, AAM is an original equipment manufacturer (OEM) for Jaguar, and the EDU4 is used on both the front and rear axles for the I-PACE, which is Jaguar's first production EV [93].

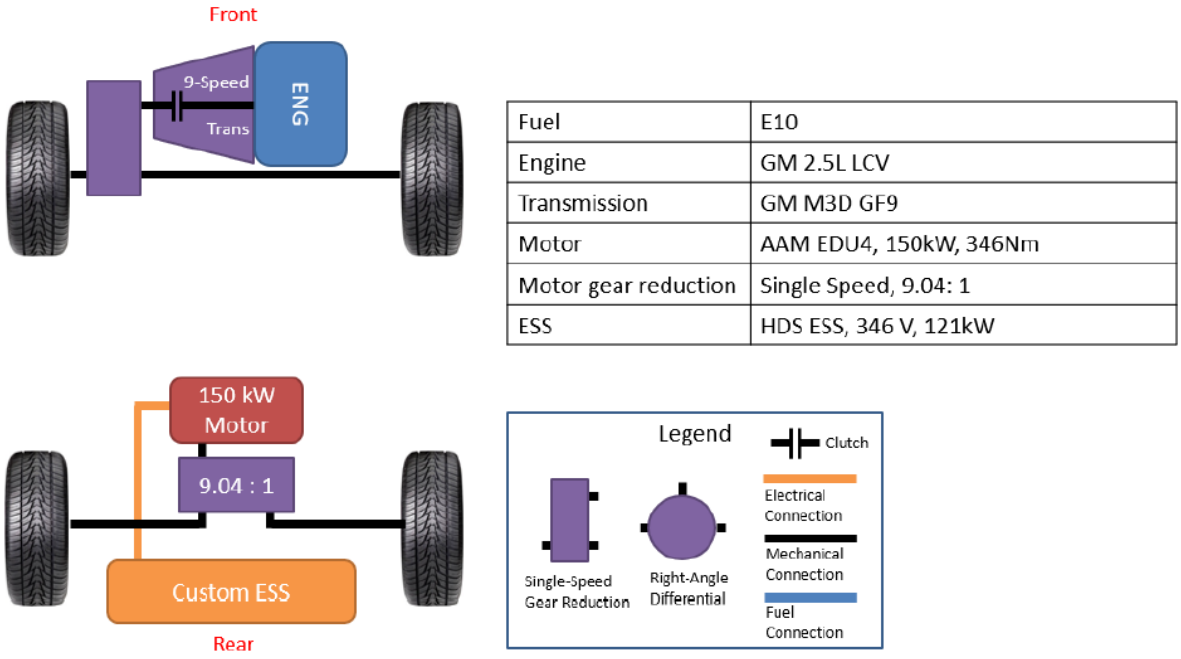

Fuel	E10
Engine	GM 2.5L LCV
Transmission	GM M3D GF9
Motor	AAM EDU4, 150kW, 346Nm
Motor gear reduction	Single Speed, 9.04: 1
ESS	HDS ESS, 346 V, 121kW

Figure 11: UWAFT Blazer Propulsion Architecture [94]

To integrate the e-axle to the Blazer's rear axle, significant modification will need to be performed to the rear cradle and any other components that could interfere. However, these modifications must suit the needs of the team and meet the requirements set by the competition.

2.5.2 Relevant Rules, Regulations, and Guidelines

As the UWAFT Blazer is being built for the EcoCAR Mobility Challenge, there are a set of rules and regulations that must be followed for the vehicle to be deemed legal to compete. All of the rules pertaining to development of the rear cradle fall under the Non Year-Specific Rules (NYSR), which dictate matters that relate to vehicle development and safety, competition support, as well as general scoring, cost, and penalties. A summary of the relevant rules are listed in Table 1.

Table 1: Summary of relevant rules for new rear cradle [95]

Rule	Summary
G-2.1 Static Ground Clearance	The ground clearance requirement for competition vehicles is 7 inches or greater
G-3.11 Crashworthiness	Sharp edges or protruding parts must not be pointed at fuel tanks, battery boxes, fuel lines, or HV lines
G-8.2 Vehicle Mass, Mass Distribution, and Centre of Gravity	Maximum vehicle mass and mass distribution limits
G-9.1 Drilling	Size and spacing limits of drilled holes into critical structural areas (includes cradle)
G-9.3 Critical Fasteners	Critical fastener requirements for positive locking and torque specifications
G-9.4 Welding	General welding requirements
H-1 General Guidelines for Structural Modifications and Waivers	General requirements for waiver process
H-2.2 Suspension Modifications	Allowable suspension modifications
H-3.2.1 Rear Cradle Modifications	Allowable modifications to cradles
H-3.6 Propulsion System Mounts	Structural requirements for propulsion system mounts
H-4 Structural Waiver Process Description	Documentation requirements for structural waiver

Some of the rules are rather simple. For example, with respect to G-2.1, the team must ensure that the new rear cradle and any related components do not go below the 7 inch ground clearance limit at static ride height. To ensure the new rear axle achieves this goal, a plane can be defined in CAD at 7 inches off the ground, and designers must ensure none of the components mounted to the vehicle go below this plane.

However, there are other rules that have strict requirements and processes, most notably in section H. Section H-1 mentions that a structural waiver is required when any structural part is modified or when new structural elements are implemented. As defined by NYSR, a waiver is a document which outlines any proposed subsystem or vehicle changes allowed within the safety and technical requirements of competition rules. Section H-4 outlines the general structural waiver process; however, as most teams are implementing parallel through-the-road hybrid systems, rear cradle modifications are expected. As such, competition has provided guidelines for the rear cradle waiver in the form of a specific process for cradle development, supporting documentation and engineering data, and ability to consult with GM engineers [96].

2.5.3 Previous Cradle and Waiver Introduction

At the time of writing this thesis, UWAFT has already integrated the e-axle using a first iteration of a custom rear cradle, as shown in Figure 12. This design is known as the *2019 cradle* when further references are made to it within this thesis, and was designed by the author of this document.

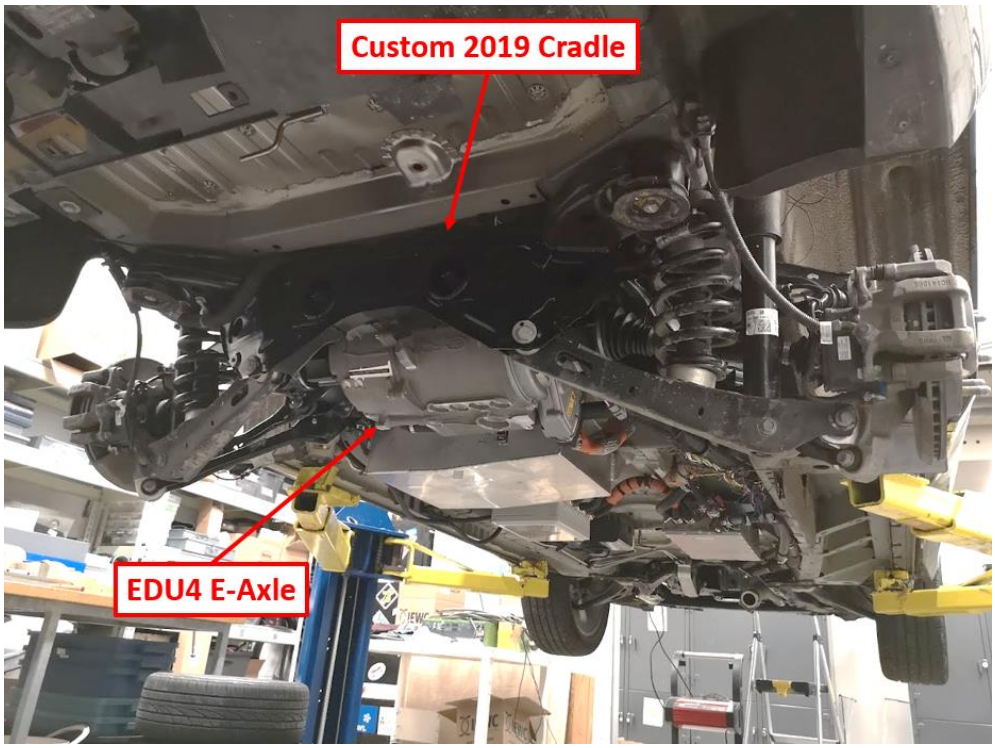

Figure 12: Integrated rear cradle assembly, consisting of the e-axle and all associated components with the 2019 cradle

Passing the cradle waiver requirements involves extensive finite-element analysis (FEA), which is a software tool that can predict stresses applied on a part as a result of input loads and constraints. To start, GM provided all teams with a baseline FEA model of the stock rear cradle for the Blazer and teams were to re-run this model and ensure that obtained results matched with what GM provided. Doing so validates the FEA software used, as there is a potential for results to vary with different solvers.

The next step was to integrate the e-axle in CAD, which involved considerations such as e-axle placement and packaging of e-axle interfaces such as high-voltage (HV) connectors, halfshafts, and e-axle mounts. Instead of manufacturing an entirely new cradle, UWAFT elected to modify the stock cradle as there was sufficient clearance for the e-axle so long as the front member was revised. Various designs were initially created, considering the manufacturing methods available to the team, and these are shown in Figure 13.

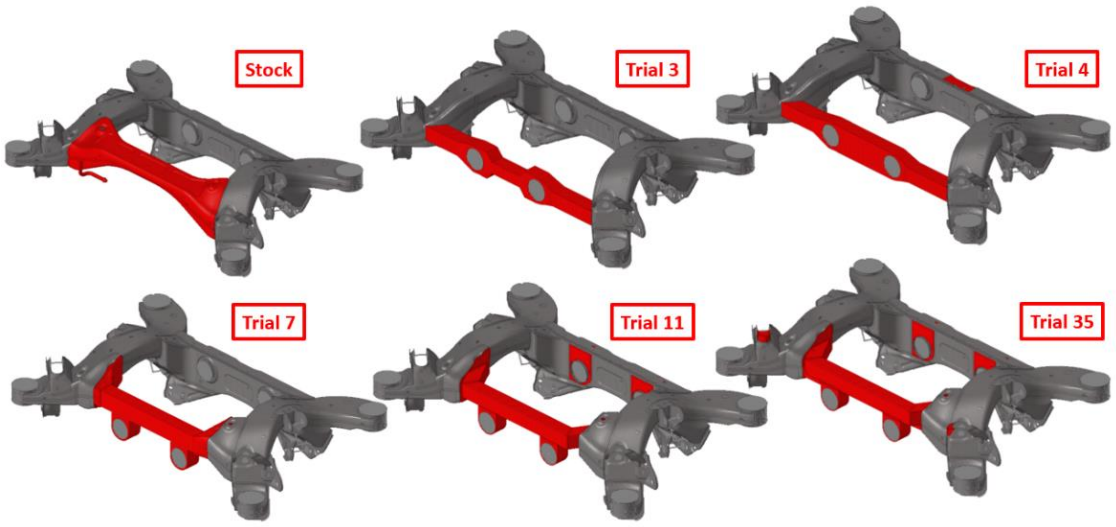

Figure 13: Various early cradle designs, showing the front member designs iterated for the 2019 cradle

FEA studies were conducted on all of these different cradles with varying degrees of success. In essence, the requirement set for the waiver were that global stresses in the cradle could not exceed those of the baseline model for each of the loadcases provided. Additionally, as the cradle serves as the mount for the e-axle, the structure must meet 8g vertical and 20g horizontal loading requirements as defined in NYSR H-3.6. Numerous designs were tested, iterating between revised geometry in CAD, and structural analysis conducted in FEA. Eventually, UWAFT finalized a design that passed the stress requirements set by GM. The last step in the waiver process was to generate a document highlighting the required modifications to the cradle, any changes to the input loads due to the addition of the e-axle, and the FEA results. Formatting requirements are mentioned in NYSR H-4.5, which the team closely adhered to.

The next step was to physically modify the cradle. To minimize downtime of the vehicle, the team opted to order a brand-new cradle, so modifications could be performed in parallel to keeping the vehicle operational. As this cradle was designed to be manufactured in-house, traditional manufacturing tools such as machining, water jetting, and welding were used to perform the

modifications required, as shown in Figure 14. The final weight of the 2019 cradle was 23.5 kg, which was 7.8% heavier than the cradle original to the vehicle, at 21.8 kg.

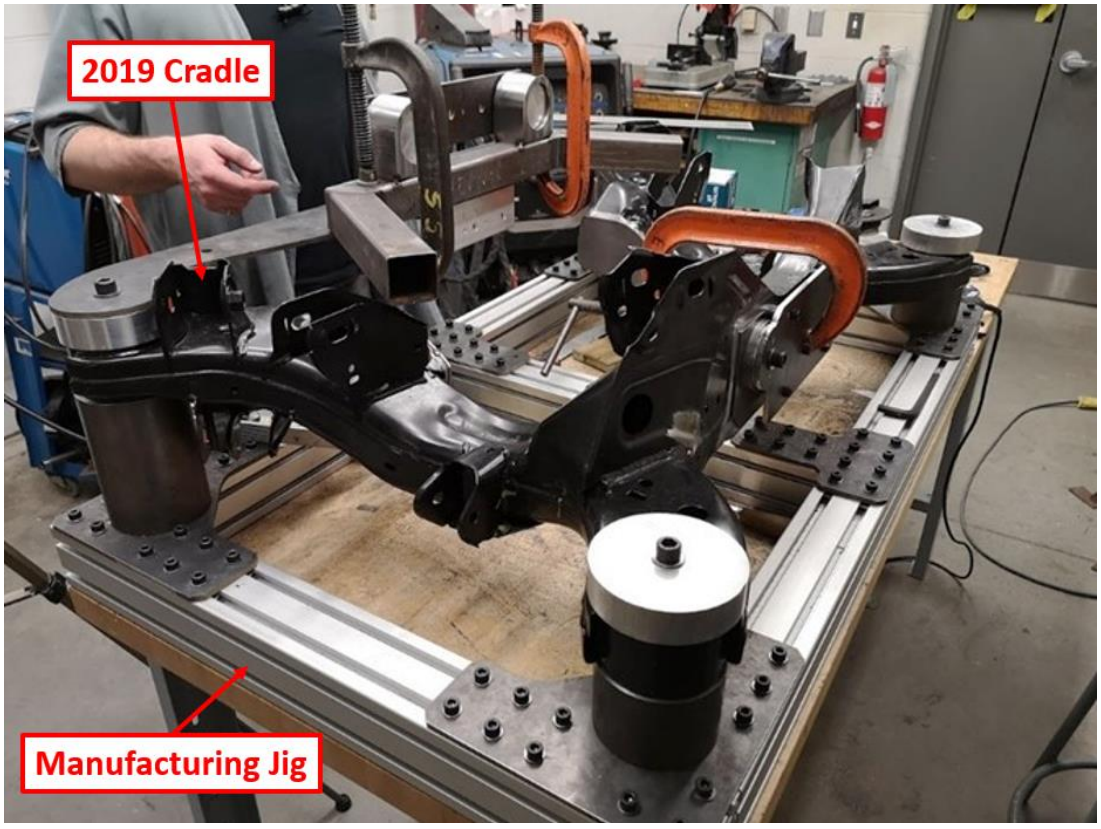

Figure 14: 2019 cradle modifications in progress

After modifications were performed, the cradle was then installed to the vehicle along with all of the surrounding components such as the e-axle, cooling lines, halfshafts, and bushings, as shown in Figure 15.

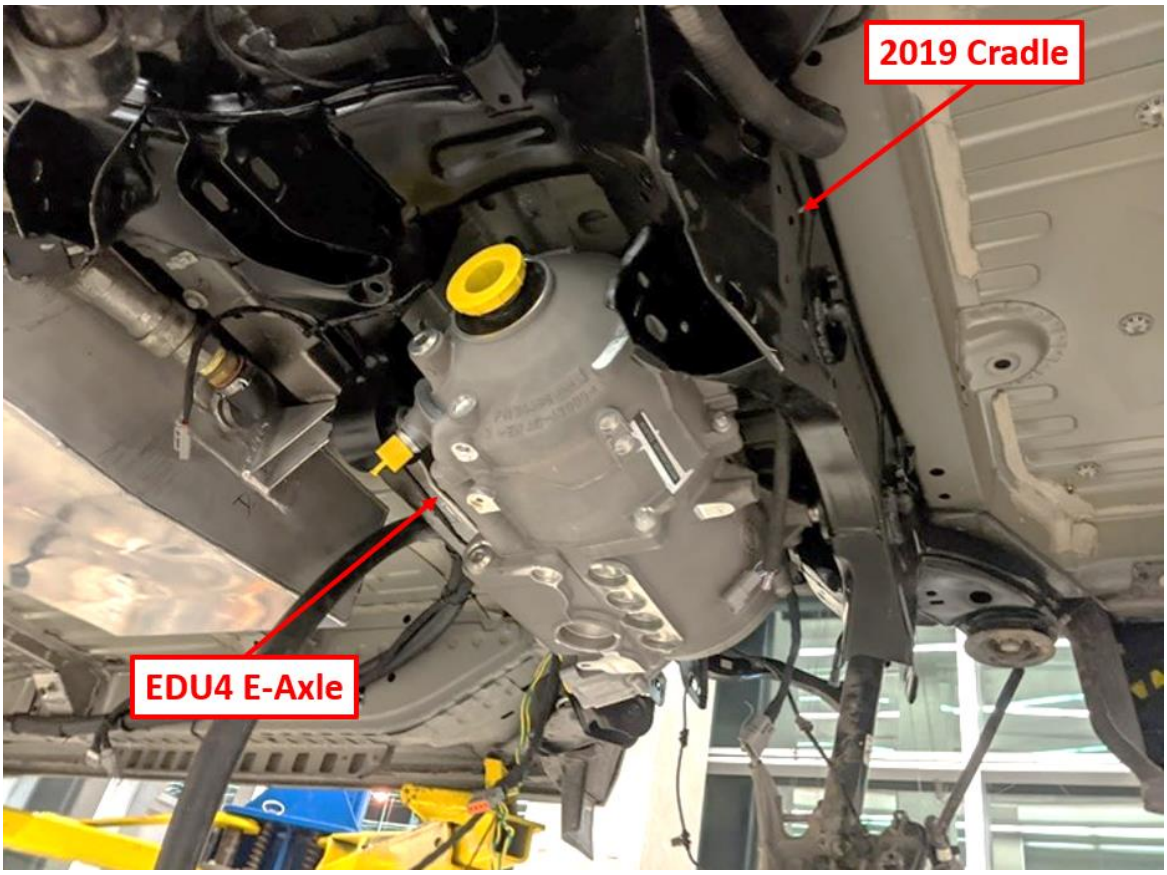

Figure 15: E-axle and 2019 cradle mounted to the UWAFT vehicle

Chapter 3
Fatigue and Maximum Stresses

One of the most important considerations with the design of structural components is fatigue and resultant stress targets. As such, this chapter will introduce the concept of stress and strain, how fatigue plays a major role in setting stress targets, and how these targets were set specifically for the cradle.

3.1 Introduction

Every object in the world is subjected to a force – whether this is the force in a rope being pulled apart in a game of tug-of-war, the force of your hand gripping around a baseball, or even the gravitation force pulling any object with a mass towards the ground. The amount of force an object can withstand is typically proportional to its cross-sectional area, so for ease of comparison between different objects and materials, the term stress was coined, which is defined as the force per unit area [97]. Similarly, materials deform when stresses are applied, so strain is defined as the change in length divided by the original dimension [97]. As stresses generally increase proportionally with strain, they are plotted against each other to create a stress-strain diagram, as shown in Figure 16.

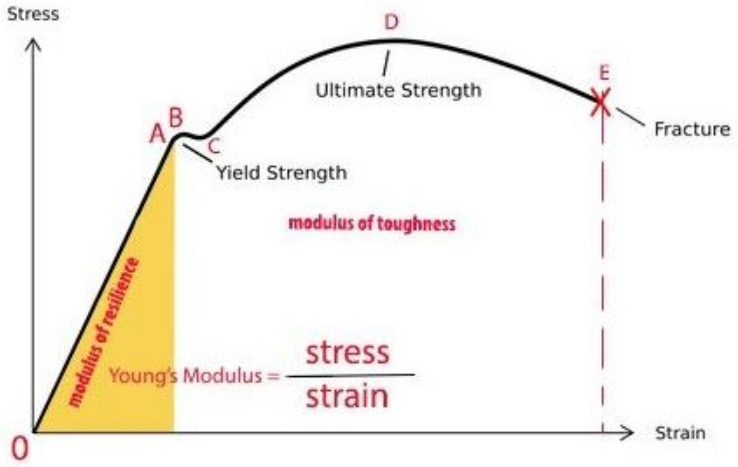

Figure 16: Example stress-strain diagram [98]

Stresses applied to a material cause a corresponding amount of strain. If the stress is removed and the strain correspondingly goes back to zero, the material is physically unchanged; this region is known as the elastic region [97]. However, large amounts of stress may cause strains not to disappear when removed, so the material has been physically altered; this region is known as the plastic region [97]. The stress level at which the elastic region transitions to plastic is known as the yield strength, with the peak level of stress being known as the ultimate tensile strength (UTS). Further increases in stress beyond the UTS result in fracture of the material and thus failure of the component.

However, materials can fail at stress levels well within the elastic region if repeated loading is applied – this phenomenon is known as fatigue. Essentially, tiny cracks form in a material and grow with cyclic load [97]. As numerous components within machinery such as aircraft or automobiles are subject to cyclic loads, fatigue is the limiting factor in maximum stress, and this is one of the most important considerations in designing a new rear cradle. Similar to the stress-strain diagram, there is a fatigue diagram known as the S-N curve, which defines stresses in conjunction with cycle count [33]. Logically, allowable stresses decrease with increasing cycle count as cracks grow, as shown in Figure 17. Therefore, similar to the stress-strain diagram, the fatigue S-N curve can be used as a tool for designing components to obtain an allowable stress level for the corresponding cycle count.

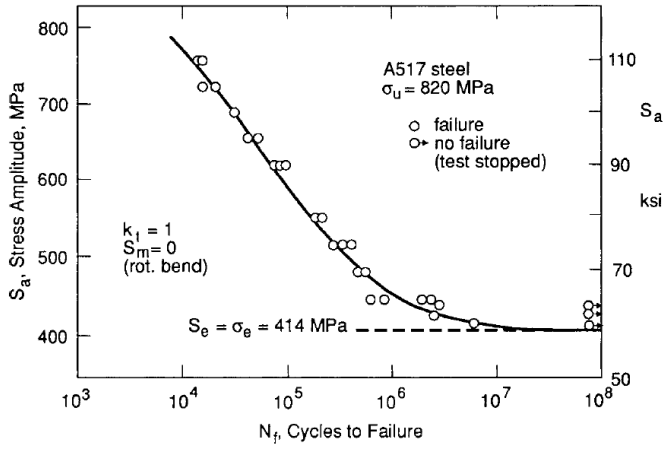

Figure 17: Example fatigue S-N curve [33]

The importance of considering fatigue in the design of the rear cradle cannot be understated. The average age of privately-owned passenger vehicles in the United States as of 2018 is 11.9 years for an estimated total of 154,874 miles accumulated throughout ownership [99]. It is not uncommon to encounter a few speedbumps or potholes while driving, so any suspension components such as control arms or cradles must bear these loads. Given the length of vehicle ownership and mileage accrued, one can only imagine how many cycles these components undergo. As such, fatigue is one of the most important considerations in the design of many load-bearing automotive components.

3.2 Competition Waiver Requirements

As the importance of fatigue is now well understood in the context of the rear cradle, there is a need to understand how competition requirements have taken this into account. As previously mentioned, there is a waiver process for the rear cradle which outlines the processes and procedures set by GM in developing this component [96]. A flow chart for this waiver process is shown in Figure 18.

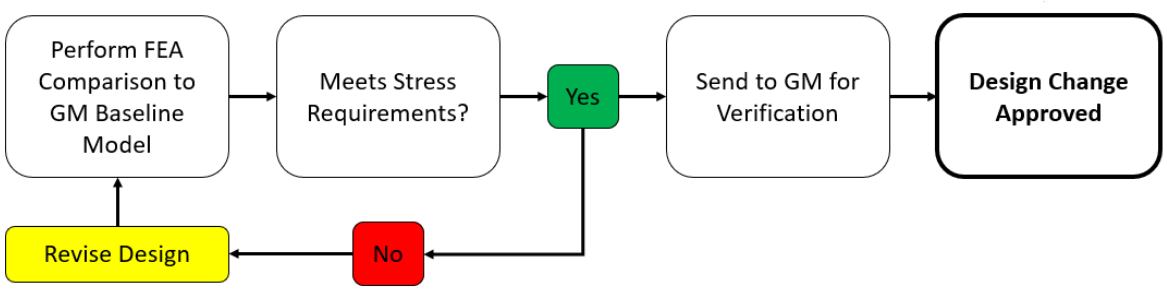

Figure 18: Competition waiver process flow chart [96]

GM has gone through the fatigue calculation process and defined a stress level that cannot be exceeded for each of the provided loadcases. Additionally, GM has defined nine specific loadcases that altogether capture the most damaging driving scenarios, such that if these requirements were met, the cradle should last the life of the vehicle. The pass/fail criteria is straightforward – if the calculated stresses exceed the requirement, the design must be revised; conversely, if the stresses are lower than the requirement, the results are sent to GM to be reviewed.

Table 2: Maximum permissible stresses for competition waiver

Loadcase	Stress Limits* (MPa)	
	Parent	Heat-Affected Zone
Two-Wheel Bump	382	389
Twist LH	403	392
Twist RH	404	397
FWD Braking	397	375
REV Braking	365	323
Cornering LH	328	313
Cornering RH	345	337
FWD Accel	429	405
Rev Accel	312	286

*Note: Placeholder values shown due to confidentiality – values depicted are within 30 MPa of those provided by GM, and represent peak stress values that cannot be exceed

However, it's important to note that these maximum stresses were defined for high-strength alloy steel. If a similar material were to be used, these stress targets can be retained; however, as fatigue properties vary with differing materials, new stress targets will have to be developed if a different material is chosen.

3.3 Material Selection

With a completely new rear cradle, there is opportunity for extensive weight savings with choosing a new material. As such, this decision would dictate whether the existing stress targets could simply be reused or if new targets must be developed.

The first decision was which general type of material to use. An overview of materials used in structural automotive applications was provided in section 2.3.4, which outline the three main categories – metals, plastics, and composites. There are many considerations to account for when choosing a material, and the rear cradle is no exception to this Typically, a decision matrix would be generated and the differing materials compared with respect to categories such as manufacturability, availability, strength, stiffness, and cost. However, the waiver process, coupled with the decision from the team as well as general logical thought processes, ruled out the need

for using one to decide at this stage. Figure 18 shows the rear cradle waiver process; however, Figure 19 shows the material modelling process for the general structural waiver glidepath.

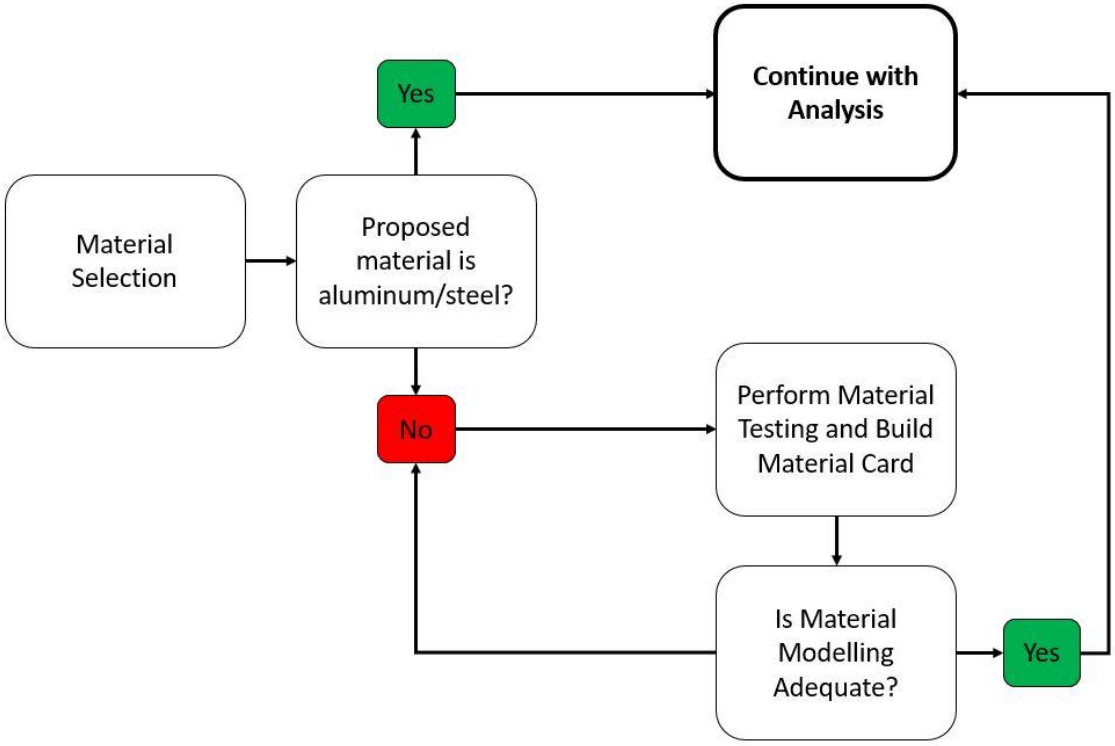

Figure 19: Material modelling process for general structural waiver

Essentially, unless the proposed material is aluminum or steel, physical material testing must be performed to obtain material properties and compared to analysis results. If there is inadequate correlation, more material testing and model tweaking is necessary, and the cycle is repeated until modelling matches results, at which point analysis can continue. It is stated in the rules that the purpose of these processes was to allow for accurate analysis in the case of anisotropic materials such as composites or 3D printed plastics [95]. As a matter of fact, as long as the material is isotropic with known material data, physical material testing and building a material card is not needed. As this is the case, it was determined that choosing an exotic material and creating its material card was not the correct choice. The big issue with doing so is time and resources, as physical testing of a material and correlating the results back to a model is very time consuming

and takes a significant amount of effort. As such, the use of composites and 3D printed plastics were automatically eliminated.

This decision left the choice of either metal or plastics with isotropic properties. Generally, plastics with isotropic properties use manufacturing methods such as injection or blow molding, which are mass production methods not suitable for the rear cradle [100]. In contrast, 3D printed plastics are generally anisotropic due to the manufacturing techniques used – for example, fused-deposition modelling (FDM) printers extrude molten plastic in multiple layers that result in differing tensile strengths for a given direction due to bonding between layers [101]. Stereolithography (SLA) is an isotropic 3D printing technology [101]; however, it is extremely expensive, especially for a large component like the rear cradle [102]. Consequently, it was determined that the ideal material choice is metal.

The next step was to determine the type of metal to be used. The four primary metals used in structural components of a vehicle are steel, aluminum, titanium, and magnesium [103]. Manufacturability, strength, weight, and fatigue were classified with utmost importance due to the low-volume production requirements, structural waiver requirements, and the primary goal of minimizing weight. Next was corrosion resistance, as the vehicle will be used in harsh winter conditions for many years, so it is important to use a material that will not degrade over time. Cost was next, as small shops or teams such as UWAFT have budget constraints; in this case UWAFT has set a limit of $3,000 CAD for this project as detailed in section 4.3.2. After was availability, as it is possible to order from external vendors with longer lead times as long as the project is planned accordingly. Lastly is stiffness, as there are no stiffness requirements in the waiver. After analyzing all of these properties for all materials, a decision matrix was compiled, as shown in Table 3 [104]. In the end, it was decided that aluminum would be used to build the new rear cradle. As a matter of fact, the use of aluminum in the automotive industry is becoming increasingly widespread due to its high strength to weight ratio, relatively low cost, availability, and corrosion resistance, and it was for these reasons that this material was selected [38].

Table 3: Metal material selection decision matrix [38]

Category (Tot. Points)	Steel	Aluminum	Titanium	Magnesium
Manufacturability (5)	5	5	3	3
Weight (5)	1	4	3	5
Fatigue (5)	5	4	5	5
Strength (5)	5	4	5	2
Corrosion Resistance (5)	2	5	4	3
Cost (4)	4	3	1	1
Availability (3)	3	3	2	1
Stiffness (2)	2	1	2	1
Placement (Tot. Points)	2nd (27)	1st (29)	3rd (25)	4th (21)

The last step was to decide exactly which grade of aluminum would be used. It is expected that low-volume production methods such as machining, welding, and forming are to be used. Additionally, it may be desired to heat treat the cradle after welding to eliminate weak spots in the HAZ. Table 4 depicts all the grades of aluminum and their general machinability, weldability, formability, and heat treatability characteristics [105].

Table 4: General aluminum grade characteristics, with 'X' marking off feasibility [105]

Category (Tot. Points)	1000	2000	3000	4000	5000	6000	7000
Machinability	X	X	X		X	X	X
Weldability	X		X	X	X	X	
Formability	X	X	X	X	X	X	
Heat Treatability		X				X	X

As shown, the only grade of aluminum that meets all needs is the 6000 series. Investigating the material properties further, as a matter of fact, 6061 aluminum is the most versatile and widely used of heat treatable aluminum alloys [105]. Furthermore, the T6 temper of aluminum has the highest yield strength and can be heat treated back to this temper post-weld [106]. Therefore, the chosen material for the rear cradle is 6061-T6.

3.4 Mileage Target

As new stress targets needed to be developed due to the new material the first task was to determine a target mileage, since this would form the basis for calculating the cycle count of each loadcase. The target mileage was derived from length of vehicle ownership as well as accrued mileage for each year owned. Oak Ridge National Laboratory (ORNL) has conducted extensive data analyses on the energy sector, that includes detailed studies on consumer vehicle ownership statistics. In particular, one of their studies outlines the likelihood of a vehicle to be scrapped, at a given age. At 15 years, roughly half the vehicles of that age are disposed or sold for parts, so accumulated mileage was calculated over the 15-year period [99].

In addition, ORNL publishes data on estimated annual miles of travel for consumer vehicles. This starts at 13,843 miles with a new vehicle, tapering all the way down to 5,358 miles for a vehicle that is 30 years old. The total mileage target can thus simply be computed by adding mileage for the first 50th percentile of survival, or 15 years, which results in 192,726 miles or 310,163 km [99]. As such, it was determined that cycle counts of the nine loadcases would be derived for this mileage.

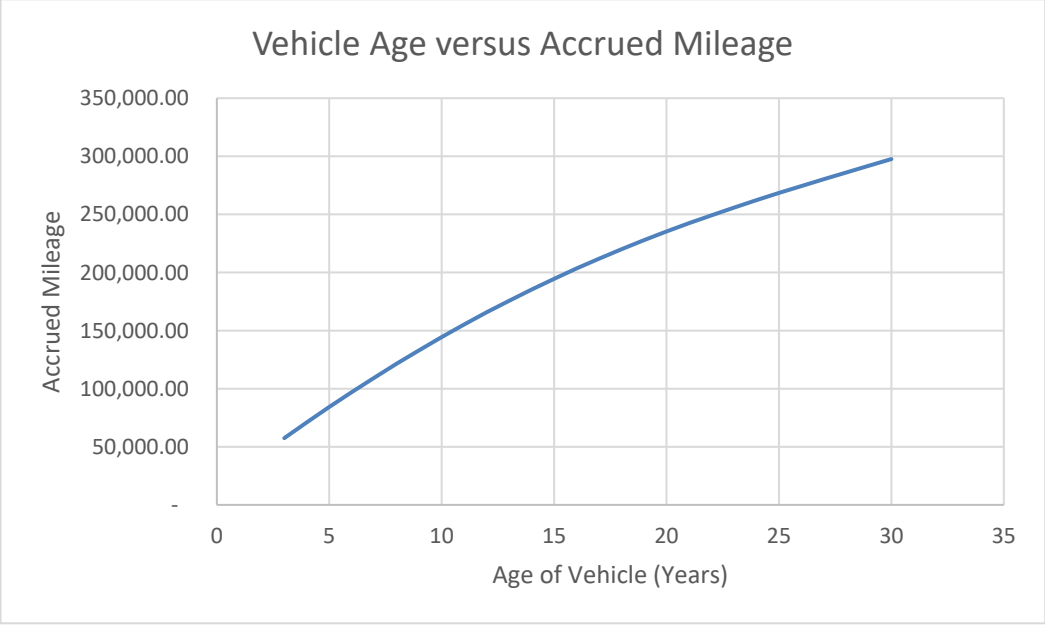

Figure 20: ORNL data for vehicle age versus accrued mileage [99]

3.5 Loadcases

Now that the mileage target was known, cycle counts for each of the nine loadcases, as shown in Table 2 could be derived. However, before direct calculations for each loadcase can be conducted, the distribution between city and highway driving must be known since certain scenarios are only observed with either type of driving or distributed unevenly between the two. Once again, ORNL has conducted studies on this, and as of 2017 consumer vehicles spend on average 44.3% of road mileage on the highway, with the remaining 55.7% spent in an urban environment. With this distribution defined, calculations for each loadcase could then commence.

The first loadcase was two-wheel bump, which is where both wheels on a single axle undergo compression simultaneously. Brainstorming various types of driving scenarios led to two main contributors, which were driving over speed bumps and railway crossings, as these obstructions in the road surface are consistent and completely perpendicular to the path of travel. As speed bumps are only present in urban environments, the total number of speed bumps driven over can be computed by calculating the speed bumps per given distance in a city and extrapolating. In this case, the city of Toronto was used, which has 2,400 speed bumps [107] in 5,358 km of urban road [108]. With the full city mileage target known, this extrapolates to 77,384 speed bumps for the life of a vehicle. Similarly, there are 102 railway crossings [109] for the same length of road, so there are 3,288 railway crossings for the designed life of a vehicle. Therefore, the total number of two-wheel bump events is the sum of both scenarios, which is 80,673.

Next are the left-hand and right-handed twist cases, which are due to both driveway entries and exits, as well as potholes, as they are driven over with one tire. Number of driveway entries and exits can be calculated by total number of trips. Once again, ORNL had data on this, which indicated that the average mileage of a trip was 10 miles, or 16 km [99]. With a total of 310,163 km for the life of a vehicle, the resultant number of trips is 38,545. Assuming one entry and one exit per trip, this equates to 38,545 driveway events. With respect to potholes, there is data that indicates a total number of potholes in the United States as 55,961,000 [110]. With 4,180,000 miles or 6,727,041 km of road [111], that equates to 8.3 potholes per kilometer. This in turn results in

2,580,190 potholes throughout the full life of the vehicle. Therefore, the total number of twist events are 2,618,735. Assuming an equal distribution to the left and right sides, it is 1,309,367 for the left and right sides each.

Next are the dynamic driving cases, namely the accelerating, braking, and cornering cases. It is assumed that the cycle counts are equally distributed between the acceleration and braking as well as left and right-handed cornering. The forward acceleration and braking cases could be computed by number of stops at a traffic signal, which were only present in urban environments. The City of Toronto shows that there are 2,376 traffic signals in Toronto [112]. Coupled with the 5,358 km of urban roads mentioned earlier, that would be a traffic light every 2.25 km. If it is assumed that every traffic light is a red, this results in 76,611 acceleration and braking events each. Reverse acceleration and braking are assumed to be due to backing out of parking spots, which is the same value as number of driveway entries and exits. As such, this equates to 38,545 each.

Lastly are the cornering cases, which is indicative of the vehicle turning left or right. However, hard cornering events are not common for the everyday driver, so instead, this value was computed from a team perspective of testing of the vehicle. It was estimated that there were on average 4 testing sessions per month for 12 total months of testing making for a total of 48 testing sessions per life. In each testing session, it was conservatively estimated that there were 30 autocross laps for each testing session. The SCCA course design book defines an average of 35 cornering events per lap [113], therefore the number of hard cornering events for life is 50,400 total, or 25,200 for the left and right sides each.

Table 5: Tabulated cycle counts for the nine loadcases

Loadcases	Cycles
2 Wheel Bump	80,673
Twist LH	1,309,367
Twist RH	1,309,367
FWD Accel	76,611
FWD Brake	76,611
Cornering LH	25,200
Cornering RH	25,200
REV Accel	38,545
REV Brake	38,545

Table 5 lists the cycle counts calculated for each loadcase. At this point, the next step would have been to translate these values to stress targets. However, as GM is responsible for inspecting waiver submissions, it was only customary to go over these results with them as a double-check. After consultation, their representative stated that these values were quite accurate, and suitable as competition requirements [114].

3.6 Stress Targets

As cycle counts for each loadcase were finalized, completing the objective of obtaining stress targets could be performed. As previously mentioned, the chosen material is 6061-T6 aluminum, which has known fatigue properties. A linear S-N curve can be generated using Equation 3.1, with A and B as material constants, N_f as number of cycles and σ_a the stress target [33]. It should be noted that a linear S-N curve is inaccurate with low-cycle fatigue, which is typically less than 10,000 cycles [33]. However, all the cycle counts to be translated to stress targets were in excess of this value, so this was not an issue.

$$\sigma_a = AN_f^B \tag{3.1}$$

The resultant stress targets are shown in Table 6.

Table 6: Resultant stress targets for the nine loadcases

Loadcases	Max Stress (MPa)
2 Wheel Bump	185
Twist LH	127
Twist RH	127
FWD Accel	186
FWD Brake	186
Cornering LH	211
Cornering RH	211
REV Accel	201
REV Brake	201

With the target stresses known, the next step was to define other requirements such as clearance, geometry, and manufacturability before proceeding with design iterations.

Chapter 4
Design Requirements

With the primary structural requirement defined, other design requirements need to be generated to start development of structural components for low-volume production. This can include requirements for packaging and interfacing with associated components, manufacturing methods available, as well as budgetary constraints.

With respect to the cradle specifically, this includes mounting requirements for the e-axle, such as its relative position to the cradle and the vehicle, overall stiffness of the cradle to ensure suspension compliances are within a reasonable range, manufacturing, and budget.

4.1 Geometrical Requirements

4.1.1 Geometry

The first requirement to investigate was geometrical, which were considerations that pertain to components integrating with the rear cradle. Primarily, these include the four attachment points to the body, all the attachment points to the suspension members, as well as the four attachment points to the e-axle. Figure 21 shows all of these attachment hardpoints using the 2019 cradle as an example.

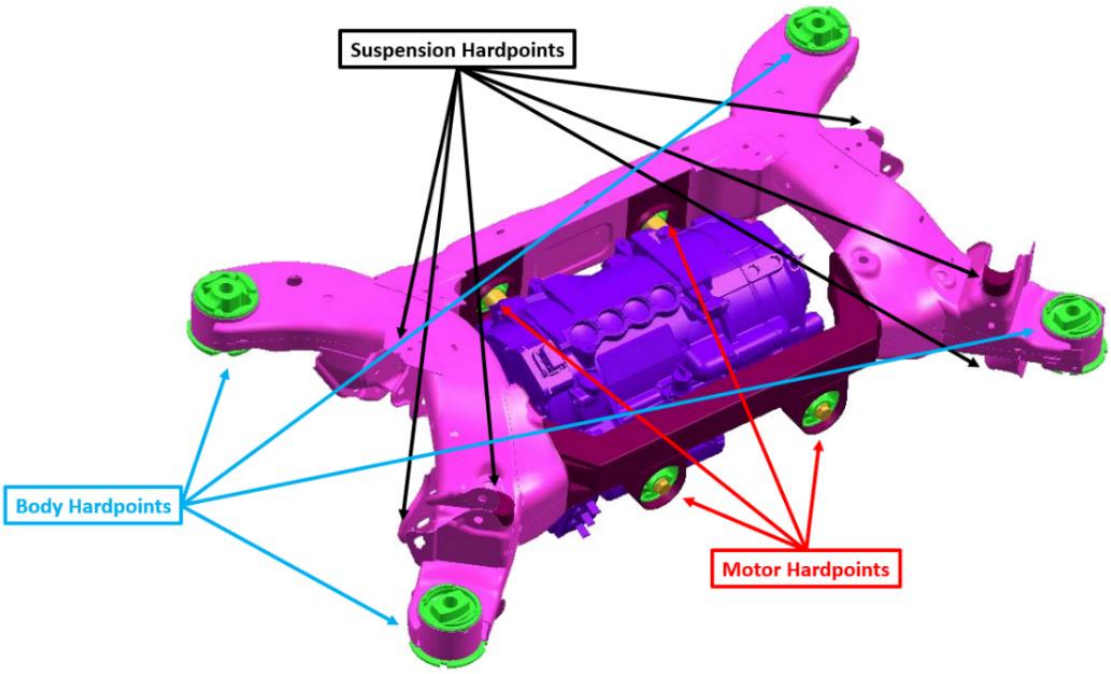

Figure 21: Body, suspension, and motor attachment hardpoints on 2019 cradle

Per competition rules, body and suspension hardpoints cannot be altered [95]. Therefore, the new cradle must replicate these interfaces in order to assemble with the stock vehicle body and suspension members. However, as the e-axle is a team-added component, there were no restrictions on its location, so emphasis was placed in determining this.

The first consideration for e-axle location was to account for all of the interfaces it has, to successfully integrate it to the vehicle. Although physical size is an obvious constraint, there were many interfaces that have specific requirements. For example, with electrical wiring, there must be ample room to access connectors, and harnesses have minimum bend radiuses according to wire gauge. Similar to electrical, the liquid cooling ports have quick-connect fittings that must be serviceable, and the cooling lines must be routed to avoid kinks. There must also be space to route hose and small filters for vent ports, and with the halfshafts, there must be adequate space around the output splines of the e-axle and clear line of sight to the outboard hub. Lastly are the mounting bushings, which are from the I-Pace and thus capable of dampening any NVH produced. As the mounting bushings are directly installed to the cradle, it was therefore

important that the new design have an interface to allow for this. Figure 22 shows all of the required e-axle interfaces, colour-coded and labelled by type as described above.

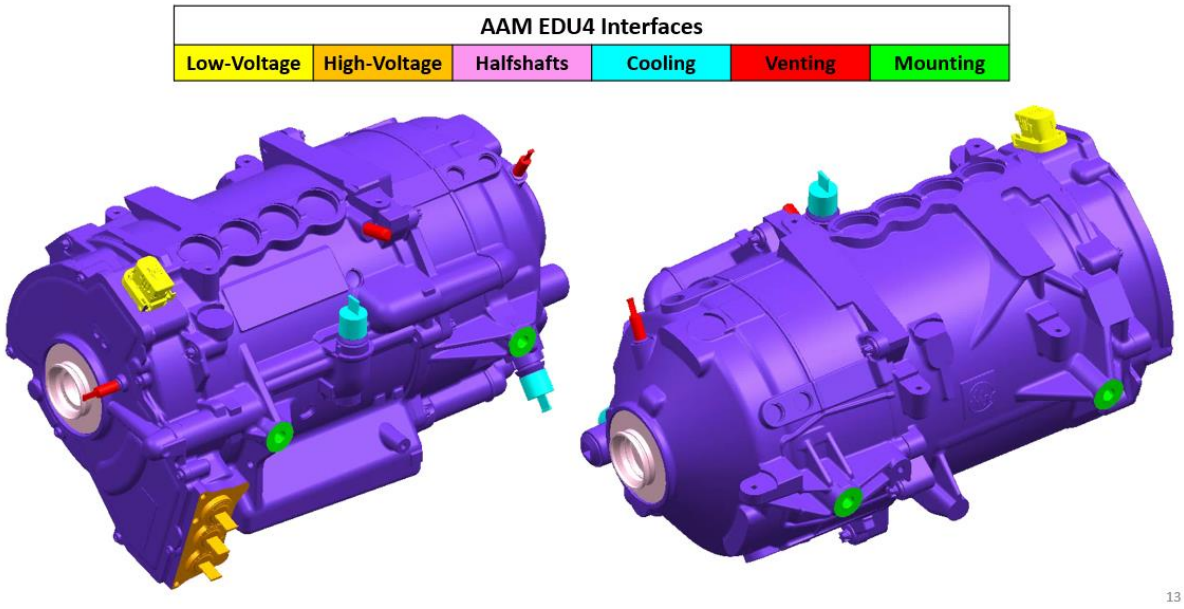

Figure 22: E-axle interfaces, colour-coded by type

Next was the orientation. Although the e-axle is relatively consistent in its shape of a large cylinder, there are some odd protrusions, such as the HV connector interface, as shown in Figure 22. As such, it may be ideal for packaging to orient the e-axle in a specific direction. Unfortunately, the e-axle's vertical orientation as well as the orientation of its forward axis for drive were defined by the AAM, and therefore the orientation of the e-axle was fully fixed [115], as shown in Figure 23.

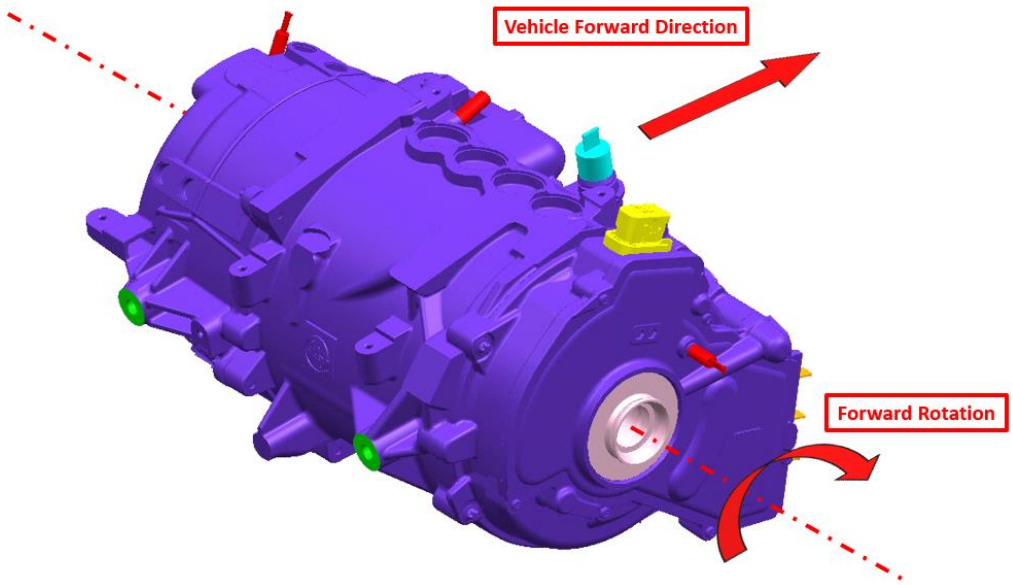

Figure 23: E-axle orientation, fixed by the supplier (AAM)

As the interfacing needs as well as the orientation of the e-axle were known, preliminary integration studies could be conducted. The stock rear cradle was used as a reference to ensure that there would be no interferences with the body or suspension hardpoints. With orientation of the e-axle fixed, the only remaining freedom with geometry was its location relative to the cradle.

First, was its position relative to the centre plane of the vehicle, which was rather quick to determine. Although the e-axle was relatively large, there was still ample space with the suspension hardpoints, as shown in Figure 24. As such, it was simply located at the centre of the vehicle, ensuring the halfshaft lengths were equal to minimize any left to right torque variation [116].

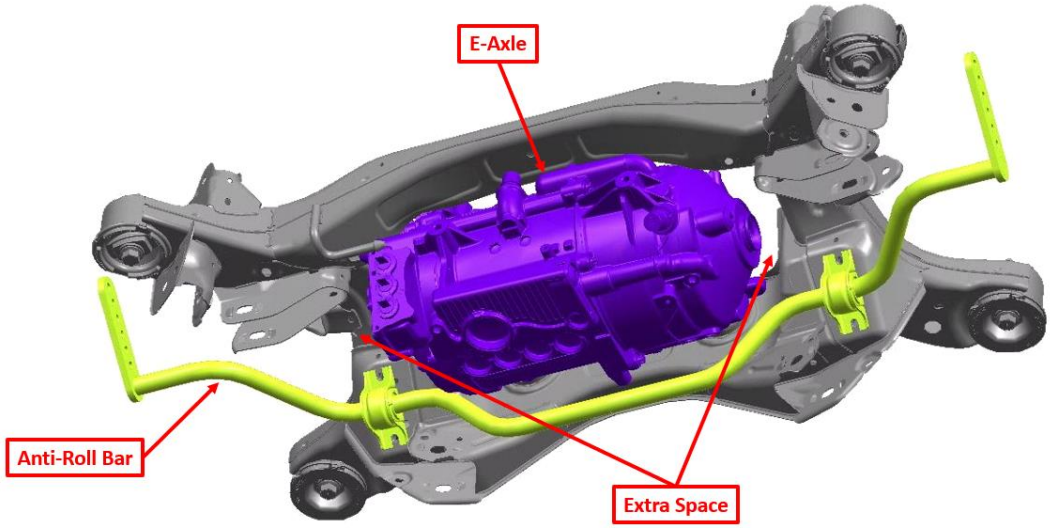

Figure 24: Left to right positioning of the e-axle, showing ample space on either side

Next was vertical positioning, which was also rather quick to determine. In this direction, the integration window was rather narrow, as shown in Figure 25. Any higher would impede on the body of the vehicle and any lower would impede on ground clearance. As such, vertical positioning was fixed as packaged.

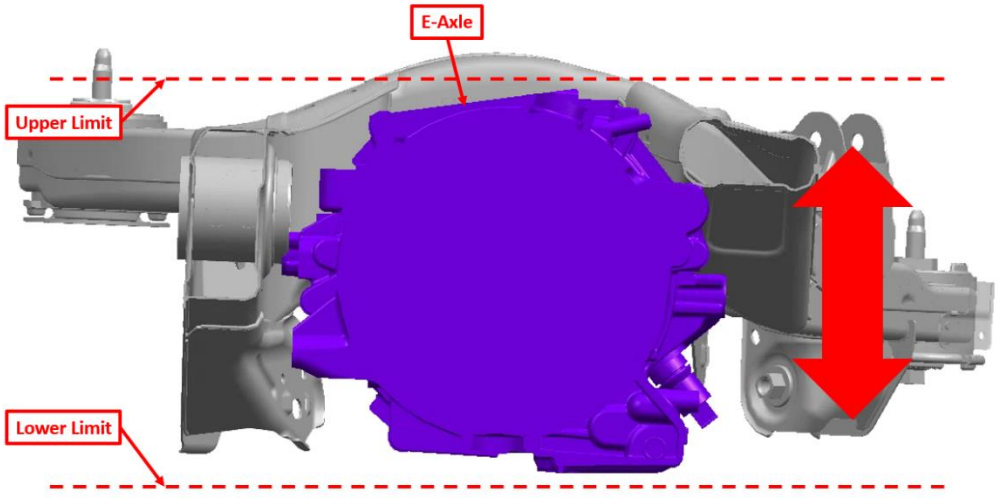

Figure 25: Vertical positioning of the e-axle, showing the narrow window for positioning as depicted with the dashed lines

Lastly was front to rear positioning. Once again, there was quite a bit of freedom in this, as pushing the e-axle forwards or backwards did not impede on body or suspension mounting points. Therefore, the e-axle was located such that the halfshaft angles were minimized for maximum efficiency [117], as shown in Figure 26.

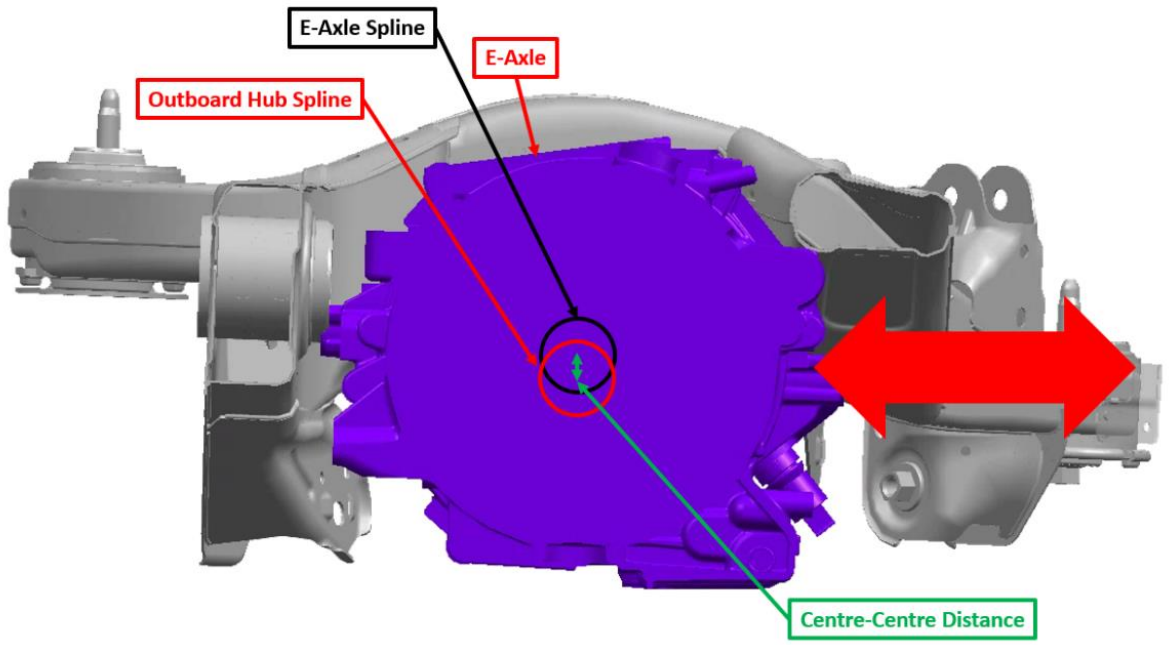

Figure 26: Front to rear positioning of the e-axle, showing the small distance between the e-axle and outboard hub spline centres in green

4.1.2 Clearance

As the e-axle positioning was finalized, the next step was to consider clearances to the e-axle. As mentioned in the previous section, ample clearance to all the e-axle interfaces were required for ease of maintenance as well as general installation. This would include not just ensuring no interferences between interfacing components and the cradle but also clearance for tools, fasteners, as well as general access by technicians. Tool clearance can be checked by using standardized tool clearance charts, an example of which is shown in Figure 27.

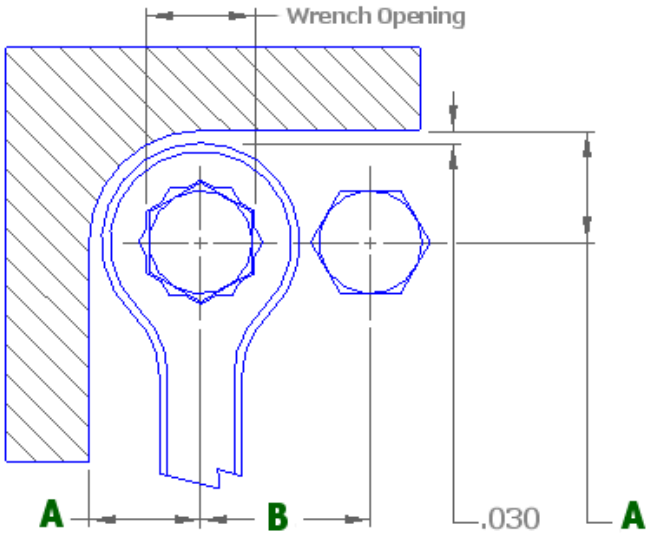

Figure 27: Example wrench clearance diagram with surrounding material in part [118]

Fastener and general access can be checked by looking at exploded views in CAD as well as taking general measurements to ensure ample hand access. However, clearance checking with the e-axle in its nominal position does not capture the full picture, as it is mounted through bushings. These bushings are made from rubber in order to isolate NVH transmission to the cabin. However, being made from such a flexible material also means that the e-axle can move nontrivial amounts relative to the cradle, which must be accounted for as it could cause temporary interferences with interfacing components. As shown in Figure 28, bushings are designed with a specific target stiffness and typically have voids to allow for movement. Bump stops are also present at the walls to provide a hard but cushioned stop as the bushing reaches the end of its travel [119]. Therefore, it was crucial that the e-axle be moved throughout the full range of bushing travel while checking for interferences between the e-axle, cradle, and all interfacing components in CAD.

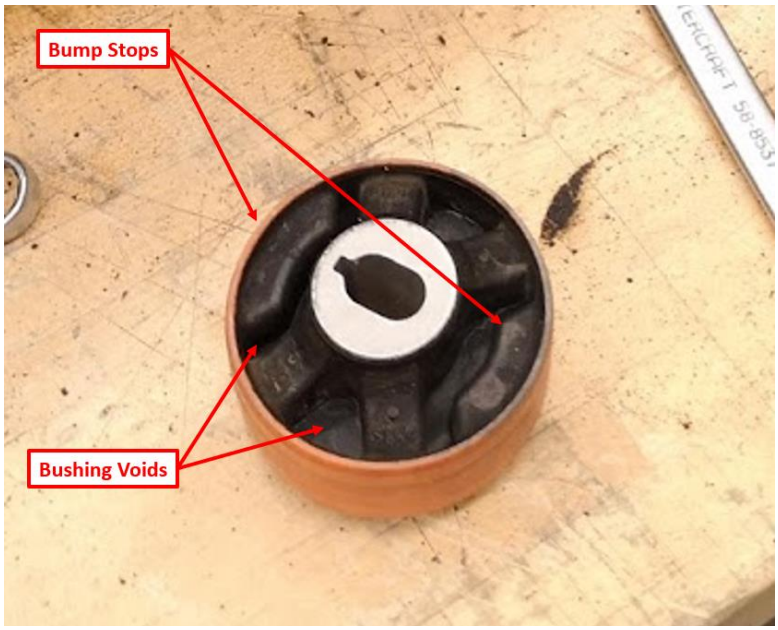

Figure 28: E-axle bushing, showing the voids for movement, and bump stops to limit

4.2 Other Structural Requirements

4.2.1 Strength

Although stress targets were defined as a result of fatigue calculations in Chapter 3, there were still other targets that had to be considered. As mentioned in section 2.5.3, the cradle must also meet 8g vertical and 20g horizontal loading, per NYSR H-3.6 [95]. Additionally, these requirements are under conditions with a safety factor of 1.5 while ensuring the structure does not undergo plastic deformation. In other words, the target stress can be calculated with equation 4.1, where σ_T is the target stress, σ_{YS} is the yield stress of the material, and SF is the safety factor.

$$\sigma_T = \frac{\sigma_{YS}}{SF} \tag{4.1}$$

Consequently, with a yield stress for Aluminum 6061-T6 of 276 MPa and a safety factor of 1.5, the resultant target stress was 184 MPa [120]. As the 8g and 20g loads were defined for propulsion system mounts, in the case of the rear cradle it was defined as the mount for the e-axle. The total

force was distributed equally amongst the four mounting points with this sum being defined by equation 4.2. F is the total force, m is the mass of the e-axle in kg, and n is the g-force multiplier.

$$F = m \text{ x } n \text{ x } 9.81 \qquad (4.2)$$

As the mass of the e-axle is 74 kg, with 8g and 20g loads this equates to 5,808 N and 14,519 N respectively. In summary, with these forces distributed amongst the mounting points, the calculated stresses in the new cradle cannot exceed 184 MPa.

4.2.2 Stiffness

Stiffness was another structural requirement for the rear cradle, though not officially defined as part of the cradle waiver process. As the rear cradle serves as the primary connection from the suspension members to the body, a certain level of stiffness to maintain suspension geometry as designed was needed. In fact, companies have developed special testing apparatus and procedures to measure suspension deflection throughout the full range of travel – these are known as Kinematic and Compliance (K&C) testers [121]. The suspension members essentially define how the wheels of a vehicle move relative to the body, and any flexibility in the system will cause the path of the wheel to deviate from what was designed. When designing a vehicle, system-level K&C targets are defined, which are then broken down into component-level targets [121]. Discussions with GM were held to obtain these values; however, due to NDA, these could not be listed in this document [37]. As a matter of fact, with the original modified cradle, deformations were negligible, especially since rubber bushings for NVH were the major contributor in compliances. However, defining this stiffness limit was still necessary in the case deformations were large, so GM defined the simple target of staying within 1 mm of deflection for all suspension hardpoints.

With respect to any structural component, defining stiffness targets can follow a similar thought process like the cradle. If excessive deflections are detrimental to the vehicle's operation, it would be necessary to investigate the degree of deflection permissible.

4.3 Manufacturing Requirements

With low-volume production parts, limitations with resources result in restrictions on the manufacturing methods that can be used. As the rear cradle was a one-off prototype build done by a student team, manufacturing methods were constrained. For example, it simply was not feasible to forge certain parts of the cradle, as forgings only make financial sense when mass produced due to the high initial startup cost [122]. Additionally, the team wanted to restrict cradle fabrication strictly in-house to keep costs low. Therefore, this section covers the manufacturing processes available to the team as well as the allowable cost.

4.3.1 Fabrication Methods and Limitations

To expand on the previous section, restricting fabrication to the tools available at the school was a decision made to minimize cost. However, manufacturing processes were not limited by this, as the school has quite the array of tools available in the machine shop. Table 7 lists the various manufacturing methods available for aluminum, marking down availability in the machine shop, as well as viability for low-volume production [123] [124].

Table 7: Availability and viability of various manufacturing methods, with 'X' marking the manufacturing methods that are available and viable

Method	Availability in-house	Viability for low-volume production
Hand Fabrication	X	X
Machining	X	X
Welding	X	X
Casting		
Forging		
Extruding		
Sintering		
3D Printing		X

It was evident that traditional manufacturing methods such as hand-fabrication, machining, and certain welding processes were both available and viable while casting, forging, extruding, and sintering were not. Metal 3D printing is a new, low-volume production technology capable of creating complex geometry with isotropic material properties [125]. However, it is an expensive process and outside help would be needed. Therefore, the manufacturing technologies used were restricted to fabrication, machining, and welding.

4.3.2 Cost

With producing one-off parts for a student team, cost was an obvious concern. Although the allowed manufacturing methods were defined, some of them were more expensive than others, so relying on high amounts of one method may not be viable. For example, heavy usage of CNC machining could drive costs up significantly such that it is no longer a sound financial decision to do so, given its potentially high cost [126].

After speaking with the project manager, the allocated funds for the rear cradle was $3,000 Canadian, based off the team's budget for all projects. To keep costs low, CNC machining would only be done as necessary, and the students could hand-fabricate or manually machine parts. As the designs were iterated, shop technician hours were accounted for, with the cost of the final design estimated through labour hours and hourly rates.

Chapter 5
Topology Optimization

At this point, with the requirements for strength, stiffness, manufacturing, and cost defined, it was possible to start design. The first step of this process was topology optimization, which uses FEA to determine the most efficient structure of a component given design spaces, input loads, and boundary conditions. At its core, the input loads and boundary conditions result in a stress and strain imparted on each element in the design space, and elements with high stresses and strains are highlighted whereas those with low values are not [127]. This tool allows the designer to minimize mass while still meeting the design requirements of the part. However, as the outputs are directly tied to the solver's inputs, it is important to ensure that the input conditions are carefully chosen and set. Figure 29 and Figure 30 show a topology optimization example of a brake pedal, where the orange areas are the design spaces where the solver is allowed to iterate, and the grey areas are the non-design spaces that cannot be modified.

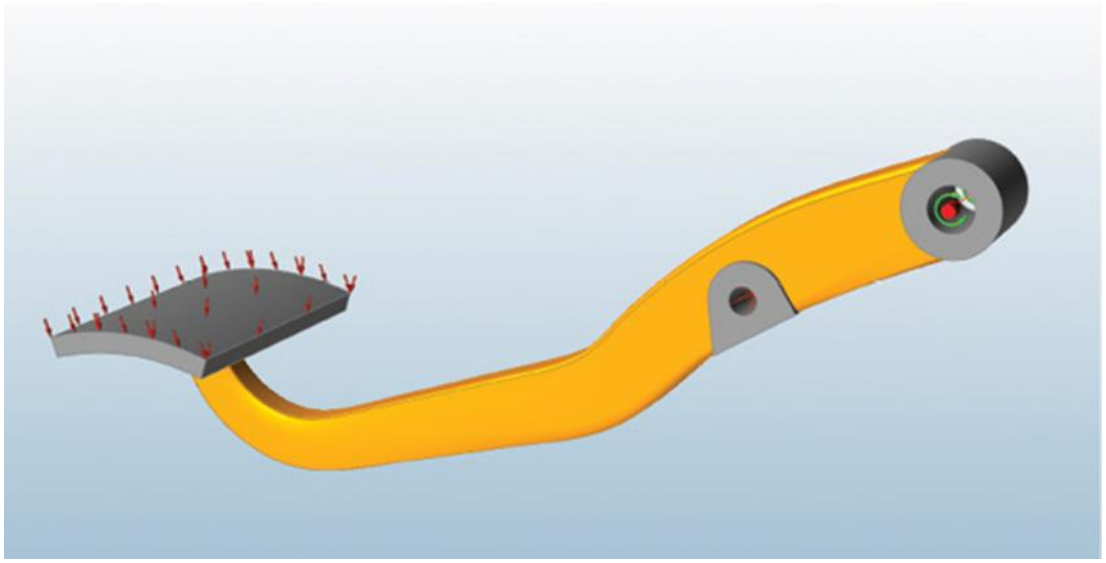

Figure 29: Topology optimization design space example setup, with orange as the design space, and grey as the non-design space [127]

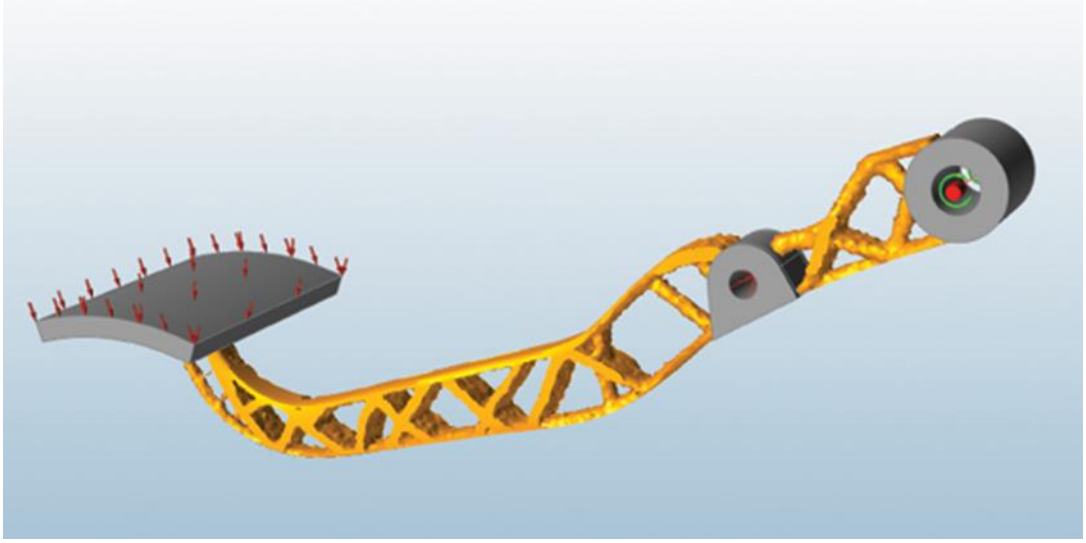

Figure 30: Topology optimization example result, with orange as the design space, and grey as the non-design space [127]

The software used for pre- and post-processing was Altair Hyperworks, which is one of the most common structural analysis tools available [128]. The solver was Optistruct, which is from Altair and included with the team's sponsorship with that company. All in all, the software used for analysis is one of the most common in the industry and can be very powerful in the right hands.

5.1 CAD Geometry

The first step in creating a CAD model of the design spaces for the cradle was to compile all the hardpoints of the suspension and driveline. These points defined the locations for all of the suspension members and e-axle. Bushing and fastener mounting geometry were replicated in CAD and positioned in exactly the same spot as those on the existing cradle. Figure 31 shows the 2019 cradle in magenta as reference, with the replicated geometry in grey. The resultant full replicated CAD geometry is shown in Figure 32, which represents the non-design spaces that all interfacing components attach to.

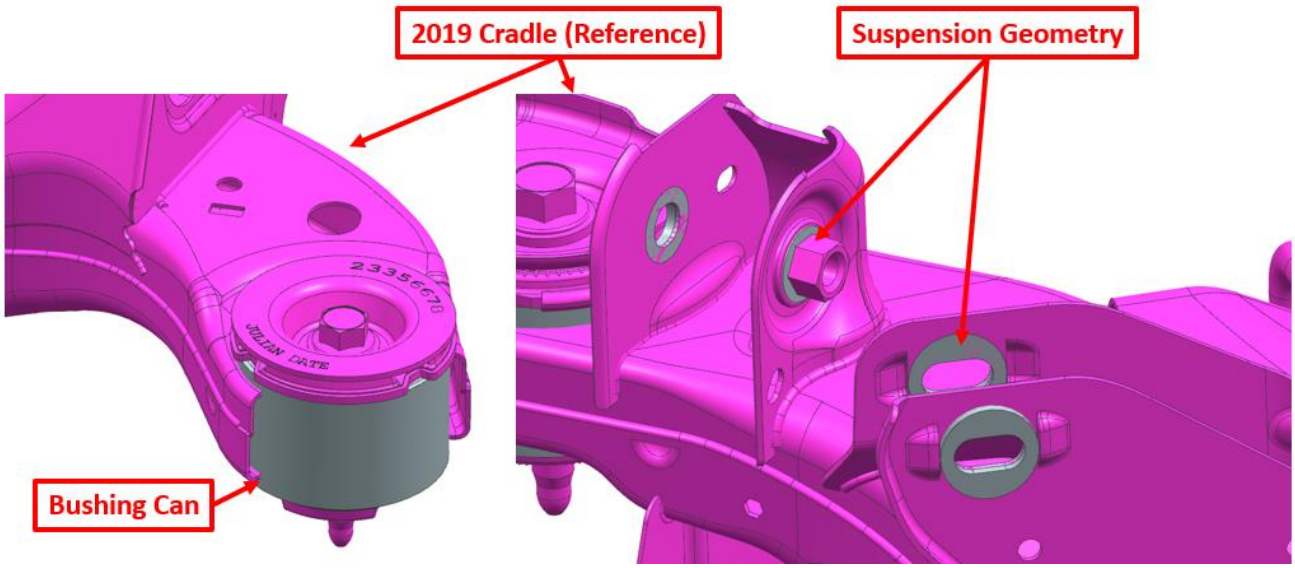

Figure 31: Replicated bushing can and suspension geometry in grey, and 2019 cradle for reference in magenta

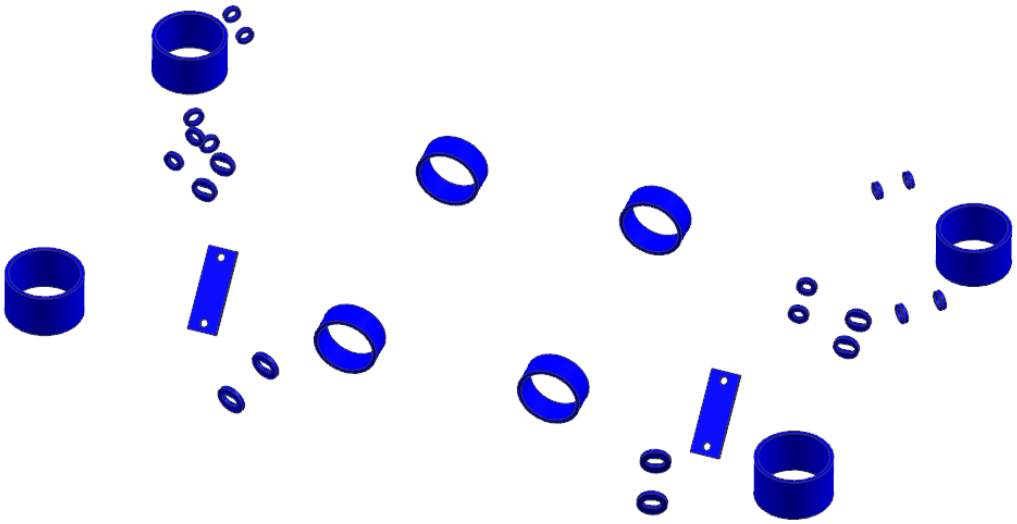

Figure 32: Resultant non-design space CAD geometry, showing the suspension, e-axle, and body bushing attachment points

The next stage, along with where the majority of the work lied, was to create the design space. As the design space dictated where material can be placed, it must not interfere with the e-axle, the body, or any of the suspension components.

The first step was to create simplified solid models, which would represent the geometry of each of these components and where the "keep-out" zones for the design space is. For example, the e-axle could be simplified into a large cylinder plus a few other small shapes attached onto it, as shown in Figure 33. In many cases, these keep-out zones were significantly larger than their actual part, for example in Figure 34 the diameter of the zone is 120 mm, when the actual size of the shaft is 28 mm. This was done to allow for sufficient clearance with surrounding components and articulation, as some of these components move with the wheel.

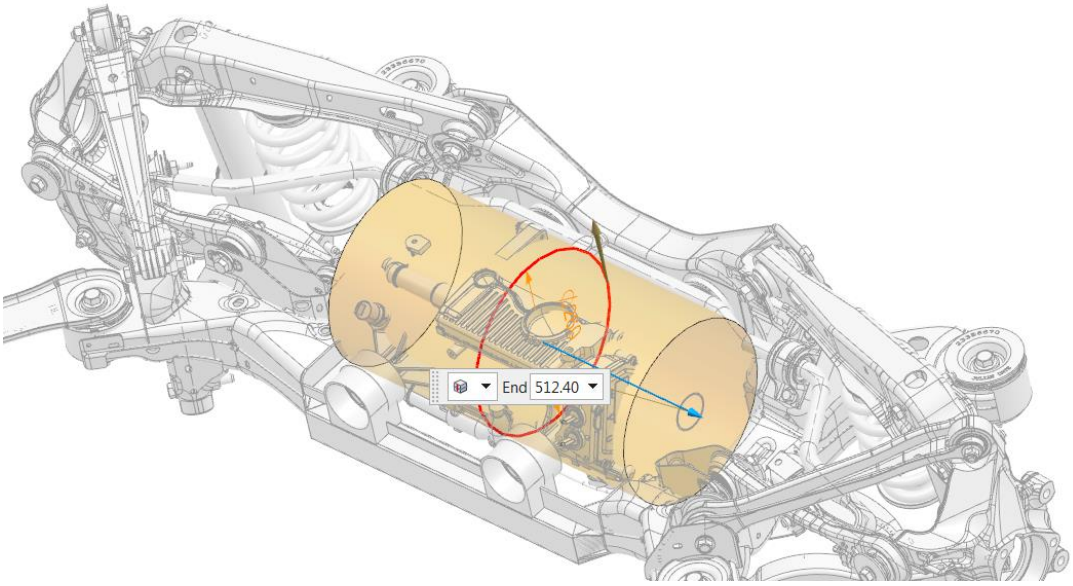

Figure 33: E-axle keep-out zone in orange, with all associated components shown in grey

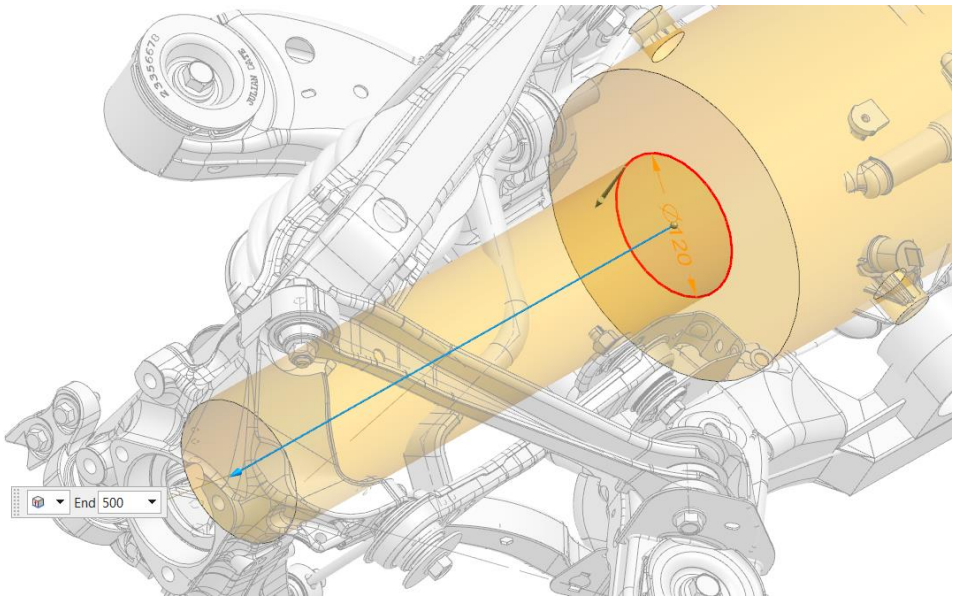

Figure 34: Halfshaft keep-out zone in orange, with all associated components shown in grey

Another consideration for these large keep-out zones was to allow for installation – for example, to allow for the e-axle to assemble into the cradle, the bottom of the cradle has to be open to facilitate this. Therefore, a very tall zone was established, to prevent any material from being placed underneath the e-axle, as shown in Figure 35.

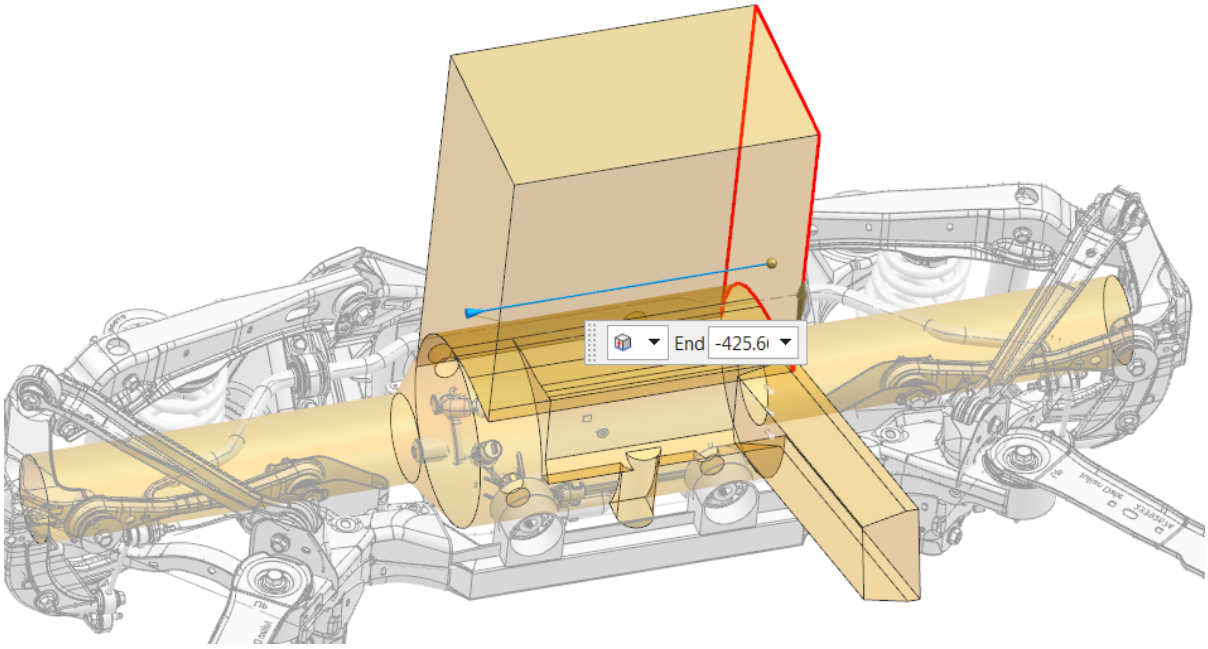

Figure 35: Vertical keep-out zone for e-axle assembly into the cradle in orange, with all associated components shown in grey

The next step was to use CAD to create similar zones for the suspension members. As the suspension members move with wheel travel, these zones must account for that and be designed accordingly. An example is shown in Figure 36, where it can be observed that the zone widens to the left to allow for clearance as the toe link pivots. Keep-out zones for all suspension member on one side is shown in Figure 37.

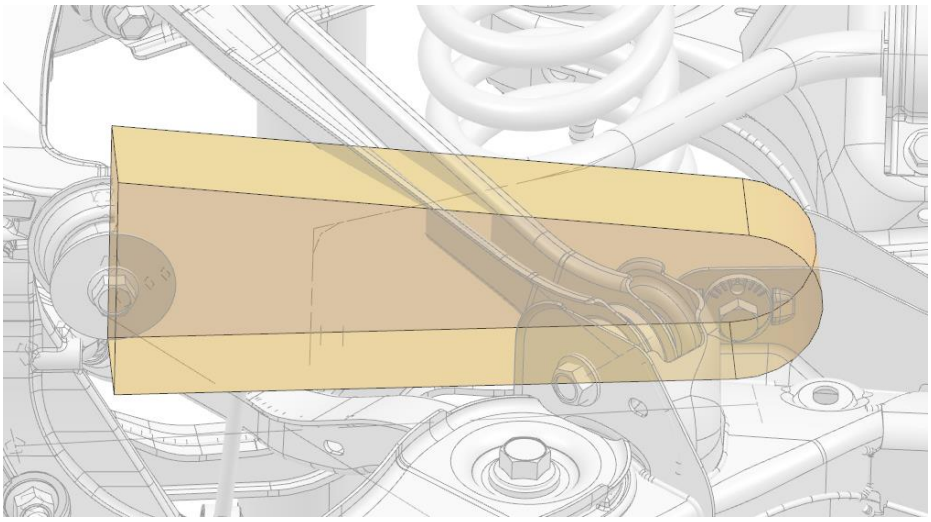

Figure 36: Keep-out zone for left toe link in orange, with all associated components shown in grey

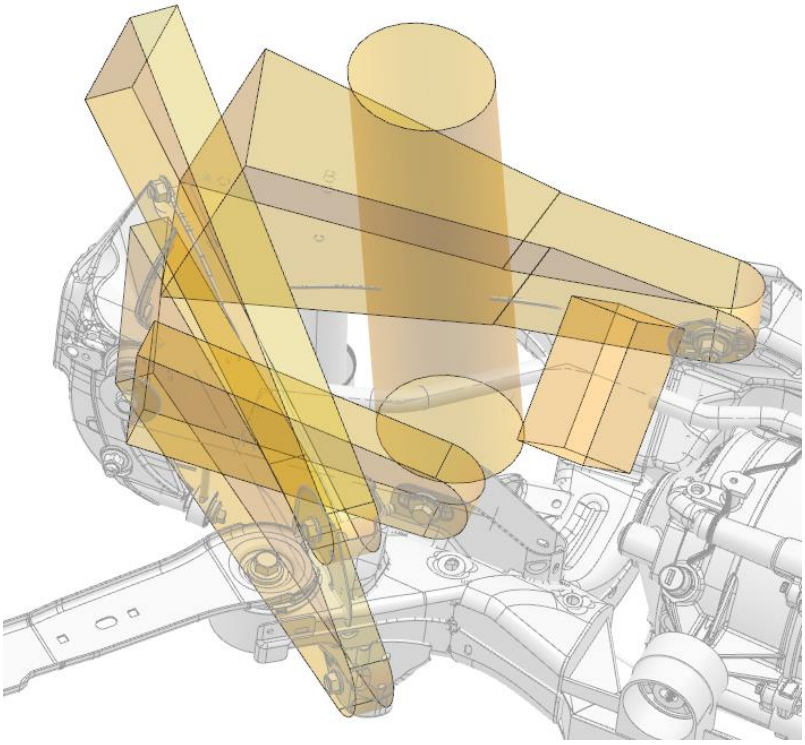

Figure 37: Keep-out zones for left-side rear suspension in orange, with all associated components shown in grey

At this point, all of the keep-out zones were complete. The next step was to use CAD to create a box that would form the basis for the design space. This box was designed such that each of the corners were at the bushings for the chassis and had similar height to the existing cradle. Figure 38 shows the orange design space box, with the original rear cradle in magenta, along with the e-axle and suspension components in dark grey.

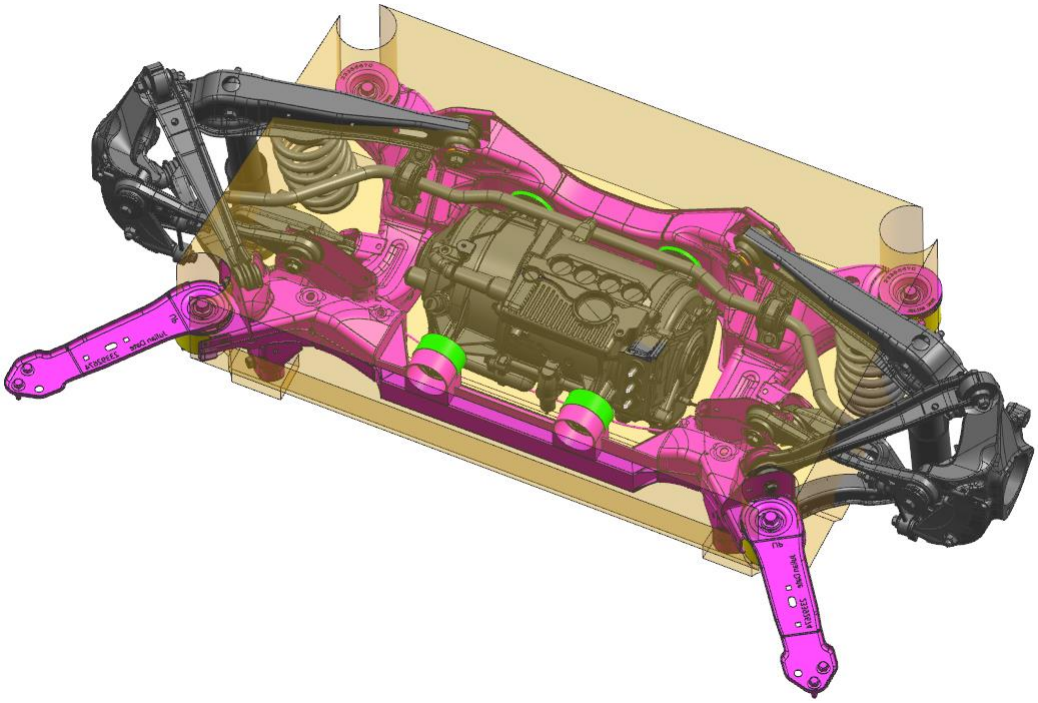

Figure 38: Isometric view of orange design space box, with 2019 cradle in magenta, and all associated components in grey

Showing all bodies resulted in what is shown in Figure 39. Taking all the keep-out zones and subtracting them from the design space box results in the shape shown in Figure 40.

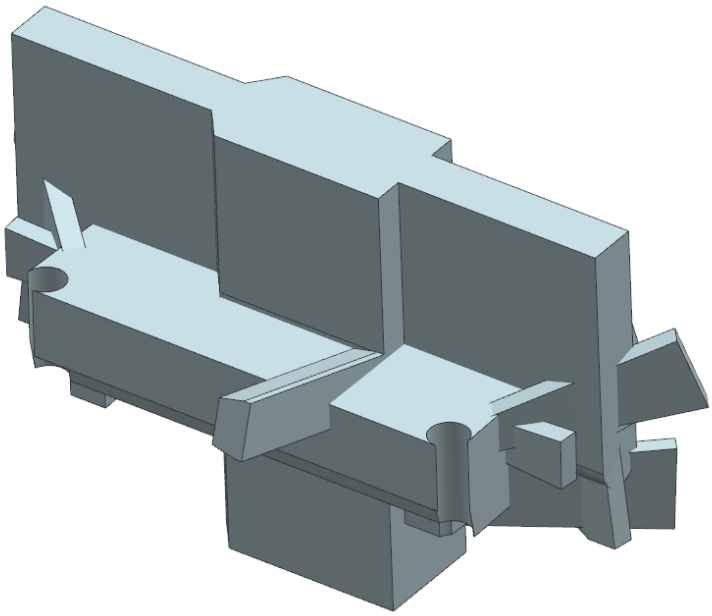

Figure 39: All compiled bodies shown for design space, before subtraction

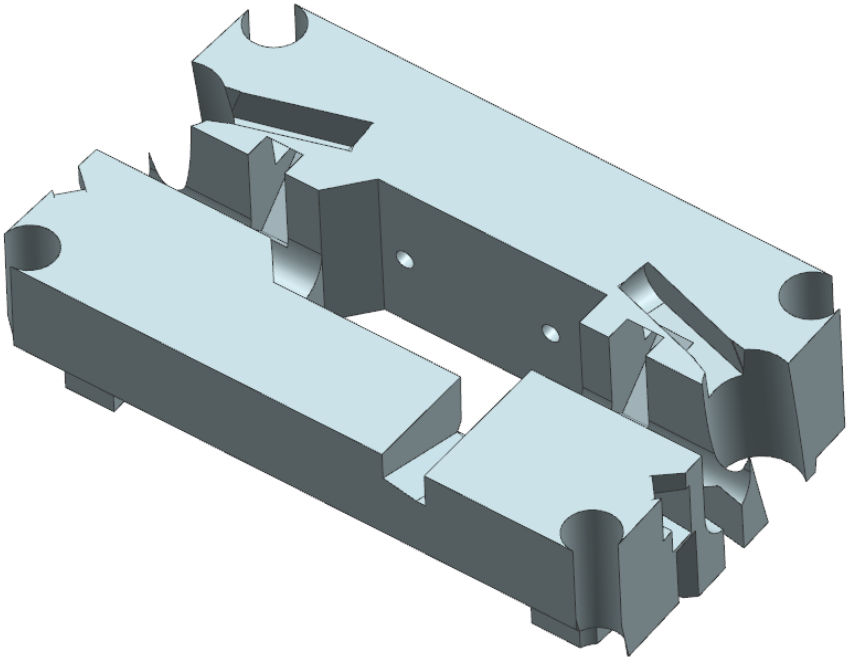

Figure 40: Completed preliminary design space, obtained from subtracting the keep-out zones from the design space box

Careful inspection of the preliminary design space reveals sufficient clearance around the e-axle, halfshafts, and suspension members. However, there were still small details missing, such as missing holes for bushing and fastener access, as shown in Figure 41.

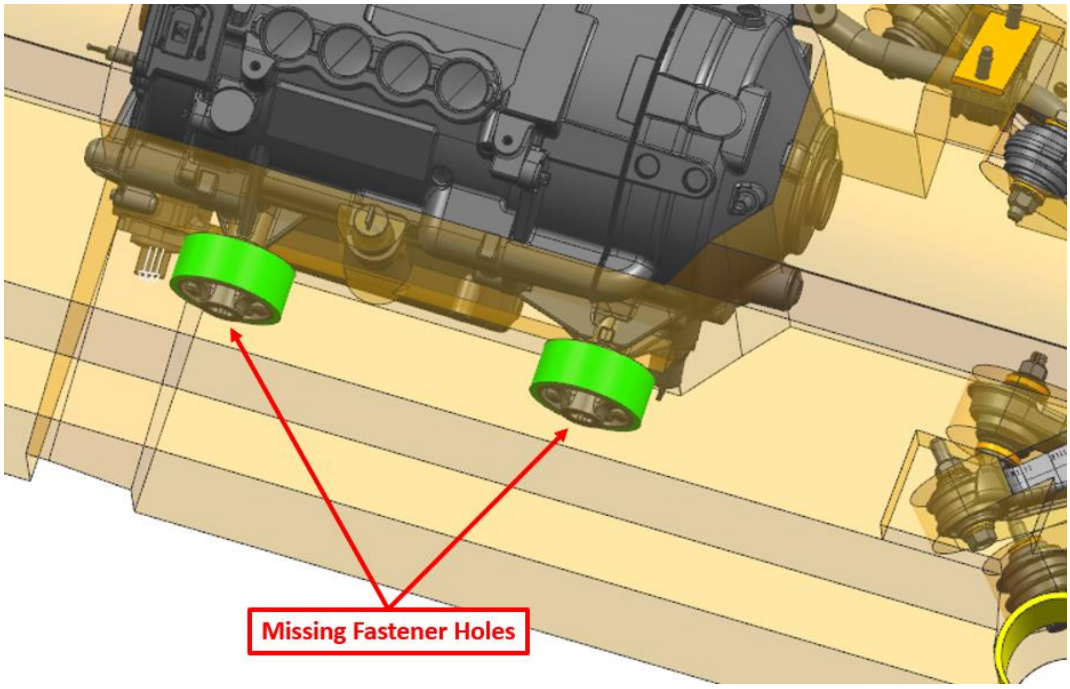

Figure 41: Missing holes for e-axle mounting fasteners, with the orange design space and green bushings for reference

After adding these holes and checking that the design space did not interfere with any surrounding components, CAD was complete, and FEA could commence. The complete CAD assembly is shown in Figure 42, where the design and non-design spaces are orange and blue, respectively.

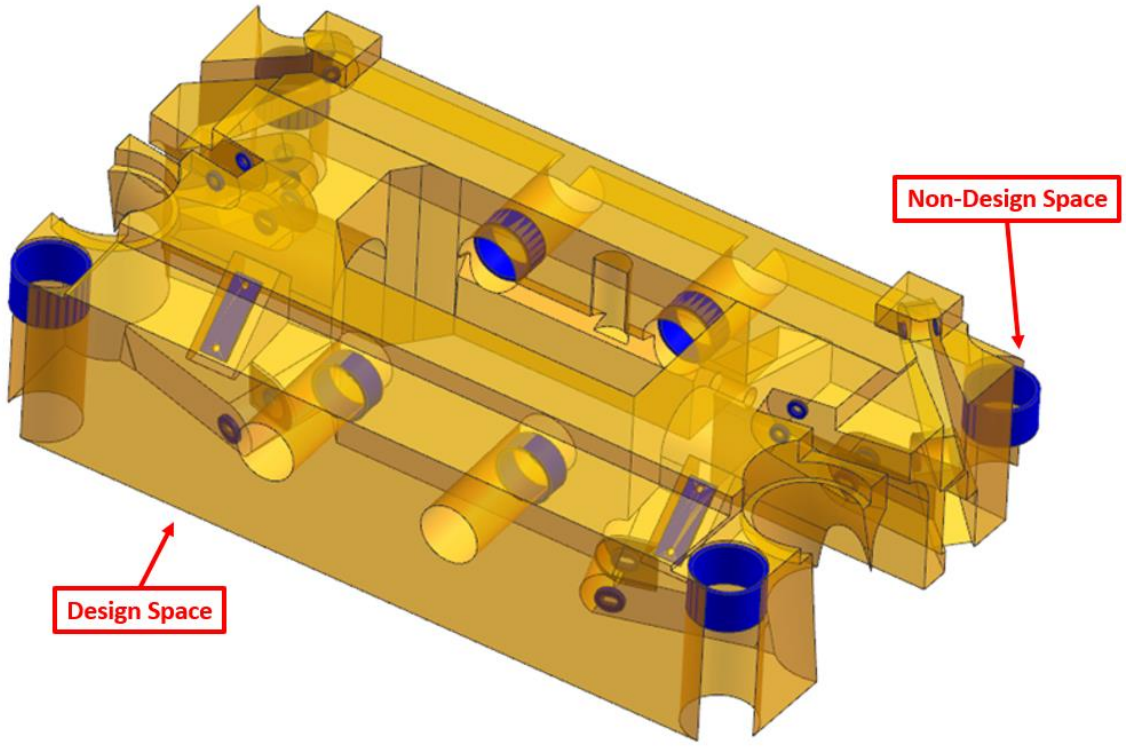

Figure 42: Completed CAD assembly, with the design space in orange, and non-design space in blue

5.2 Initial Model Setup

5.2.1 Meshing

The next step was to import the CAD assembly into HyperWorks. Organization was key with using HyperWorks, thus all CAD bodies and surfaces were organized into two component collectors, design and non-design spaces, similar to how the CAD assembly was organized. Firstly, the non-design spaces were meshed, following GM modelling guidelines for meshing quality and size, as shown in Figure 43 and Figure 44 [129].

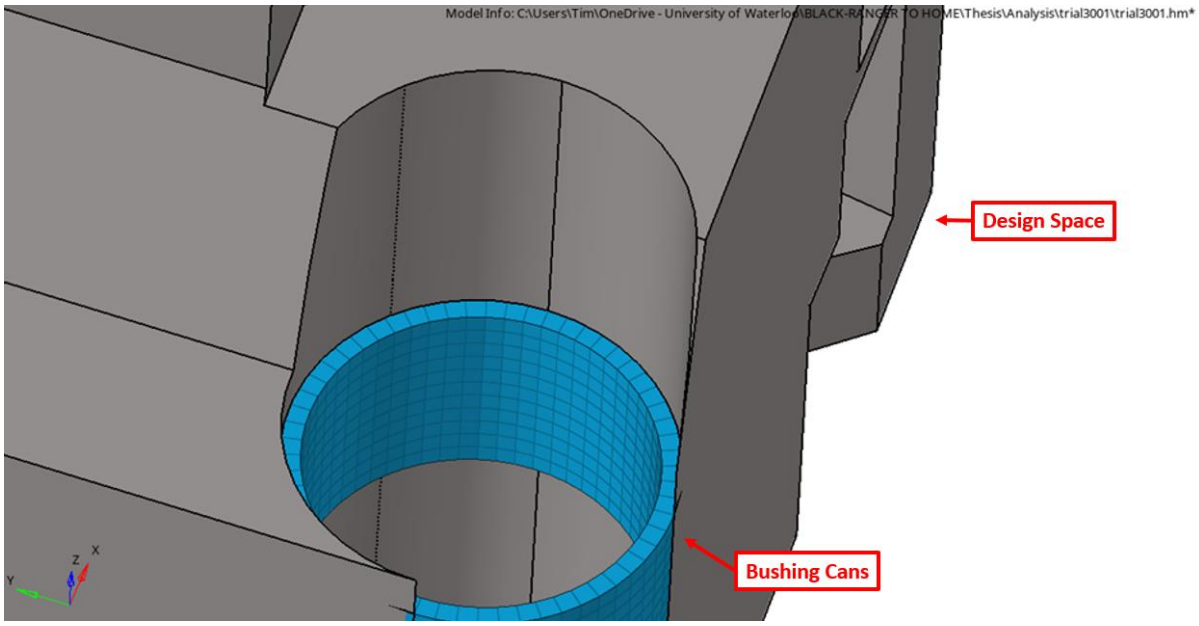

Figure 43: Meshed bushing can in blue, and design space geometry in grey

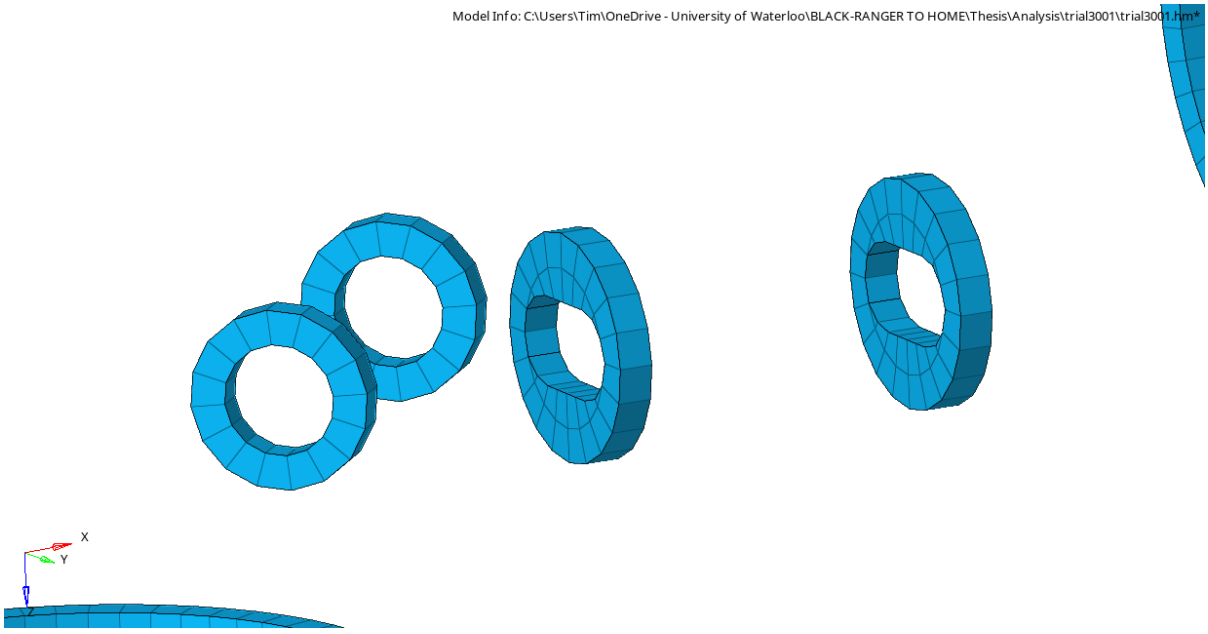

Figure 44: Meshed suspension mounts in blue

Next, the design spaces were meshed, while ensuring the nodes facing the non-design spaces were coincident to ensure transfer of loads between the two, as shown in Figure 45. The full mesh of the design and non-design spaces are shown in Figure 46.

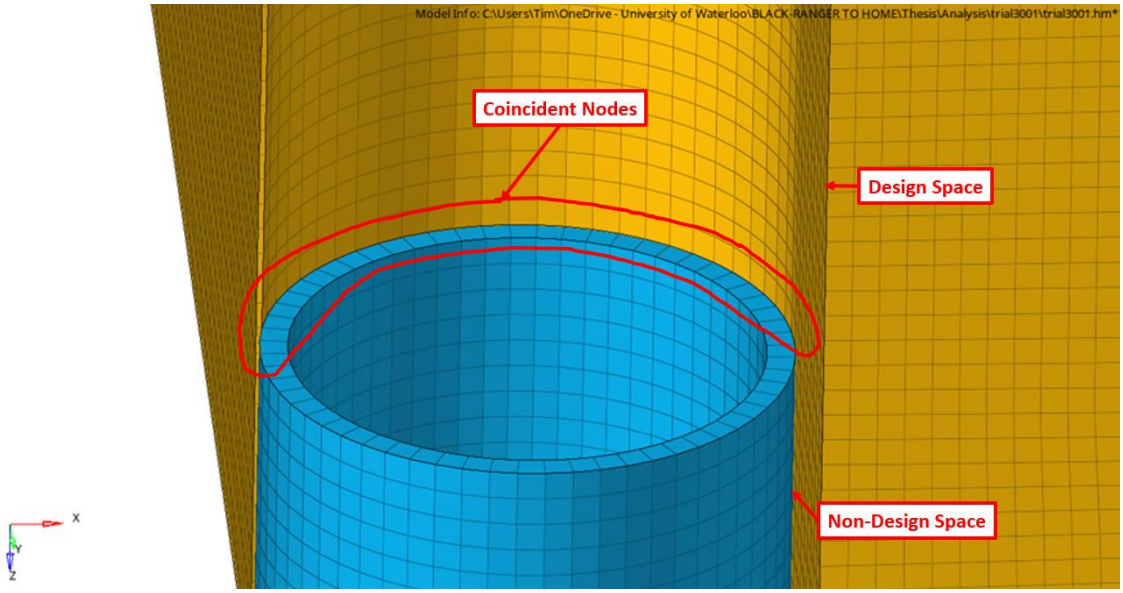

Figure 45: Ensuring coincident nodes between the non-design space in blue, and design space in orange

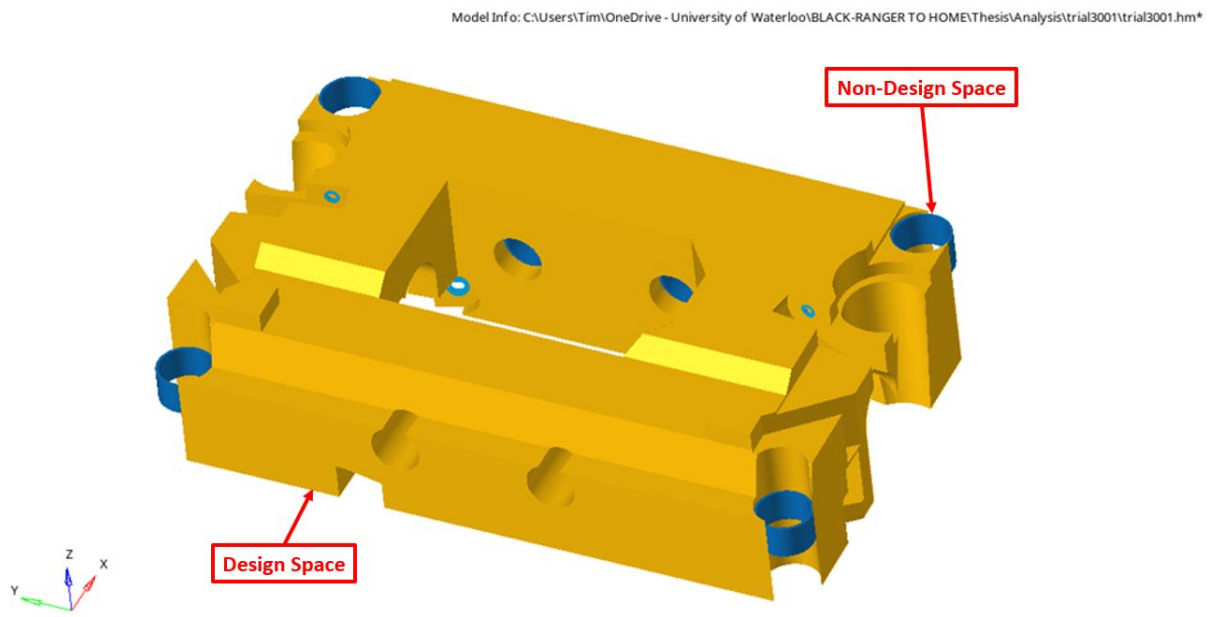

Figure 46: Meshed design and non-design spaces in orange and blue respectively

Lastly, rigids were required, to facilitate input of loads from loadcases to the structure. These were done by creating a point at the geometric centre of the body, suspension, and e-axle mounting points, and rigidly connecting them to the adjacent non-design nodes. This is a fairly common practice with mesh setup, which is also mentioned in GM modelling guidelines [129]. Figure 47 shows this, where the rigids are in red, and the non-design spaces are in blue. The completed mesh is shown in Figure 48.

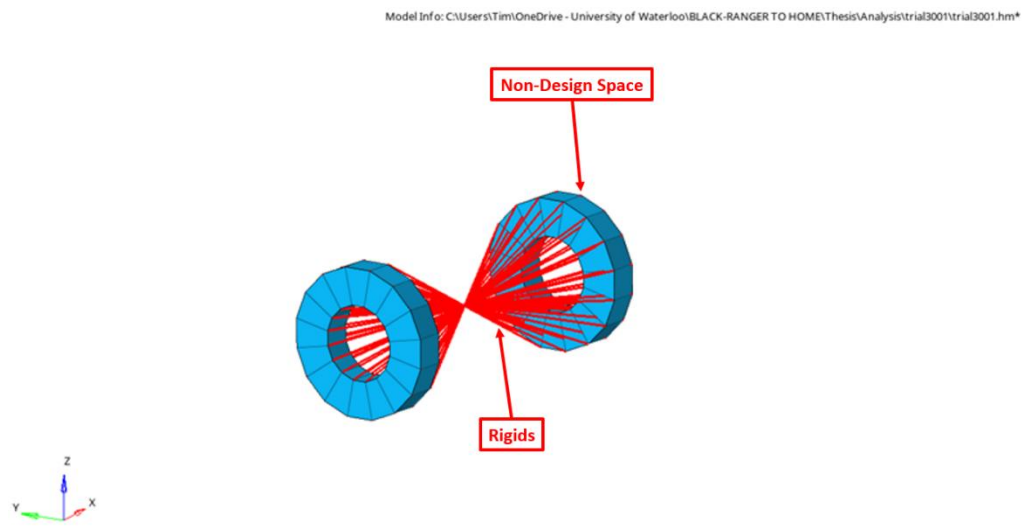

Figure 47: Rigids in red, tying into suspension hardpoints in blue

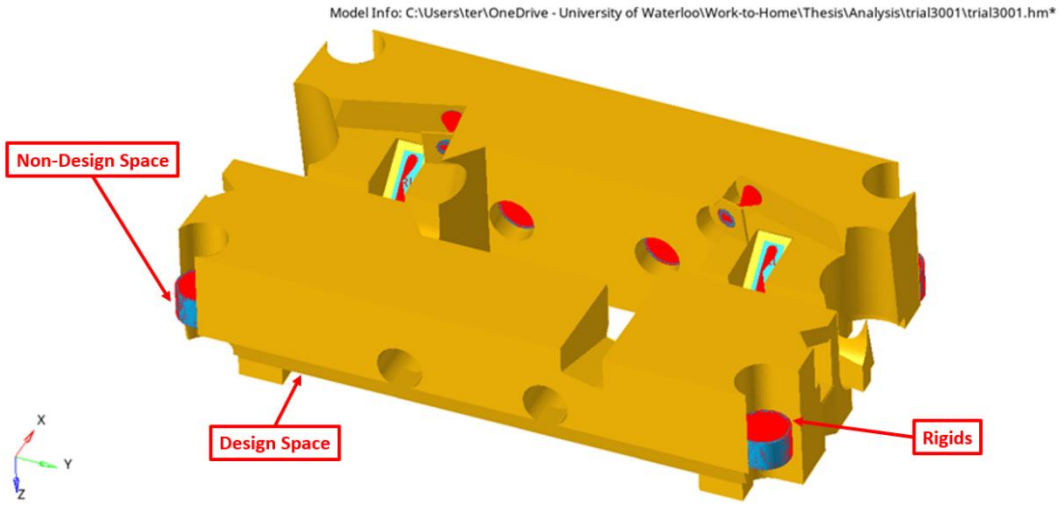

Figure 48: Completed mesh, showing the design space, non-design space, and rigids in orange, blue, and red respectively

With all the elements in the mesh, it was then possible to move onto setting other parameters necessary for the analysis.

5.2.2 Material and Optimization Targets & Constraints

After meshing, there were other inputs to the model that were required for it to run. Firstly, a material needed to be defined, in this case aluminum, as previously mentioned. As this is a simple linear static analysis, the only properties required were a Young's Modulus of 69 GPa, Poisson's ratio of 0.33, and density of 2700 kg/m3 [120].

Next, optimization targets and constraints needed to be set. Optimization targets define what the end goal of the analysis is, and constraints define set boundaries in which the defined property cannot exceed. In this case, the only target was to minimize mass, as it was expected that deformations in the hardpoints would be negligible, because there are rubber bushings which have significantly lower stiffness than the cradle itself. The constraints were set to a maximum global stress level for each of the 9 loadcases corresponding with the values set by the fatigue calculations in Chapter 3.

5.2.3 Loads

After materials and optimization, loads for both components needed to be defined. The loads were simply taken from the provided GM model, which was not totally accurate given the significant increase in weight of the vehicle. However, after consultation with GM, the way the waiver process was defined by rules means that passing the waiver with these loads would result in a cradle that is structurally sound and safe for competition [32].

Another concern with loads were input loads to the cradle, imparted as a result of reaction loads from the e-axle. Taking these reactions into account must be done, as they were not negligible. As a matter of fact, the stock vehicle had a rear differential as shown in Figure 49, which input loads to the rear mounts on the cradle that had to be removed, as shown in Figure 50.

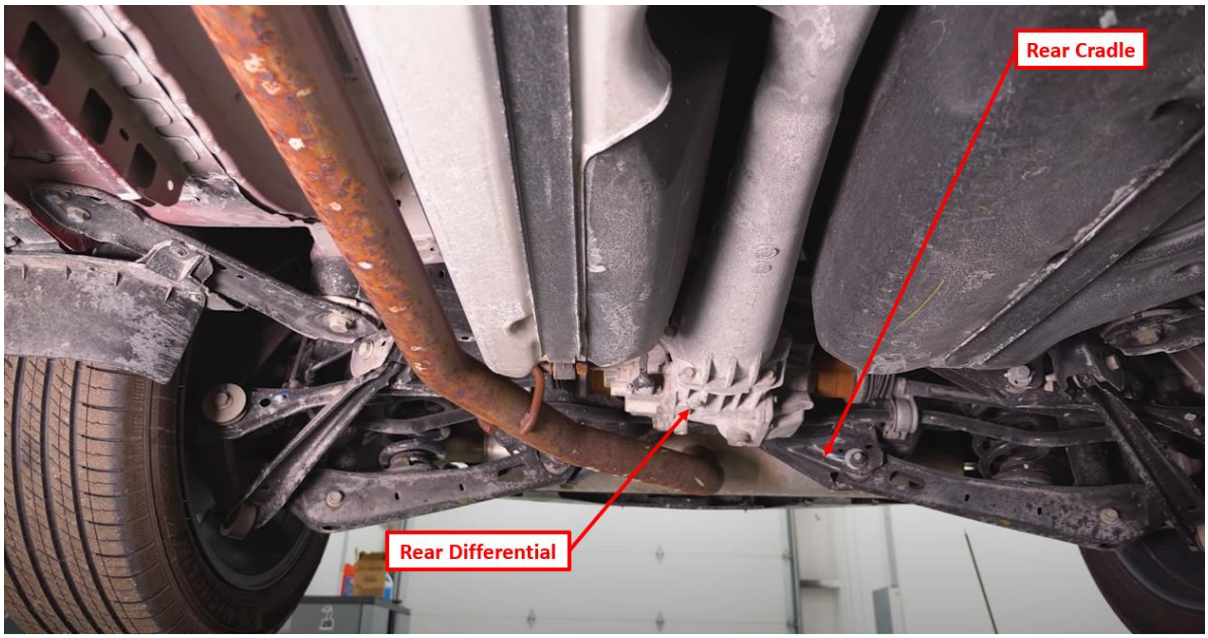

Figure 49: Stock rear differential and cradle in 2019 Chevy Blazer [130]

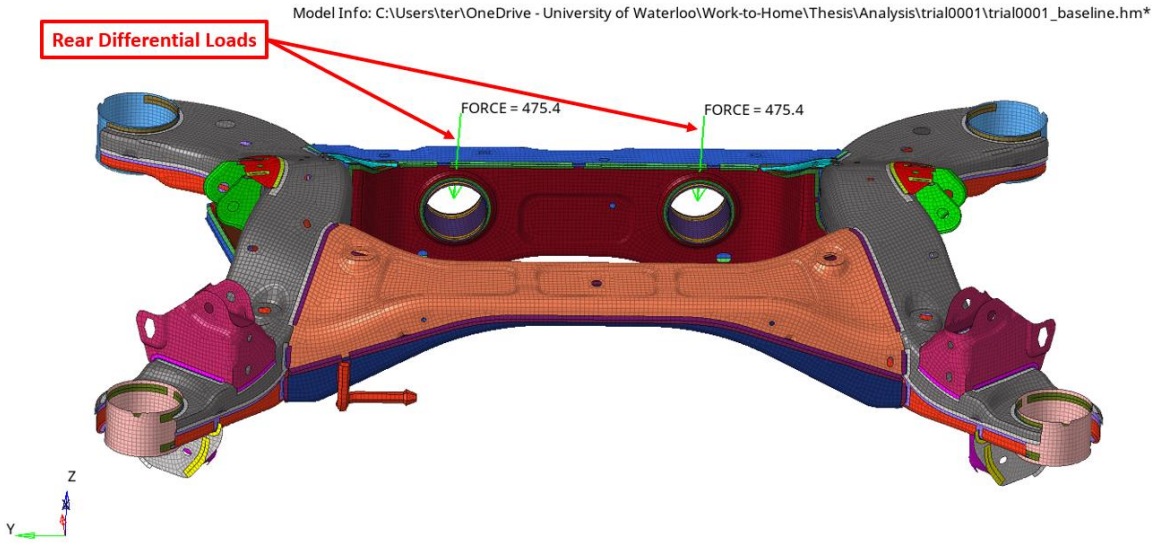

Figure 50: Added loads from rear differential to stock cradle

The first step with calculating the input loads to each of the mounting points for the e-axle was to consider what each of the loadcases represent. The 2-wheel bump case represents going over a

speed bump or railroad tracks. From research, it was determined that maximum vertical accelerations typically do not exceed 2g, therefore this value was used [131]. Driving over speed bumps or railroad tracks are typically done at a consistent speed, so no other accelerations were needed. Next were the twist loads, which represent entering or exiting a driveway. Once again, this is done at typically low speeds, with minimal acceleration, so only 1G vertical load was needed due to gravity.

The braking, cornering, and accelerating loadcases were different. A typical SUV can get close to, but not exceed 1g for each of the three loadcases, so these values were used as a conservative estimate for all [132]. However, with acceleration and braking, there is additional load due to torque output from the e-axle, either from full forward thrust or maximum regenerative braking. The forces at each of the mounting points were calculated by taking the peak torque of the e-axle at the output shafts and dividing it by the moment arm length to the centres of each mount. A summary of the added loads from the e-axle are listed in Table 8, and Figure 51 is a diagram that shows the added loads from the forward acceleration loadcase. Detailed calculations are included in Appendix A.

Table 8: Added loads from e-axle

Loadcase	E-axle Loads
2 Wheel Bump	2G vertical bump
Twist LH	1G gravity
Twist RH	1G gravity
FWD Braking	1G gravity + 1G decel + 351 Nm rev motor torque loading
REV Braking	1G gravity + 1G accel + 351 Nm fwd motor torque loading
Cornering LH	1G gravity + 1G LH cornering
Cornering RH	1G gravity + 1G RH cornering
FWD Accel	1G gravity + 1G accel + 351 Nm fwd motor torque loading
Rev Accel	1G gravity + 1G decel + 351 Nm rev motor torque loading

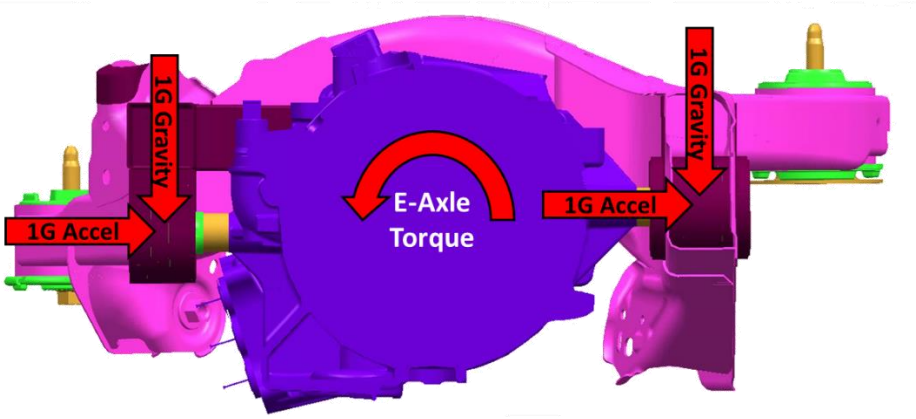

Figure 51: Side view diagram showing all the e-axle loads due to forward acceleration

To minimize computation time, the 8g and 20g loadcases as required by competition rules were excluded from the optimization. During the design phase of the 2019 cradle, it was observed that resultant stresses from these loadcases were an order of magnitude lower than the stresses due to the GM loadcases. Therefore, it was assumed that the ideal design for the GM loadcases would have minimal issues with passing the 8g and 20g loadcases, and thus these were not needed for optimization.

5.3 Initial Results

With all the inputs for the topology optimization defined, it was at this point the first analysis study could be conducted. A couple things to note are the intricacies of the solver and the results. The topology optimization method utilized was the element density method, which essentially varies the density of the material according to where it should ideally be placed. As such, the resultant shape was extracted by only plotting above certain element densities, and the colours represent the densities of the displayed [133]. Results from the initial optimization are shown in Figure 52.

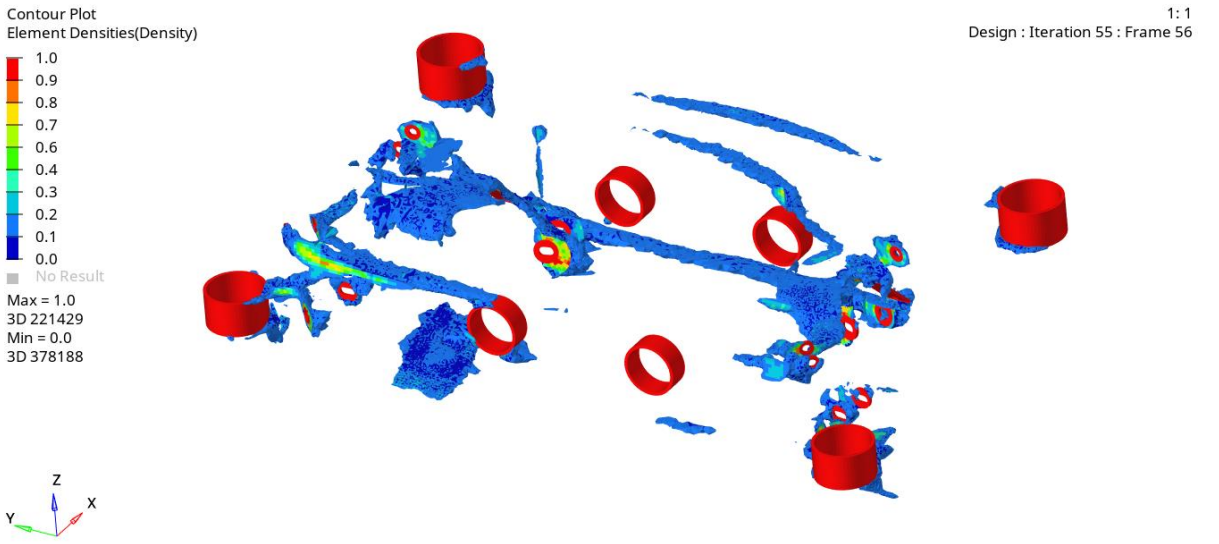

Figure 52: Initial topology optimization results, showing element densities >0.15

It was observed that the initial shape and element density plot results were not meaningful. Element densities were extremely low throughout most of the part, with the only high spots in areas adjacent to the non-design spaces. However, the primary issue was not having any connections between all of the separate non-design space bodies, so there is no clear visualization for the ideal load path for the most efficient structure for the GM loadcases. As such, some investigations needed to be carried out to check if there were other inputs or settings that could be changed to yield usable results.

5.4 Adjustments

There are numerous settings for topology optimization that allow a designer to target parameters such as mass minimization or stiffness maximization. Additionally, there are various settings to allow a designer to account for manufacturability, for example the draft setting in Optistruct prevents the software from producing geometry that may create undercuts that are hard to machine, as shown in Figure 53 [134].

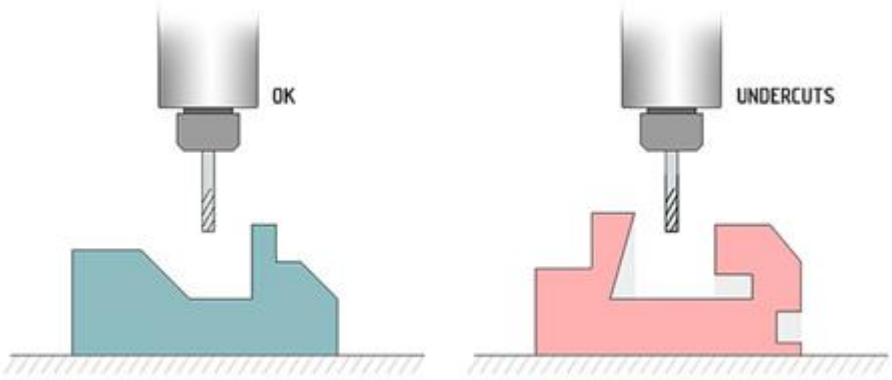

Figure 53: Example visualization showing difficulty of machining an undercut [135]

One of the first settings to be tweaked for the rear cradle was the minimum and maximum member size, which had a drastic positive effect. Setting a constraint on the size of members effectively tells the solver that groups of elements can only be together within that range, rather than distributing load throughout as many or as little elements as desired. This more closely reflects a fabricated part, where sheet or tube are joined together.

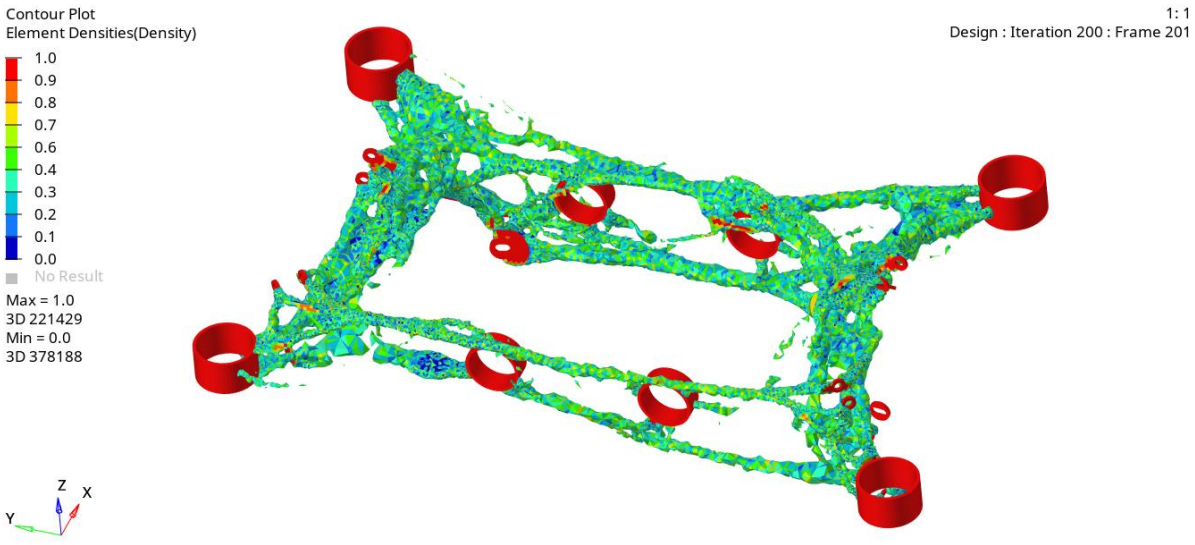

Figure 54: Revised results with member size constraint, showing element densities >0.35

Figure 54 shows the revised shape, as a result of adding member size constraints. As shown, the plot is a lot more meaningful, and in a form factor that could be fabricated. However, as observed in Figure 55, there were still connection issues between some of the e-axle mounts and the rest of the structure. This meant that there was little load transfer from the e-axle input loads to the cradle, so more revisions were needed.

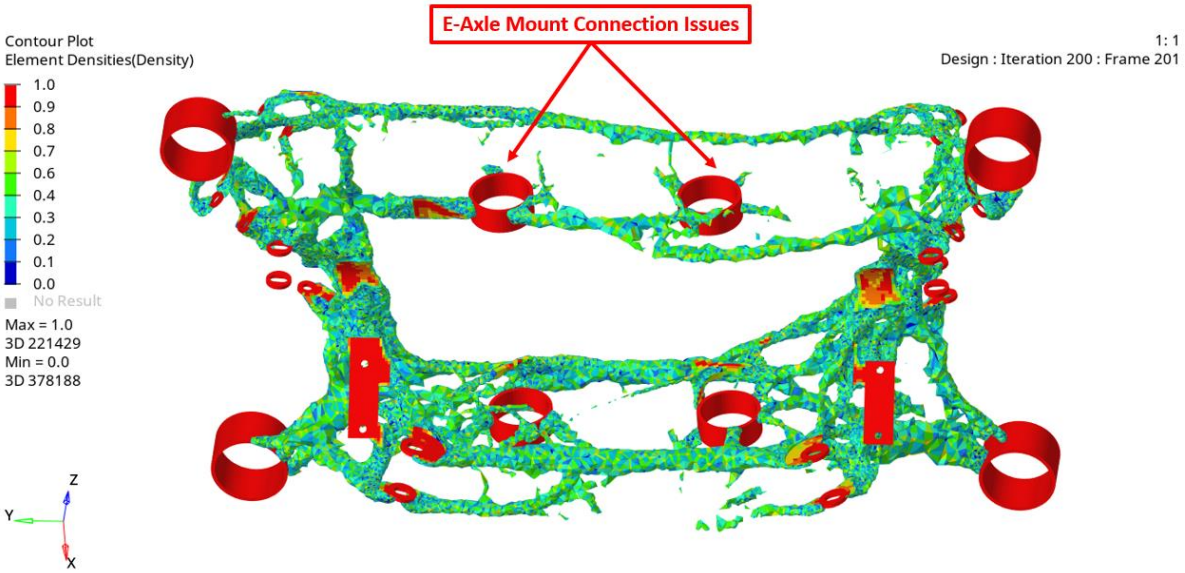

Figure 55: Disconnects from e-axle mounts to rest of structure

The next setting was to delete a few of the stress constraints. Since all nine GM loadcases were input, the solver has to compute for all loadcases, which takes a significant amount of computation time and makes it more difficult for the solver to arrive at a feasible solution. Therefore, only five of the nine loadcases with the lowest allowable stresses were retained, as highlighted in Table 9. It was expected that due to the difference in stress levels, the other four loadcases would not be as big of an issue to pass.

Table 9: Loadcases for optimization, with those retained highlighted in yellow

Loadcases	Max Stress (MPa)
2 Wheel Bump	185
Twist LH	127
Twist RH	127
FWD Accel	186
FWD Brake	186
Cornering LH	211
Cornering RH	211
REV Accel	201
REV Brake	201

The last thing to do was to account for the 8g and 20g loads, as shown in Figure 56. As mentioned, there were connectivity issues from the e-axle mounting points to the rest of the structure, so doing this would hopefully alleviate this issue.

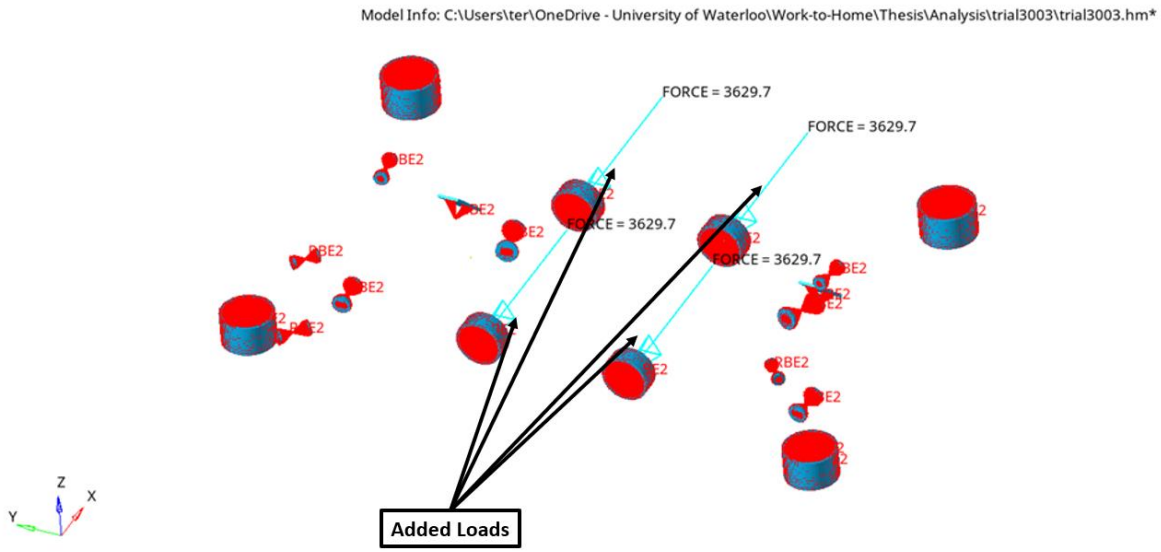

Figure 56: Added 8g and 20g loads to the e-axle mounting points

5.5 Final Result

With all of these changes applied, the analysis was re-run, and the results are shown in Figure 57. It was apparent that all the settings applied resulted in a shape that logically made sense and was potentially useful.

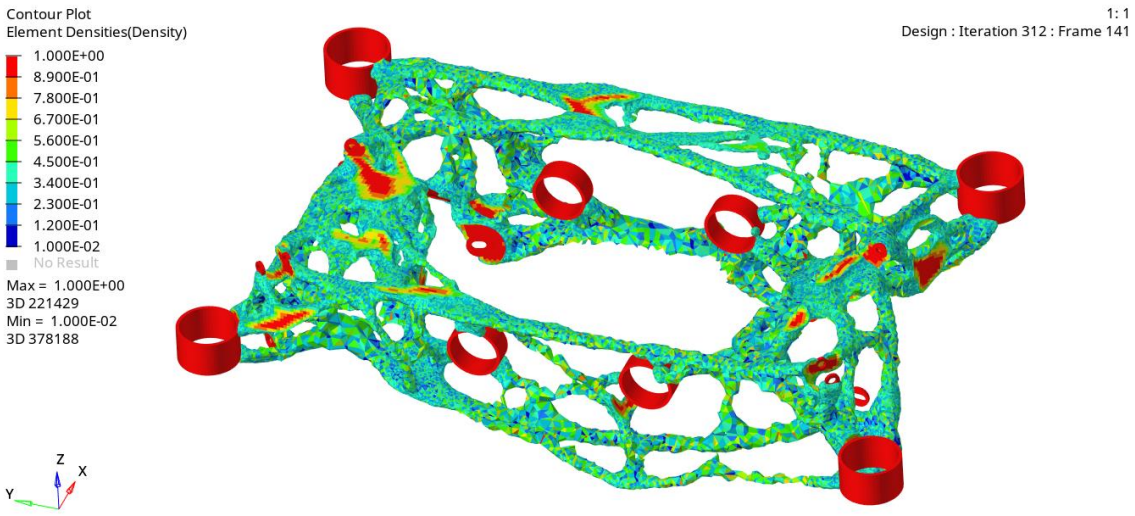

Figure 57: Final topology optimization result, showing element densities >0.35

First, there were clearly defined members within the structure that could easily be manufactured with tube or bar welded together, as shown in Figure 58. Next, the e-axle mounts have a direct connection to the rest of the structure, indicating good load transfer, as shown in Figure 59. Therefore, these optimization results seem to be something that can be used as reference for cradle design.

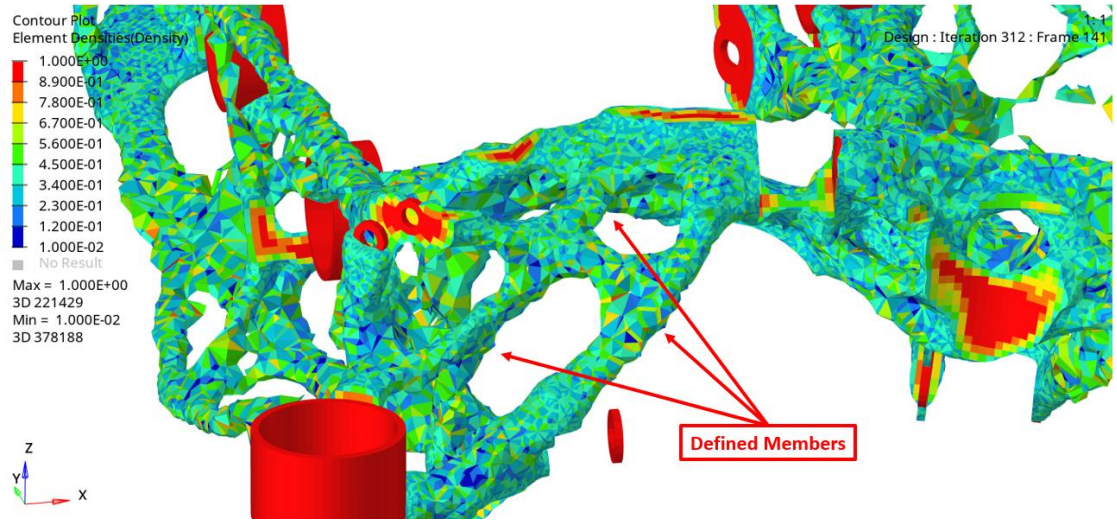

Figure 58: Clearly defined loadpaths that are manufacturable

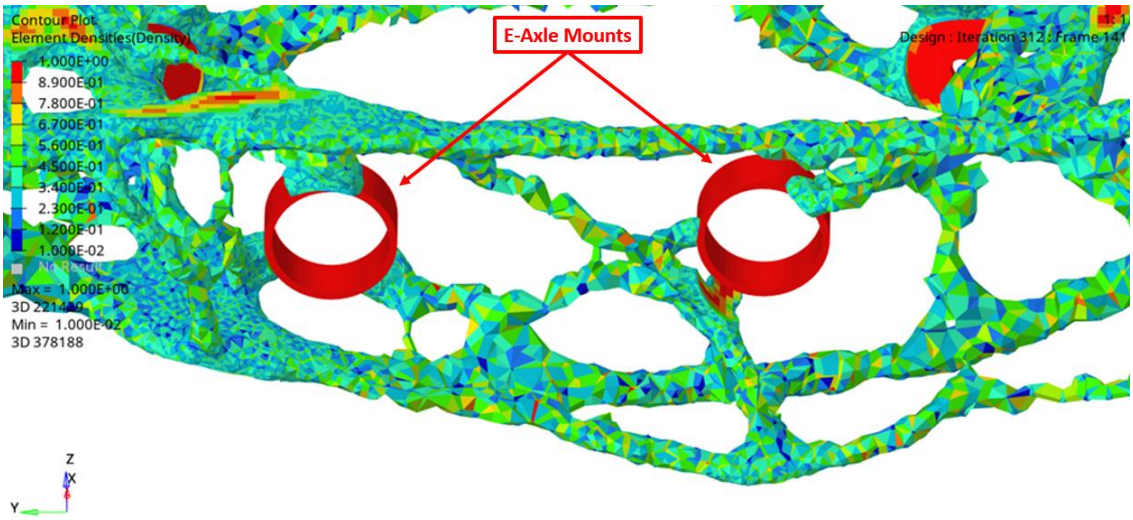

Figure 59: E-axle mounts connecting to rest of structure

The last step before proceeding to design and structural analysis iteration was to verify that the resultant structure would pass waiver requirements. The optimized structure mesh was re-imported back to the pre-processor and analyzed for the nine GM loadcases. The ideal structure for these loadcases would be one that has a relatively even stress distribution throughout the part, which is indicative of material efficiency. Figure 60 and Figure 61 show stress contours for the 2-

wheel bump and forward braking cases respectively. Although there were low and high stressed areas throughout the entire part for each individual loadcase, all the areas of the cradle were equally utilized to bear load for all loadcases collectively. As such, the results were indicative that the structure was material efficient. With the structure verified, it was then possible to start rear cradle design.

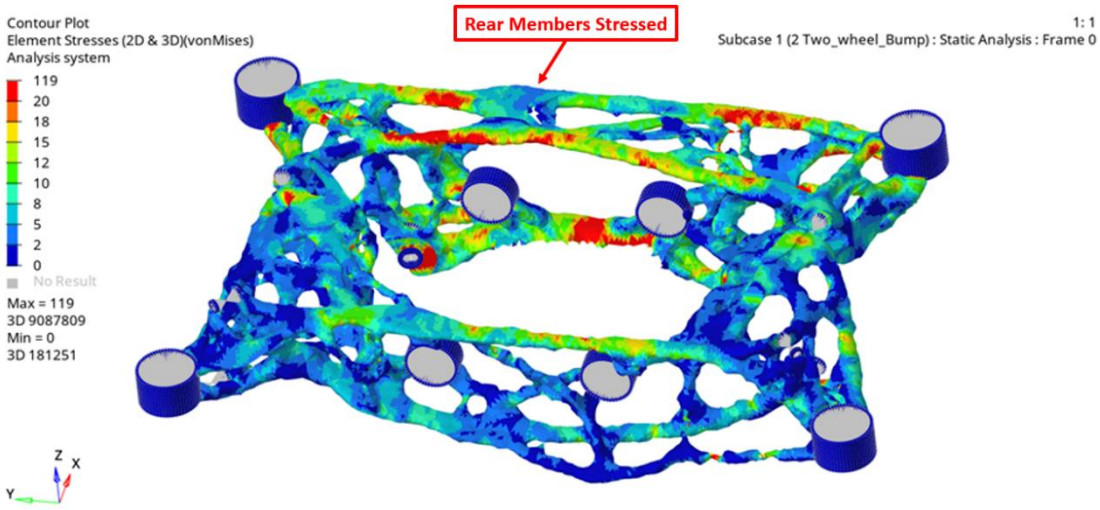

Figure 60: Optimized structure re-analysis, 2-wheel bump stress contour

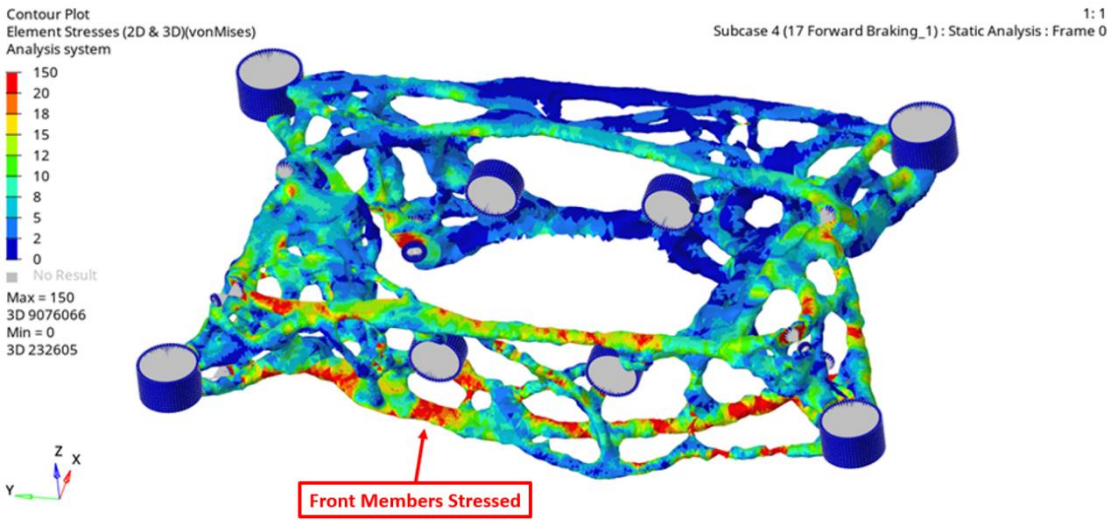

Figure 61: Optimized structure re-analysis, forward braking stress contour

Chapter 6
Structural Analysis

With topology optimization complete and an optimized shape generated, iteration between CAD design and FEA can be conducted. At this stage, geometry of the component is generated in CAD, while being mindful of manufacturing constraints. FEA is conducted to assess strength and stiffness of a component, and CAD is modified accordingly. By the end of this stage, designs should be nearly finalized, with minimal modifications needed for the final product.

6.1 Initial Design Studies

With the ideal structure for the nine GM loadcases defined, design studies for the cradle itself could be started. The first decision to investigate was the general construction of the cradle. Cradles developed by an OEM are typically stamped or formed from sheet metal, however some cradles have been cast [19], as shown in Figure 62 and Figure 63 respectively.

Figure 62: Various production cradles from aluminum sheet [19]

Figure 63: Die-cast aluminum cradle for Porsche Panamera [19]

However, cradles designed by an OEM do not have the same manufacturing limitations as one designed for prototyping. As previously mentioned, casting is a higher volume production method unsuitable for one-off builds, which is the same case for the sheet forming techniques employed by these manufacturers. Sheets are typically stamped or hydroformed, both of which require a high initial investment cost for tooling [38]. Therefore, using sheet or thin-wall material in a low-volume setting would usually employ the use of pre-formed sections, such as tubing, or flat sheet metal with simple bends and welded together.

Conversely, the fact that OEM cradles are high production also means certain other manufacturing methods are unavailable. For example, a complicated tubular spaceframe structure requires a lot of manual labour due to welding and jigging, which would not be economically feasible for high-volume production.

Therefore, the primary methods for the rear cradle are from flat sheet and bent, or from pre-formed sections of material such as tube, or extrusions such as I-beams. Since the overall goal of

this project is to minimize weight, preliminary design studies were conducted to analyze the construction method that would weigh the least while still meeting waiver requirements.

6.1.1 Preliminary Sheet Metal Design

To create a preliminary sheet metal design, the 2019 cradle model was used, and the material simply changed from steel to aluminum. This was done because the 2019 cradle was entirely made up of flat sheet. However, it was important to note that the 2019 cradle, being modified from stock, consists of the original stamped steel geometry, not feasible for a low production design. As such, the geometry for the original sections are optimized more for the input loads than fabricated sections, as there was more freedom with the design with the stampings versus fabricated from flat sheet. Therefore, this approach was still valid, though it erred on the conservative side.

However, given the material change and thus reduction in yield strength, the stresses were significantly increased, as shown in Figure 64. Luckily, the model was set up such that the entire structure was defined with 2D elements, so its thickness was defined just by inputting a value. Therefore, the analysis was run, and the wall thicknesses of the cradle were increased in varying amounts iteratively until the stresses met requirements. Displacements of all the hardpoints were checked and were well within the requirement as well.

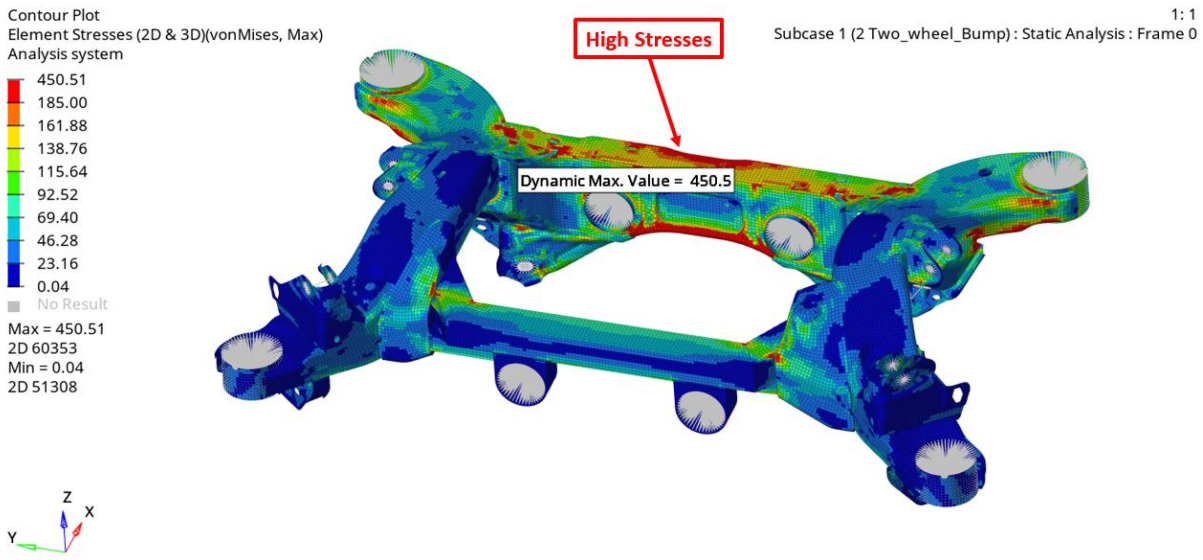

Figure 64: 2-wheel bump stress contour for initial sheet metal study

With both the stress and stiffness requirements met, the weight of the structure was calculated at 13.89 kg.

6.1.2 Preliminary Spaceframe Design

To create a preliminary spaceframe design, the resultant shape from the topology optimization study was exported as a CAD file and imported to the SolidWorks CAD software. Straight tubes were primarily used for the structure, and the centrelines of the tubes were set to follow those from the optimization using 3D sketches, as shown in Figure 65.

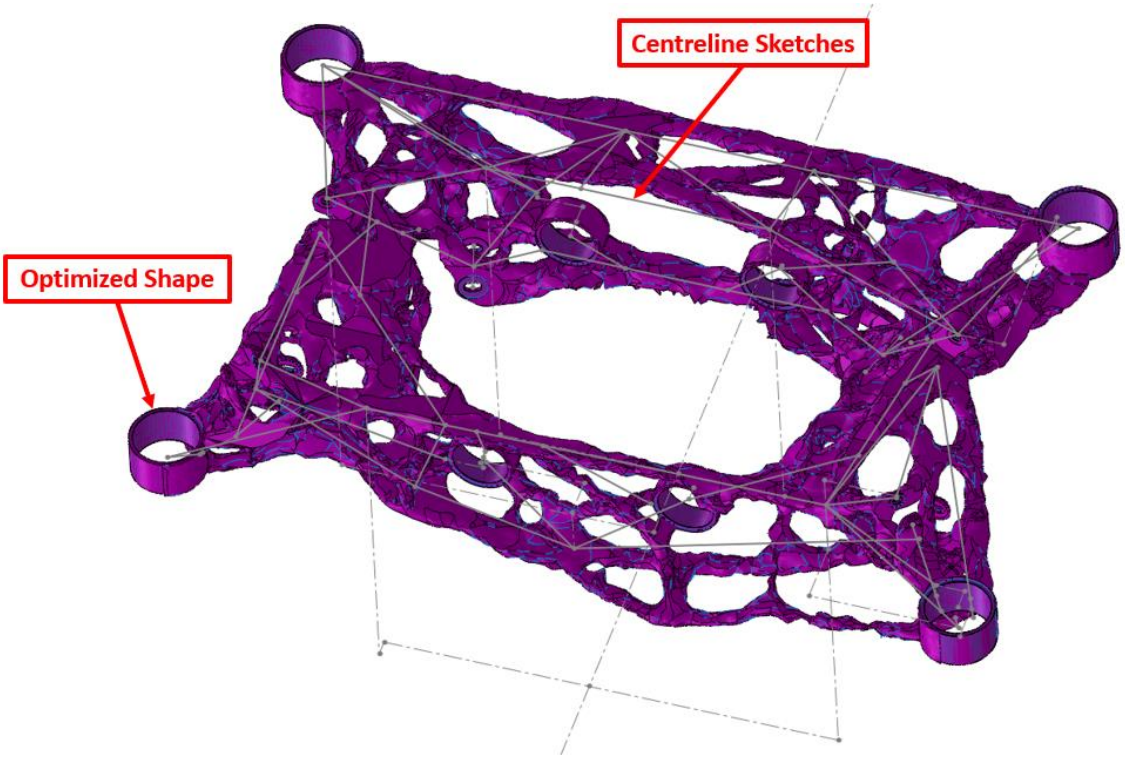

Figure 65: Optimized shape CAD export in magenta and centreline sketches in grey

These centrelines were then exported back into HyperWorks for analysis. Instead of using traditional elements and FEA theory, beam theory was used. As all members had consistent cross-sectional areas, known equations for forces and moments could be used to compute resultant stresses and displacements [136]. Consequently, beam elements were defined along all the centrelines, connecting all the nodes and hardpoints together. Figure 66 shows the 1D analysis setup with member size visualization enabled. To start, all members were set to 0.75" x 0.095" circular tube.

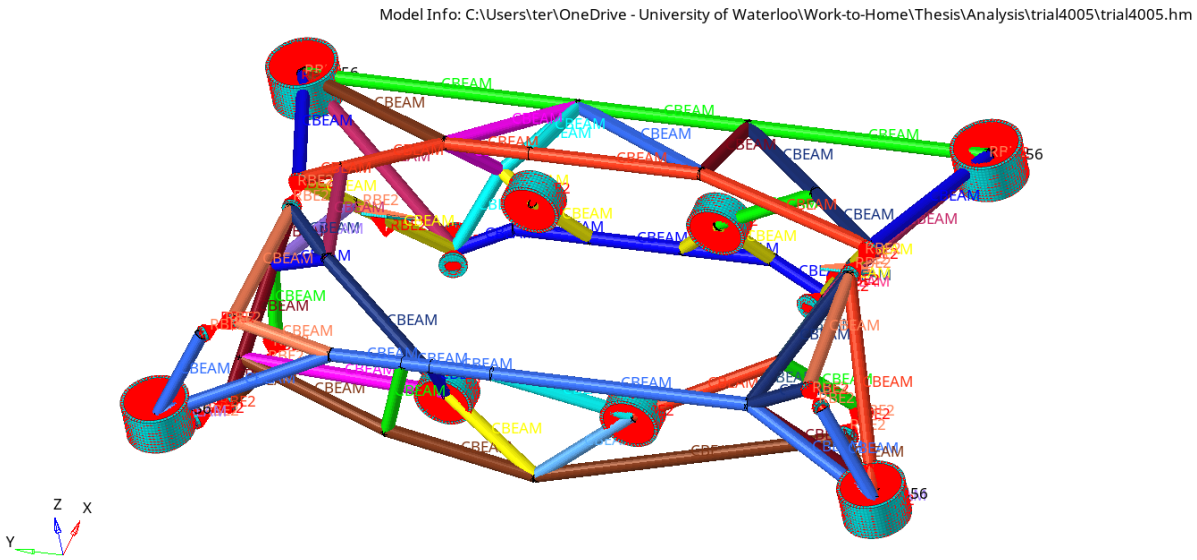

Figure 66: Initial spaceframe 1D analysis setup with member size visualization

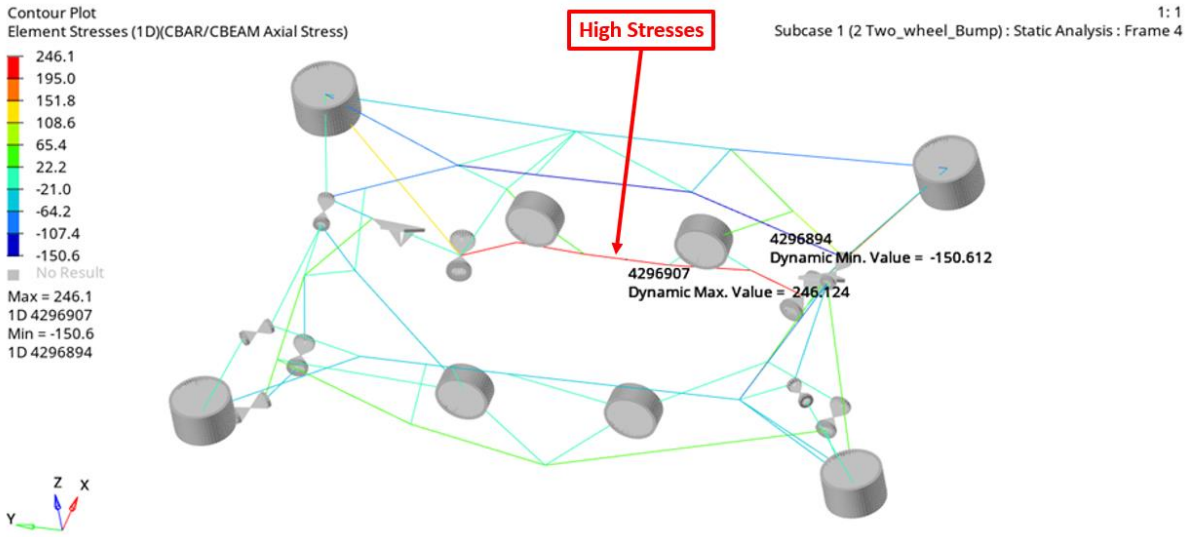

Figure 67: Initial spaceframe 1D analysis resultant stresses

The analysis was run, and resultant stresses displayed in Figure 67. Stresses were reasonable, aside from two loadcases, where the peak stress was 246 MPa. However, even this high stress value was not unreasonable, and thus not too difficult to eliminate with either more members, or members with thicker cross-sectional area. Stiffness was also a huge concern, as displacements were in the

magnitudes of 10-15 mm. Therefore, some new members were added for support, and all member sizes increased to 1.00" x 0.095". Stress results of this revised design is shown in Figure 68.

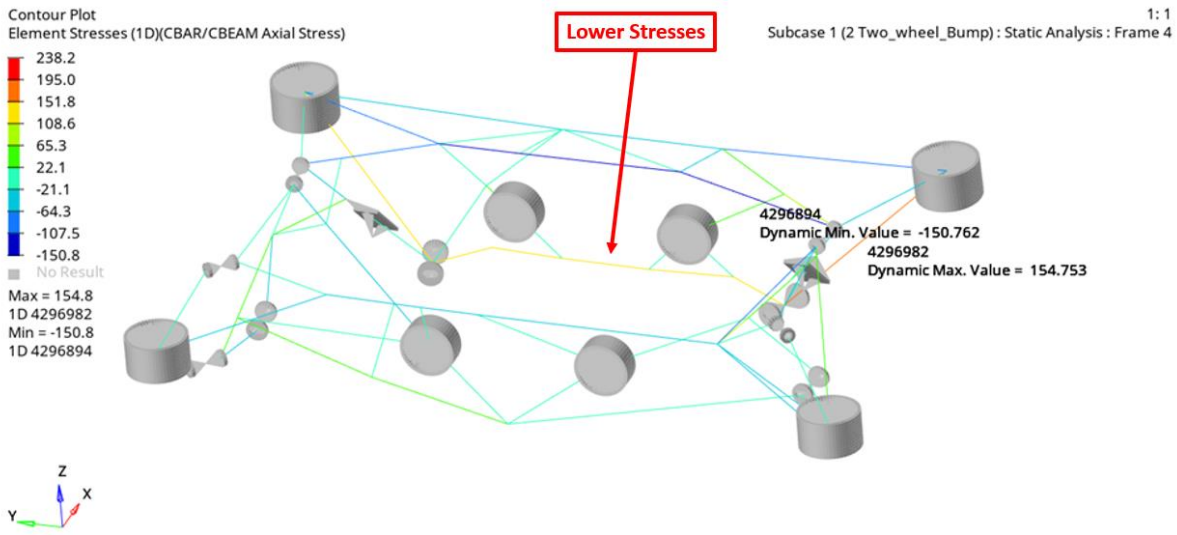

Figure 68: Revised spaceframe 1D analysis resultant stresses

With these larger members, the resultant stresses met waiver requirements. Unfortunately, displacements were still in excess of the stiffness requirement, though significantly reduced from the initial study. The estimated weight for the initial and revised models were 4.24 and 4.40 kg respectively.

6.1.3 Results

Although the tubular spaceframe structure had displacements that were exceeding the stiffness requirement, it was obvious that this construction method would be more optimal. Once again, the sheet metal design was 13.89 kg, and this represents a conservative approach given the geometry from the stock sections of the cradle that would be extremely difficult to manufacture in a machine shop. As such, it was likely that a feasible design would be even heavier, given the limitations in form factor. Conversely, the tubular spaceframe design met strength requirements at only 32% the weight of the sheet metal design. Although stiffness requirements were yet to be met, the significant difference in weight was indicative that it would be possible to meet the

requirement while still being lighter. Therefore, detailed design studies were to be conducted, with a primary focus to manufacture the cradle using pre-formed sections such as tube or extruded beam.

6.2 Detailed Design

Design studies were further conducted with 1D beam elements due to the ability to quickly iterate different sectional areas for each element. Rather than having to constantly re-import CAD geometry and mesh, new cross-sectional areas could be applied to any element in a fraction of the time.

Although it was determined that a tubular spaceframe would be the most weight-efficient construction method, the handful of analyses run did not yet pass stiffness requirements. Therefore, the design iterations will focus on lowering deflections to meet these requirements while keeping in mind the primary requirements for stress.

6.2.1 Design Iterations

To diagnose the cause of the excessive deformation, the 1D model was closely analyzed. The first task was to qualitatively investigate the root cause by inspecting the deformation modes of the cradle. For a given structure, bending usually results in higher deflections compared to tension or compression for the same load, due to higher localized stresses, and resultant strains [137]. As such, deflections could be reduced by minimizing any observed bending. In a tubular spaceframe structure, this can be done by increasing the member size, as well as triangulating nodes, which are the joints at which members meet [138].

An example of this is shown in Figure 69, which is the 2-wheel bump case. The deformed shape was amplified 10 times for visualization purposes and contoured to stresses, while the undeformed shape is in black. From these results, it was observed that the rear member had significant bending upwards, which caused high stresses in the lowermost member. Therefore, the design had to be revised to lower these deflections.

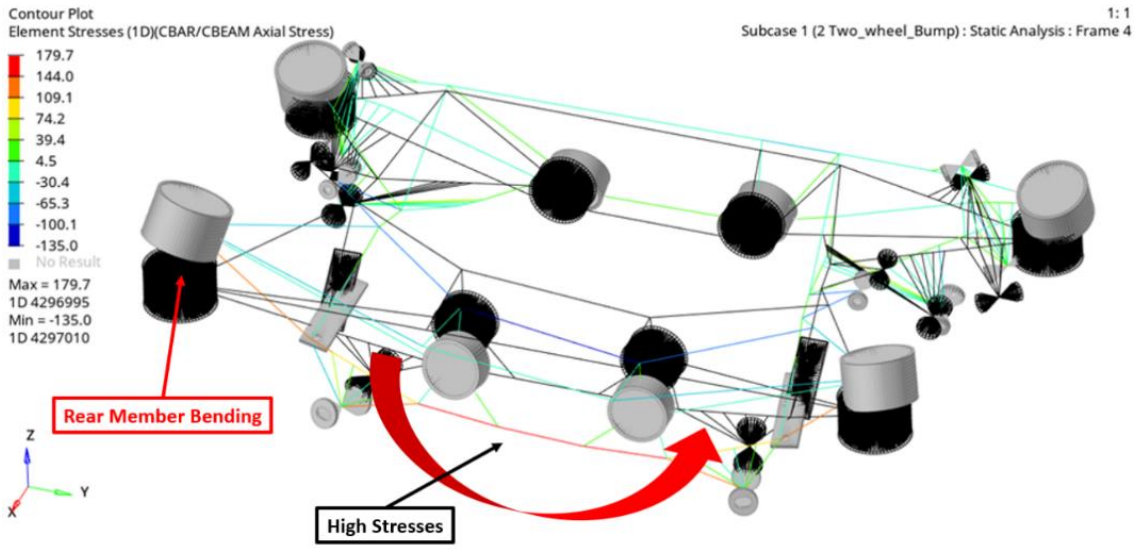

Figure 69: 10x deformed versus undeformed shape isometric view, highlighting the high amounts of bending in the rear member

Figure 70 shows the revised design to mitigate these deformations and lower stresses. The side and rear lowermost members were increased in diameter and wall thickness. An additional rear member was added as well, connecting from the rear body hardpoint to the rear lower member. As a result, projected weight increased by 1.12 kg.

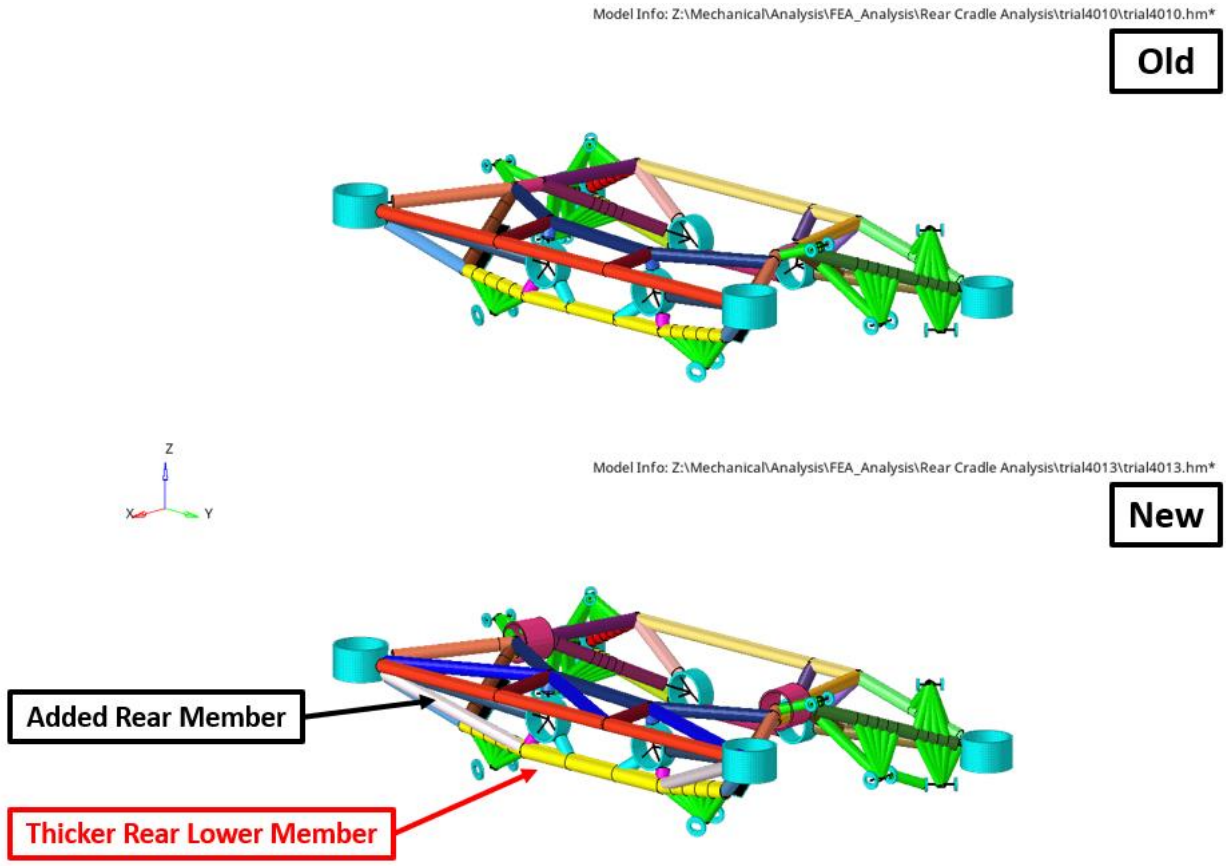

Figure 70: Revised design showing differences in member sizes to mitigate bending in rear member

With the analysis re-run for the new design, resultant displacements and stresses for both the original and revised design were plotted directly against each other for a comparison. As shown from Figure 71, deformations in the rear member have been significant reduced, with peak displacements decreased from 12.1 to 5.5 mm.

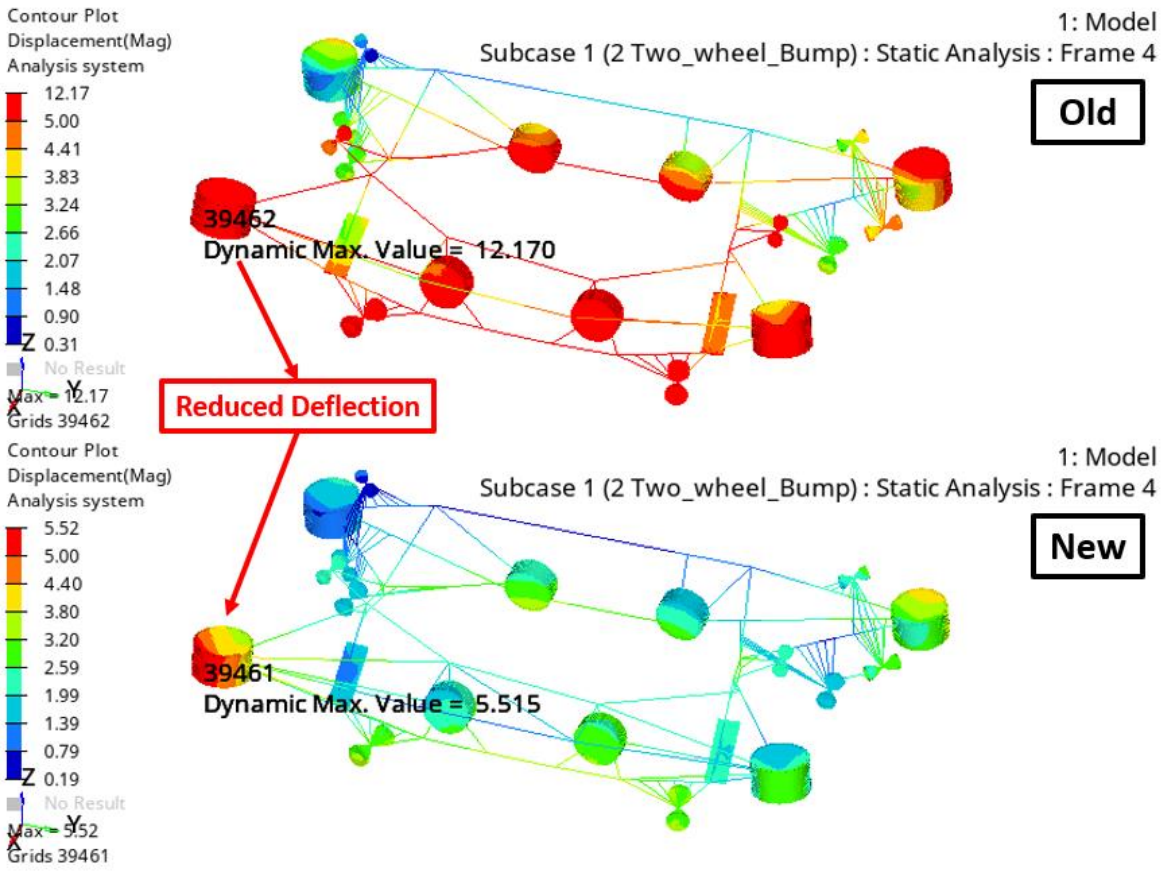

Figure 71: Resultant reduction in rear member deflection due to revised member sizes

One other notable solution for significantly reducing deformations was adding a member connecting the front to the rear half of the cradle. As shown in Figure 72, there was significant bending in the side member, which follows the original design of having the sole connection from the front to the rear of the cradle above the halfshaft. After a few design studies, it was evident that adding a secondary connection was necessary; this was simulated by connecting from the Anti-Roll Bar (ARB) to the toe hardpoint, as shown in Figure 73. In doing so, side bending was effectively reduced, evident in Figure 74.

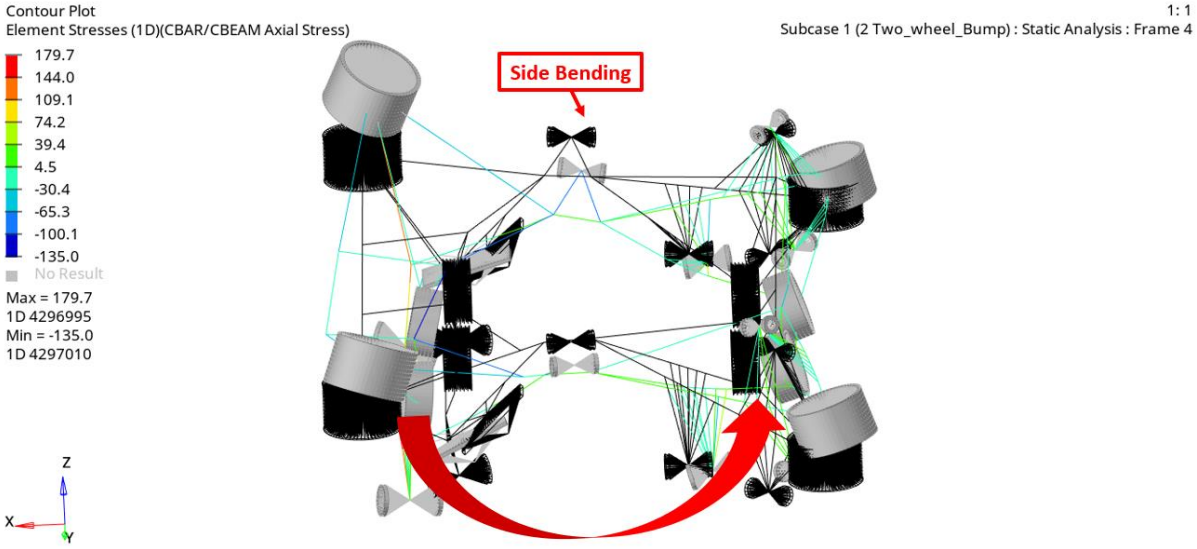

Figure 72: 10x deformed versus undeformed shape side view, showing high amounts of side bending

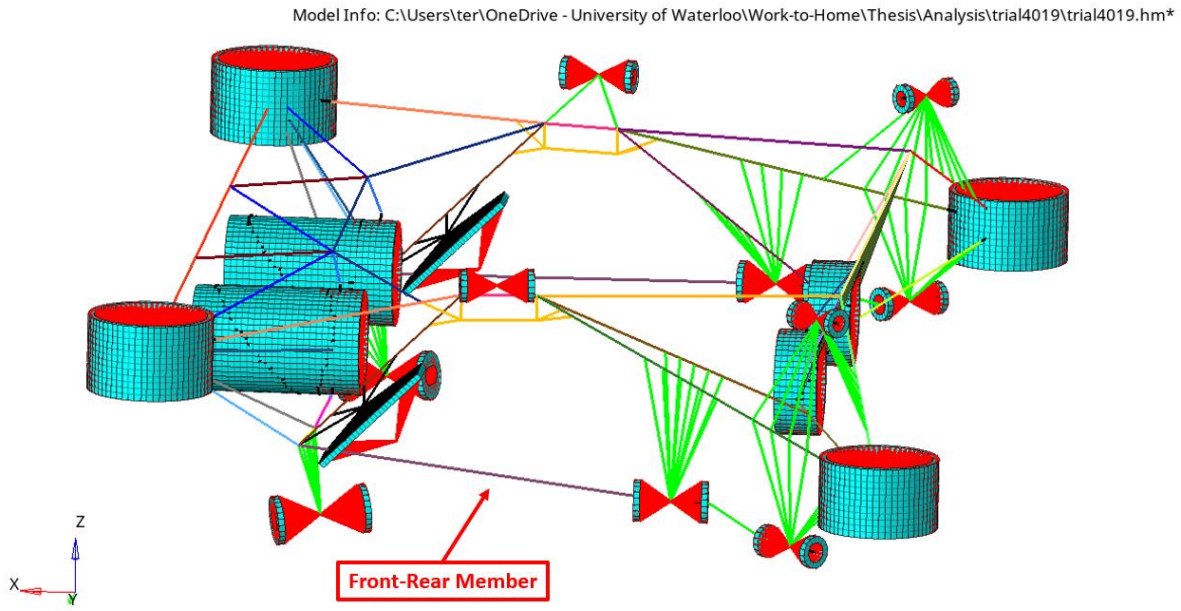

Figure 73: Added front-rear member to mitigate side bending

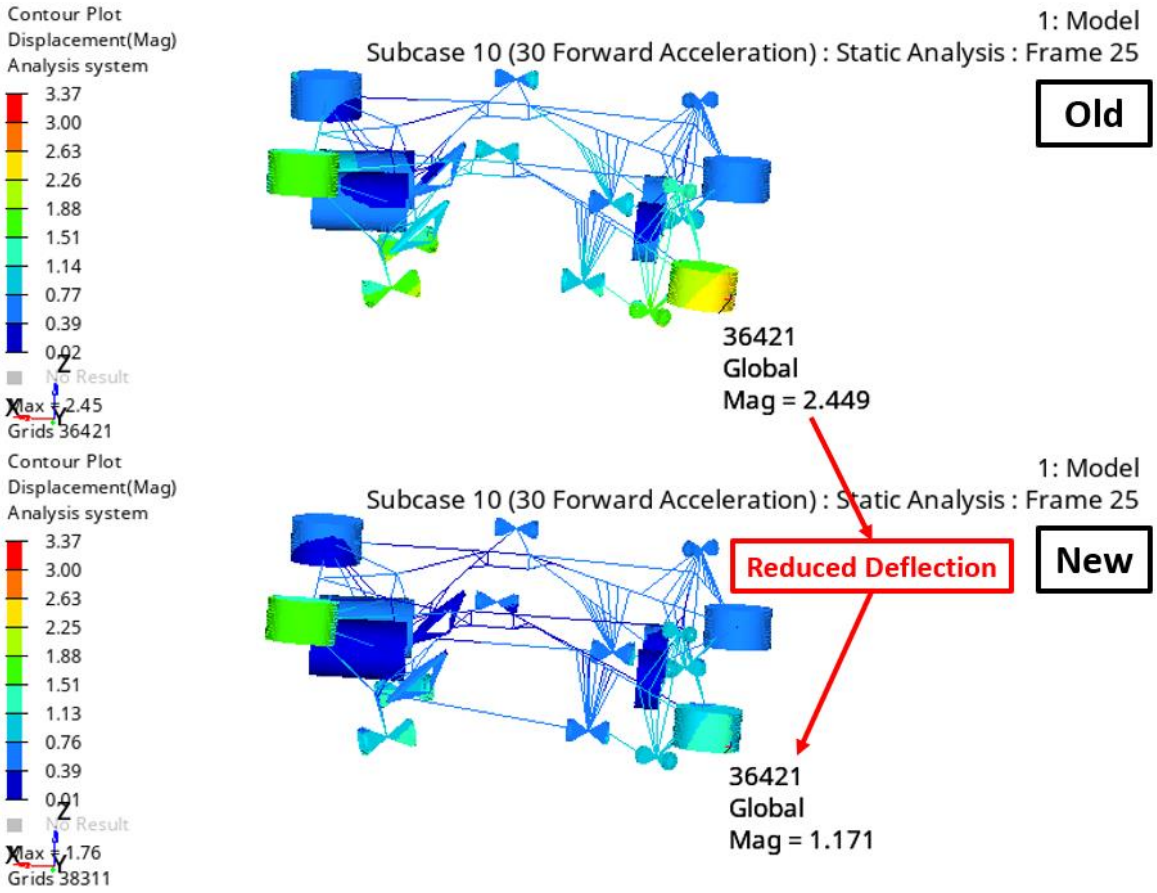

Figure 74: Resultant reduction in side member deflection due to added front-rear member

All in all, these methods of qualitatively analyzing root causes for deformations and implementing solutions through increasing member size or adding members for triangulation was the method primarily used to iterate the model. To speed up this process, numerical values for hardpoint deflections were set to output automatically when the analysis was run. This allowed for quick iterating and comparing of results between models. A screenshot of the tabulated displacement values for all hardpoints are shown in Figure 75.

	A	B	C	D	E	F	G	H	I
1	Node #	Hardpoints	2-Wheel Bump Model Number						
2									
3			Stock GM	4014	4015	4016	4017	4018	4019
4	70000430	L Toe		0.573	0.566	0.468	0.565	0.646	0.443
5	70000431	R Toe		0.636	0.512	0.627	0.629	0.753	0.376
6	70000432	LR Lower		1.428	0.992	1.397	1.409	1.020	0.484
7	70000433	RR Lower		1.467	1.013	1.376	1.445	1.107	0.508
8	70000436	LF Chassis		0.911	0.968	0.968	0.907	0.835	0.525
9	70000437	RF Chassis		1.443	1.211	1.387	1.436	1.331	0.621
10	70000438	LR Chassis		2.281	2.059	2.216	2.276	1.733	1.360
11	70000439	RR Chassis		1.777	1.857	1.842	1.777	1.406	1.252
12	70000440	LR Upper		1.186	1.063	1.257	1.174	0.936	0.877
13	70000441	RR Upper		1.175	0.983	1.201	1.160	0.967	0.915
14	70000442	LF Lower		0.772	0.707	0.743	0.763	0.864	0.318
15	70000443	RF Lower		1.150	0.934	1.102	1.143	1.207	0.401
16	70000444	LF Upper		0.505	0.647	0.601	0.506	0.415	0.335
17	70000445	RF Upper		0.961	0.892	0.908	0.960	0.820	0.487

Figure 75: Screenshot of tabulated hardpoint displacements, to allow for quicker iteration

Outlining every single design change implemented would convolute this report. Instead, all of the major properties of each design iteration were noted, which was then used to plot trends as designs were iterated. One such example of this is shown in Figure 76, where the absolute maximum displacement of any hardpoint for any loadcase was plotted for a few of the design iterations. From these trends it was observed that there was less return on investment with decreasing displacement, by increasing weight. Plotting these two variables allowed easy visualization of which design was the best, that is the one that just meets stiffness requirements while minimizing weight.

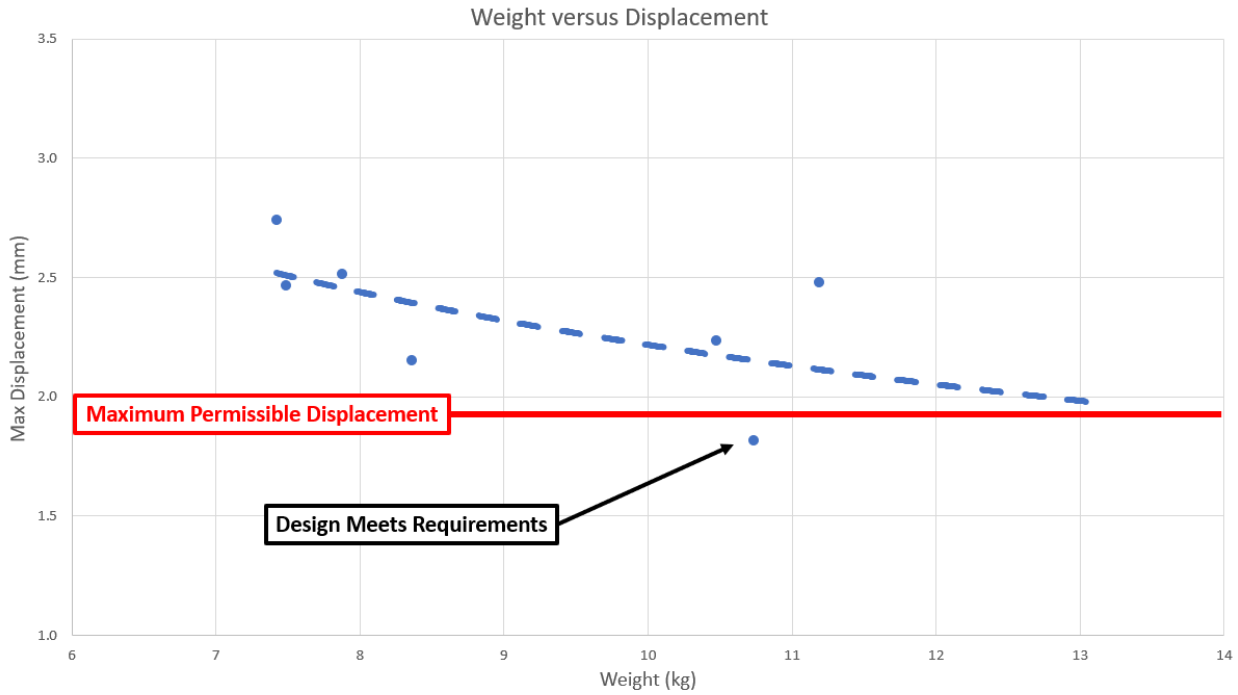

Figure 76: Scatter plot with trendline in blue of designs with respect to weight and displacement, with the maximum allowable displacement in red

The result was a 1D model that met both strength and stiffness requirements, and this was used as a basis for the final design.

Chapter 7
Final Design

With a preliminary design passing requirements, this section outlines the remaining work needed to complete the project. It is at this stage that all details, however minute, are included in CAD to ensure the design is inclusive of everything that is to be manufactured. All of the requirements set in Chapter 3 and Chapter 4 are also verified by inspecting the CAD and FEA models. With all requirements verified, the design is then considered complete.

7.1 Overall Layout

The final design of the new rear cradle was a tubular spaceframe weldment composed primarily of 1.5" diameter round 6061-T6 aluminum tubes. Body and e-axle attachments were made through bushings, pressed into cylindrical housings, similar to that of the stock cradle. Suspension attachments were through brackets composed of flat sheet and welded to the tubes. The final design was relatively easy to manufacture, had adequate clearance to all surrounding components, and met all structural requirements set by GM. As such, all design requirements were met, while only weighing 9.4 kg, as estimated from CAD, which is only 43% of the stock cradle, which weighs 21.8 kg. Front and rear isometric views of the full assembly are shown in Figure 77 and Figure 78 respectively.

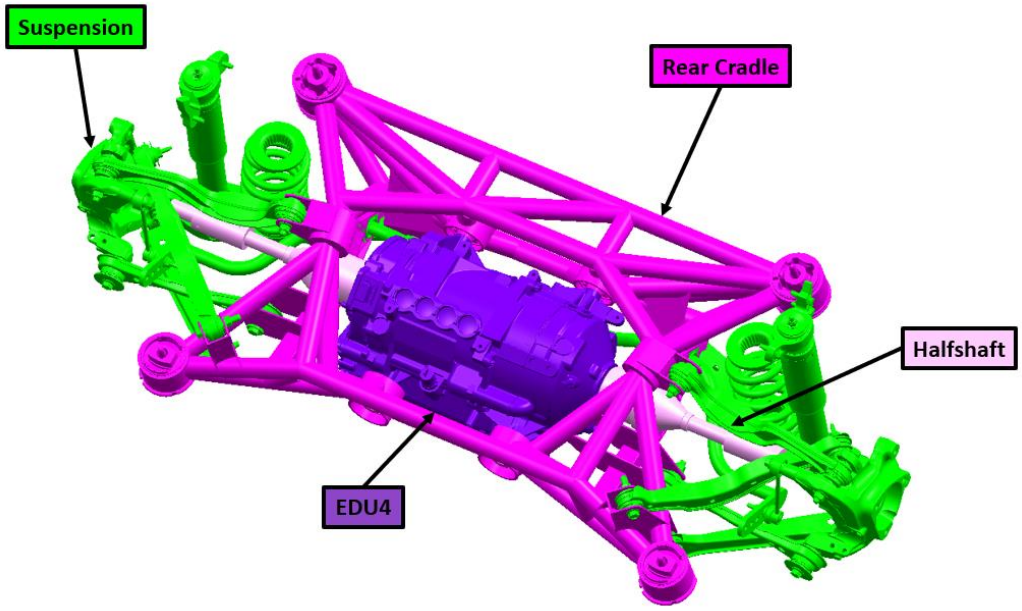

Figure 77: Front isometric view of cradle with e-axle, halfshafts, and suspension in magenta, purple, pink, and green respectively

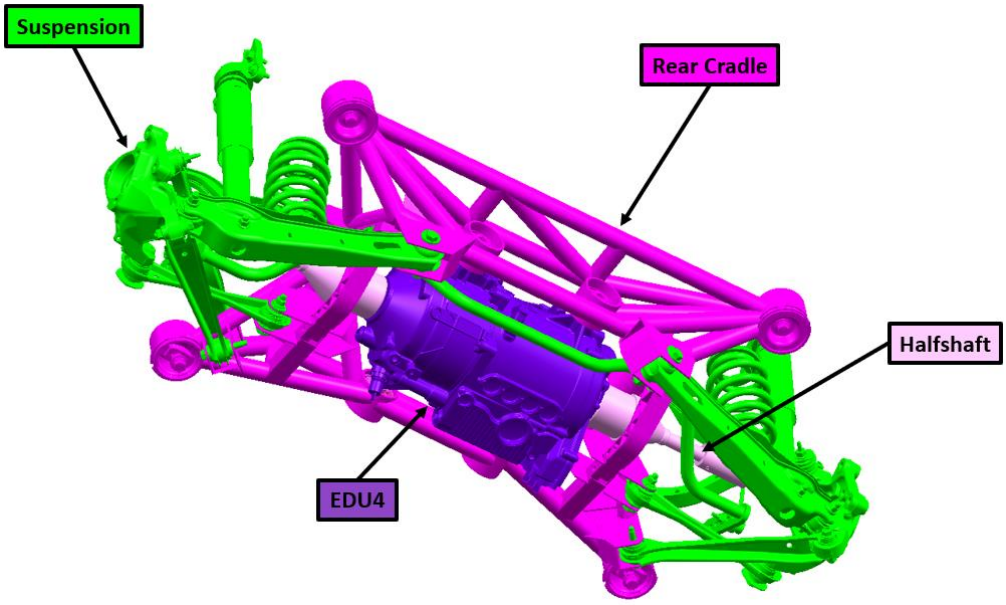

Figure 78: Rear isometric view of cradle with e-axle, halfshafts, and suspension in magenta, purple, pink, and green respectively

7.2 CAD Design

Following the 3D sketches with the initial tube frame design, the SolidWorks weldment tool was used to create most of the CAD. This tool was quick and easy to use, as 3D sketches were set up to define the tube centrelines and a cross-section defined along these paths to create the geometry [140]. The original CAD bodies from topology optimization for the bushing cans and suspension hardpoints were used as a visual reference, as shown in Figure 79. Once all of the tube bodies were generated, the ends needed to be trimmed, so the SolidWorks trimming tool was used, as shown in Figure 80.

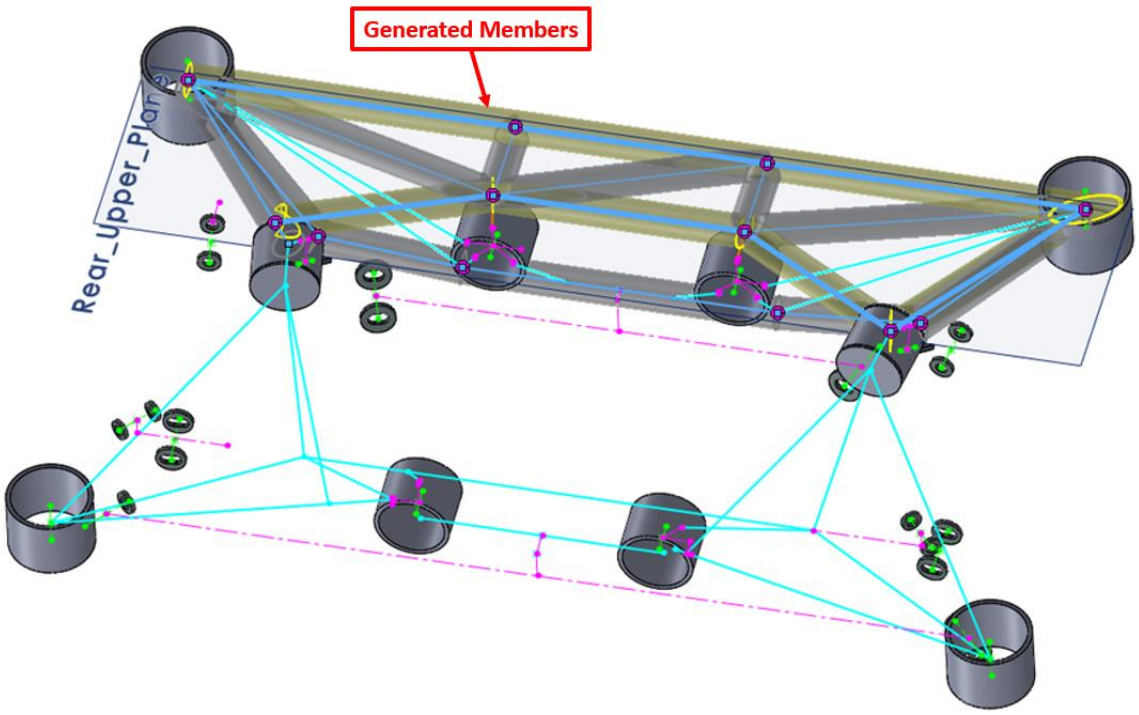

Figure 79: Using the SolidWorks weldment tool, with the generated members in yellow

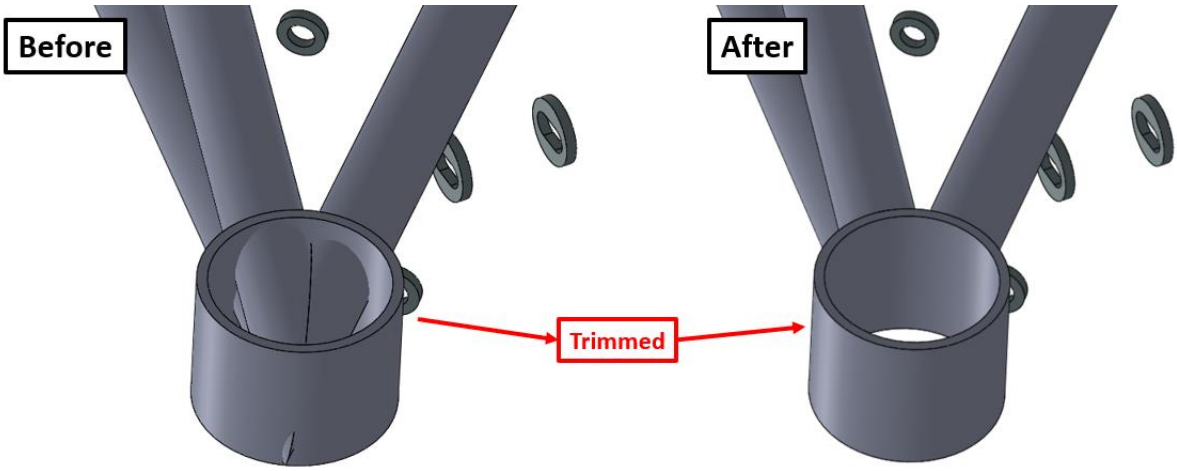

Figure 80: Tube ends with bushing can, before and after trimming

The next step was to create the brackets at the suspension hardpoints to provide a place where the suspension links could assemble to the cradle. The profile of the flat panels were sketched out using reference geometry of the tubes for fit up, as shown in Figure 81.

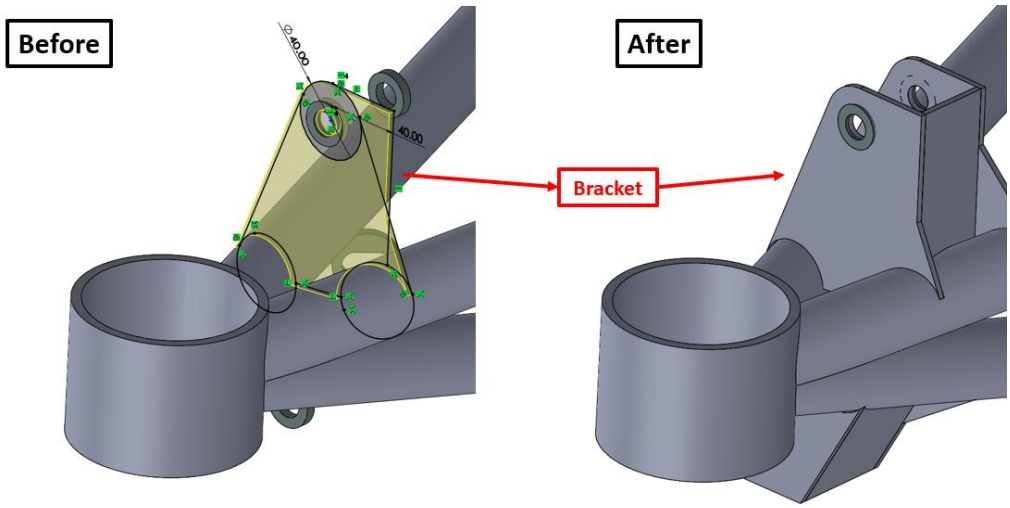

Figure 81: Flat panel creation, highlighted in yellow

Lastly was the design of the front-rear member. To aid with installation of the halfshafts, it was determined that this member should be a removable part. To simplify design and manufacturing, the ARB mounting points were re-used, and to keep manufacturing simple and maximize

strength, the member was to be oriented perpendicular to the ARB mounting surface. As such, the rough location of these members were set, as depicted in Figure 82.

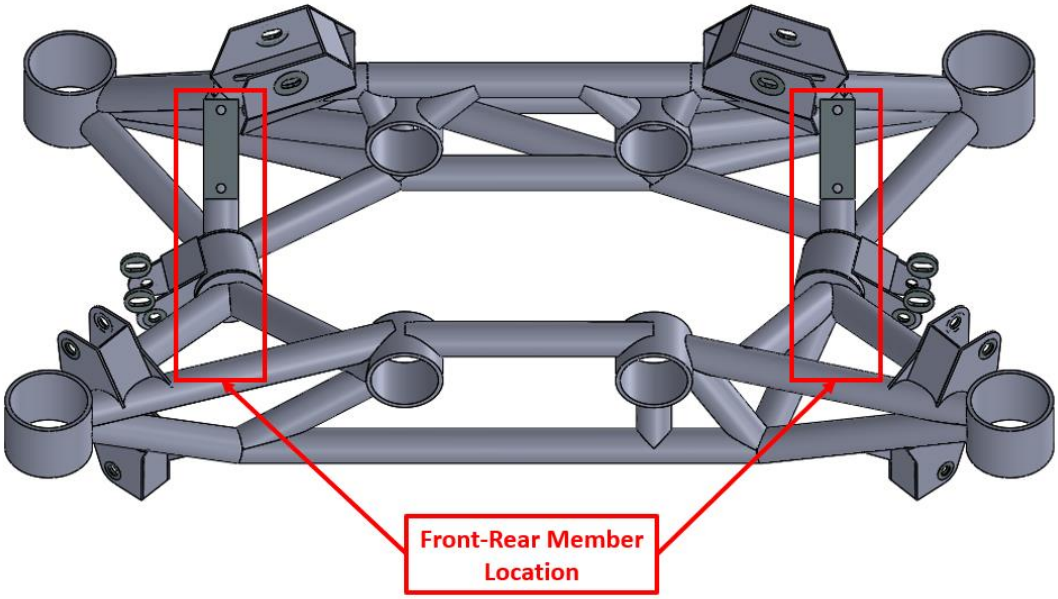

Figure 82: Rough location for front-rear member, shown in red

There must essentially be an attachment point on each side between the ARB mounting point and the front half of the cradle. The front-rear member could be designed to extend all the way to the very front of the cradle; however, it was noticed that the toe attachment was located approximately halfway from the front to rear. By extending the sheet metal brackets for this attachment point further inboard, it was apparent that there was the possibility of attaching at that point instead of all the way forward. Doing so brought a couple benefits, primarily simplified geometry of the front-rear member as well as further stiffening of the toe attachment point, reducing displacements. A layout of this member is shown in Figure 83. Basically, the front-rear member connected from the ARB to the toe brackets, and an additional support was included to provide a load path from this middle node to the front.

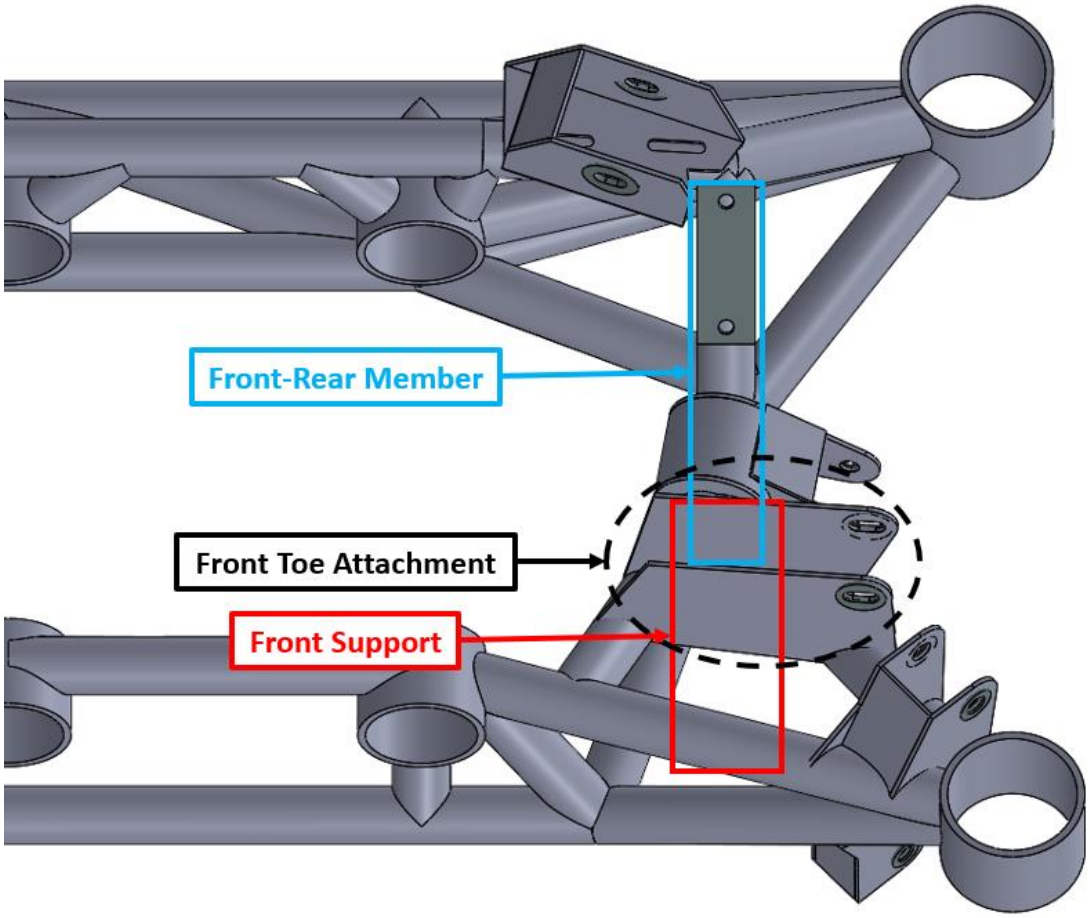

Figure 83: Front-Rear Member Layout, with front-rear member in blue, front support in red, and the attachment point circled in black

Given that the side profile of the front-rear member is parallel with the side view of the vehicle, sketch geometries of the ARB bushing and halfshaft were generated as reference, as shown in Figure 84. To minimize toe bracket bending, the front attachment point of this member was situated in the centre of the bracket. A square tube was added, which was welded to the very front of the cradle, and between the toe brackets. The front attachment point of the front-rear member was then bolted to the tube. An isometric view of the assembly is shown in Figure 85.

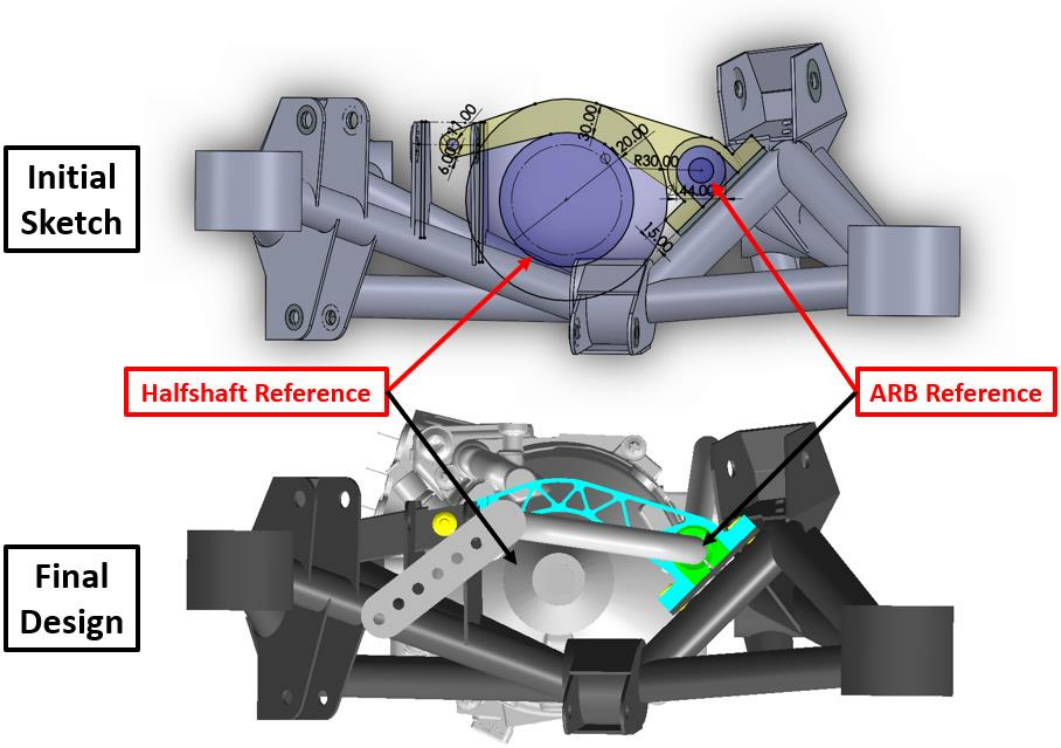

Figure 84: Initial and final design of the front-rear member

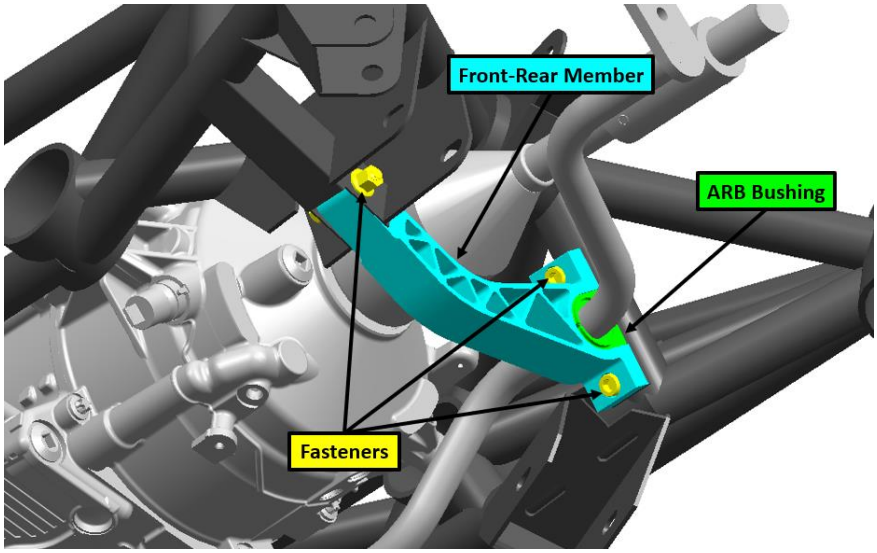

Figure 85: Isometric close-up view of front-rear member with the ARB bushing and fasteners, shown in cyan, green, and yellow respectively

7.3 Geometrical, Manufacturing, and Cost Verification

With the final design complete, requirements with respect to geometry, manufacturing, and cost were verified. This section outlines how the final design meets requirements with respect to clearance with surrounding components, manufacturing within the confines of campus and budgetary constraints.

7.3.1 Clearance

As recalled from Chapter 5, a design space volume was created for topology optimization. When this volume was generated, clearances to all surrounding components were accounted for at that stage. Therefore, as long as all the geometry of the cradle remained within this volume, there was a guarantee that there would be adequate clearances to all surrounding components. Screenshots of the cradle and design space volume overlays are shown in Figure 86 and Figure 87. It was observed that although some of the geometry got close to the edges of the volume, none exceeded this limit.

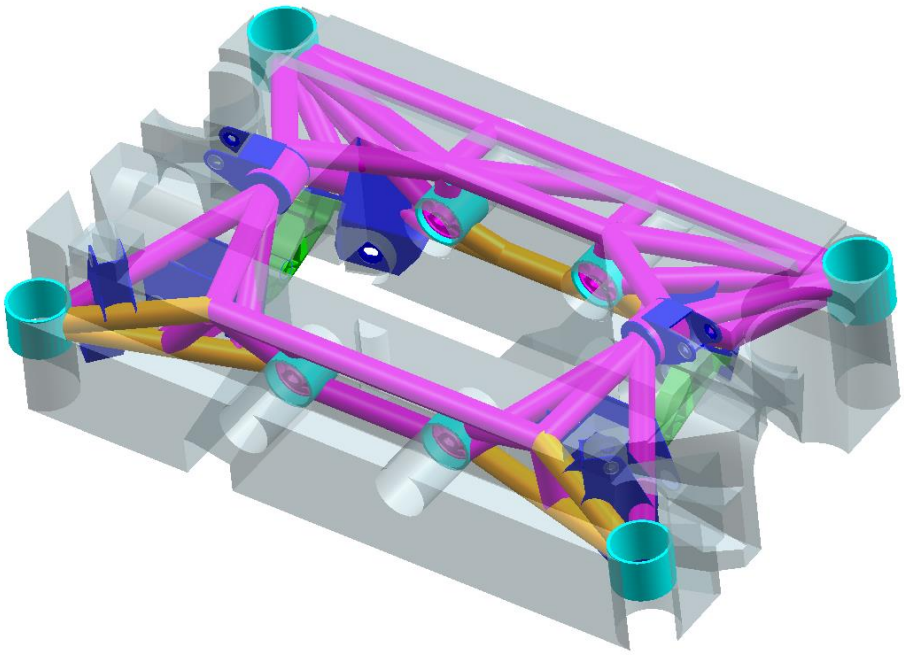

Figure 86: Design space volume in transparent grey overlaid with cradle

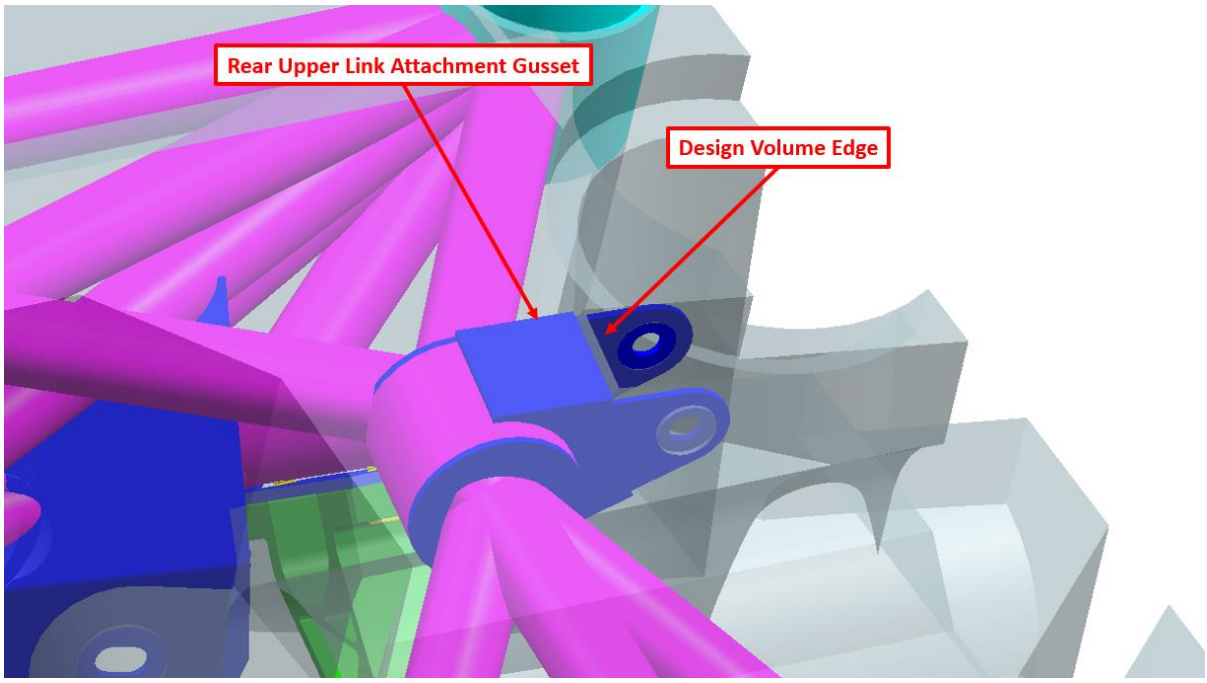

Figure 87: Close proximity of rear upper link gusset in blue to edge of volume in transparent grey

However, there was an exception to this rule. The geometry of the volume was designed assuming the cradle would be completely open on the bottom, therefore all the areas underneath the e-axle and halfshafts were dictated as non-design spaces for the optimization as shown in Figure 88. As mentioned in Chapter 6, a member connecting the front to rear, spanning the lower portion of the cradle was needed for extra stiffness. As such, verifying clearances using the volume was not possible, and CAD geometry with all other components had to be used.

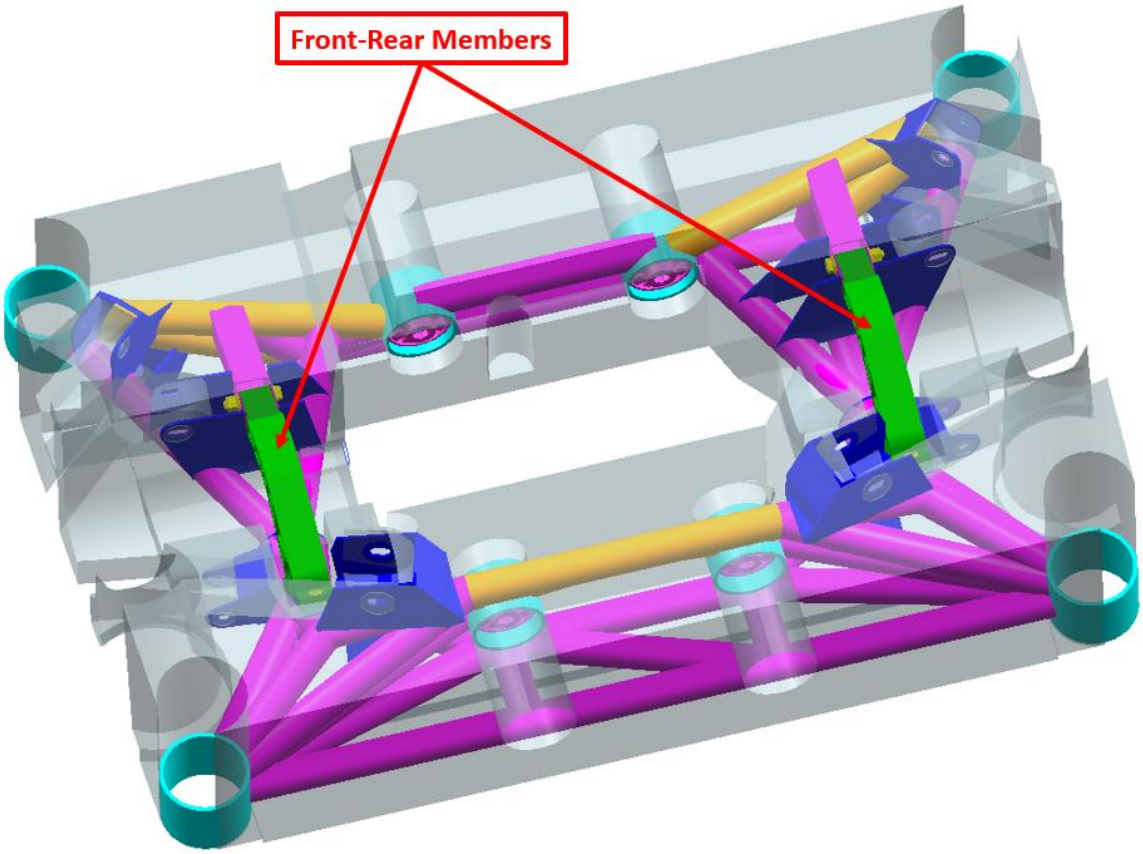

Figure 88: Front-rear members in green exceeding design volume limits in transparent grey

With respect to surrounding components, the front-rear member was in close proximity to only the rear lower suspension link and the halfshaft. At nominal ride height, the minimum distance to the rear lower link was 30 mm, as shown in Figure 89. At the lowest possible ride height, this gap reduced to 10 mm, which is still ample clearance. As for the halfshaft, there was a 10 mm clearance as shown in Figure 90. As halfshafts move with suspension travel, this could have posed an issue. However, the clearance was to the inboard stub shaft assembly, which does not move, and the section of the shaft that does move is not in the immediate vicinity. Therefore, clearances for the front-rear member, and consequently the rest of the cradle, were more than adequate.

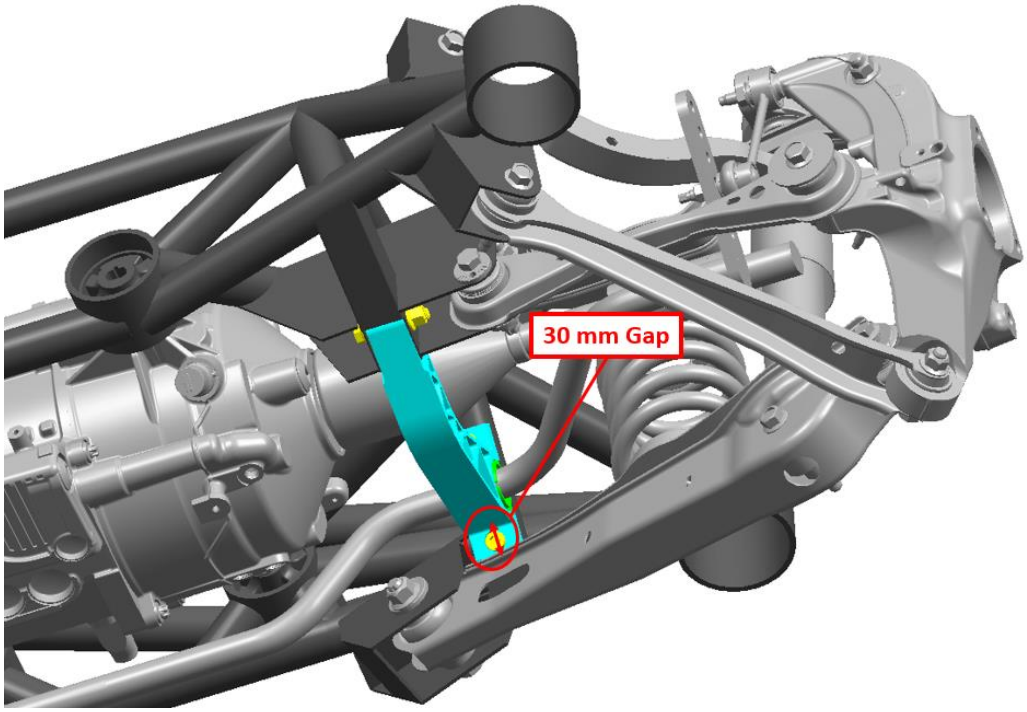

Figure 89: Gap between front-rear member in cyan and rear lower link in grey

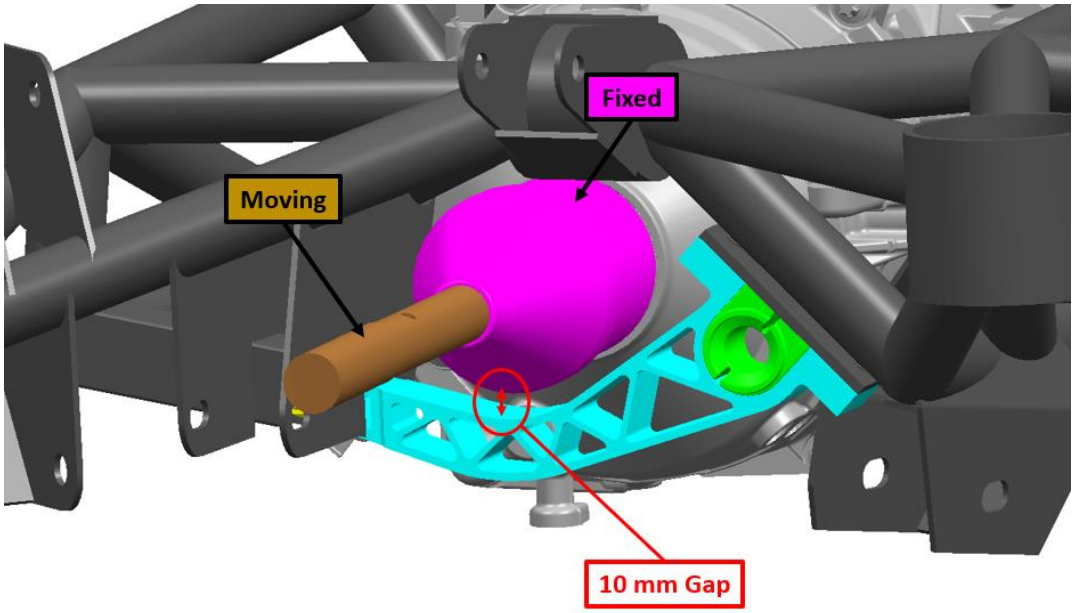

Figure 90: Gap between front-rear member in cyan and halfshaft in magenta

7.3.2 Manufacturability

The new rear cradle was designed to be manufactured with the resources available on campus. Most of the cradle was composed of readily available aluminum tube, which could be easily sourced from a metal supplier. The ends of these tubes were contoured such that they fit perfectly together at the places where they joined up, which are called *nodes*, as shown in Figure 91.

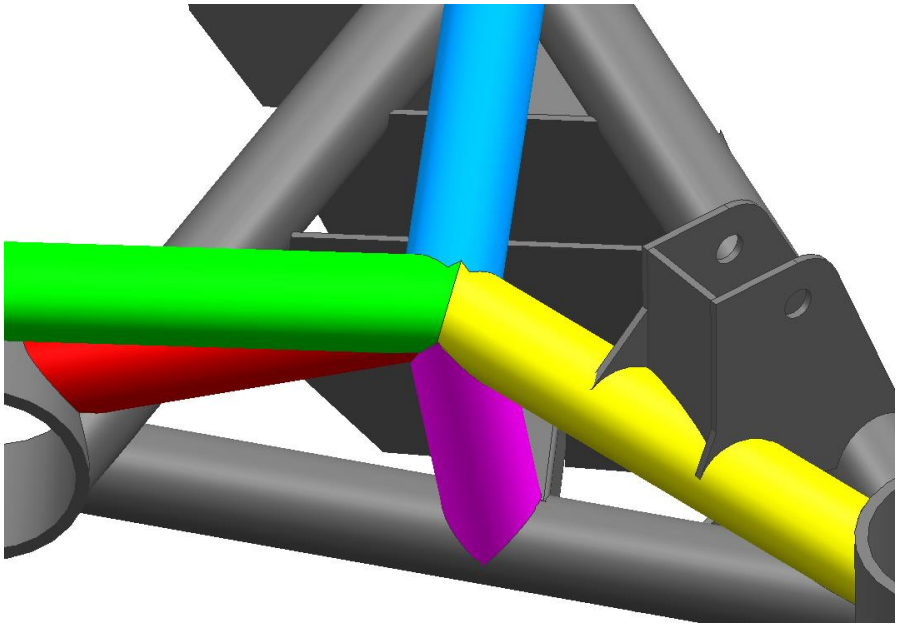

Figure 91: Example node, showing all the coloured tubes that attach together

Generally, the ends of these tubes could be manufactured a couple different ways. The first way would be to use a template tool, shown in Figure 92, which would aid in marking the contour onto the tube end, which could then be cut with a variety of tools such as an angle grinder or file. Similarly, the tube end could be unwrapped to a flat sheet in CAD, printed on a piece of paper, and wrapped around a tube to achieve the same template.

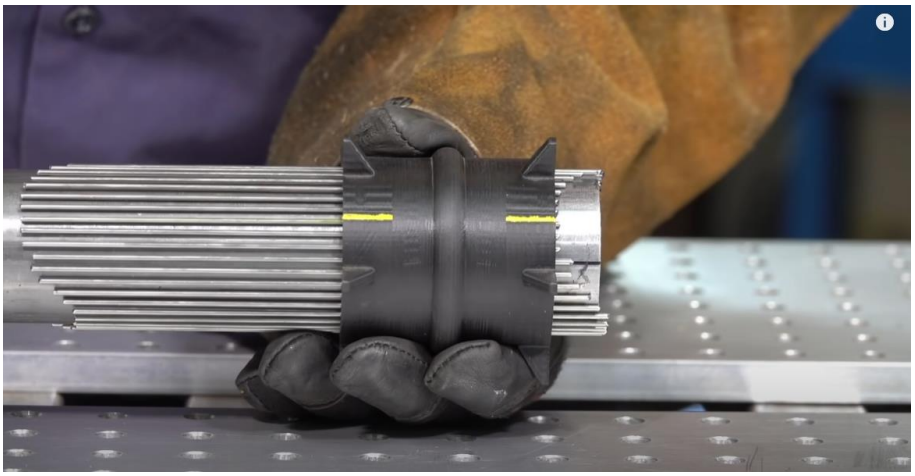

Figure 92: Example of tube notching template tool, allowing the tube profile to be traced onto the end of the tube [139]

The next method would be to outsource to a company with CNC tube notching capabilities, such as VR3 Engineering. These companies have proprietary processes and machines that notch tubes to dimensions closely matching CAD, as shown in Figure 93 [140]. In using these services, the only step would be to weld the tubes together to form the primary structure. However, given that manufacturing was to remain in-house, only the first method would be used for tube notching.

Figure 93: Example of VR3 Engineering's tube notching capabilities [140]

With the primary tubular structure welded together, the next step would be to manufacture the suspension brackets, as shown in Figure 94 and Figure 95. For simplicity, these were all designed to be cut from 1/8" thick sheet. Once again, there were a couple different manufacturing options available. The first was manually cutting the profile with a bandsaw, then drilling holes with a drill press. Both of these tools are available in the student machine shop, however another tool also available is the waterjet, which would be significantly quicker and easier to cut. Additionally, material waste is reduced, as long as proper nesting of the flat panels is done, an example of which is shown in Figure 96.

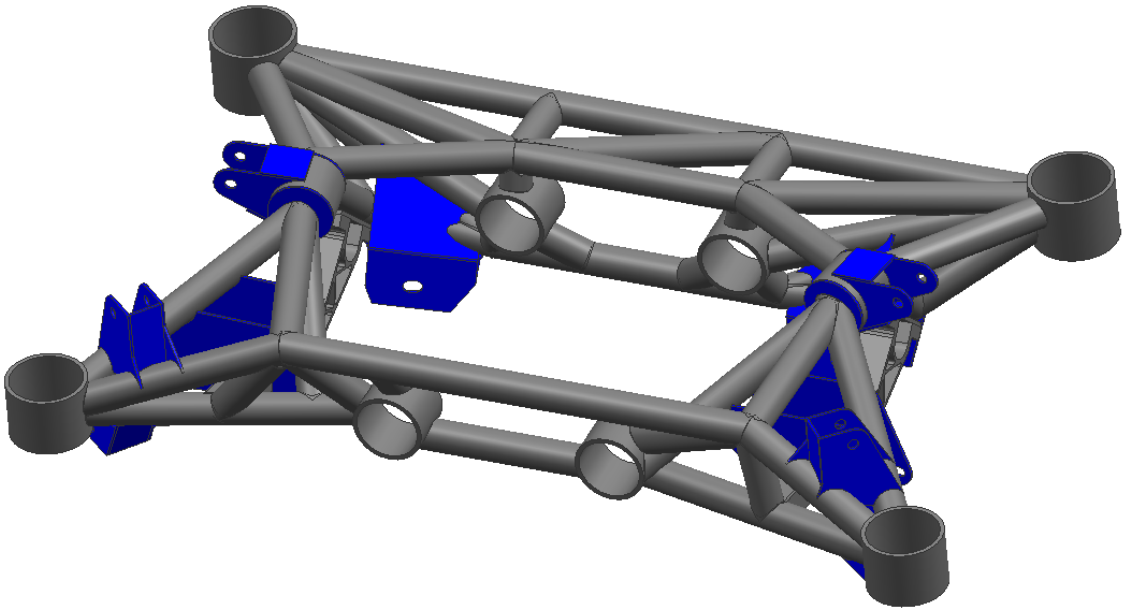

Figure 94: Flat panel brackets in blue on cradle in grey

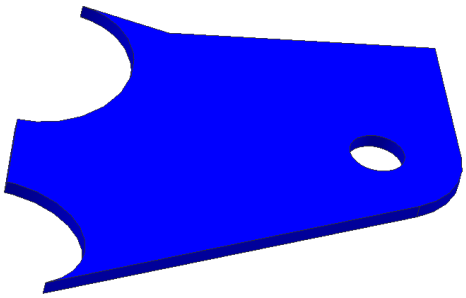

Figure 95: Closeup example of a flat panel bracket in blue

Figure 96: Example of waterjet nesting, showing close proximity of parts to minimize material waste [141]

The last two parts involve some machining. First, were the front-rear members, which are the most complicated individual parts to make. Nevertheless, as mentioned during the design phase, steps were taken to ensure ease of manufacturing to keep cost low. Given the two-dimensional nature of the front-rear member, the basic shape was intended to be waterjet, as shown in Figure 97.

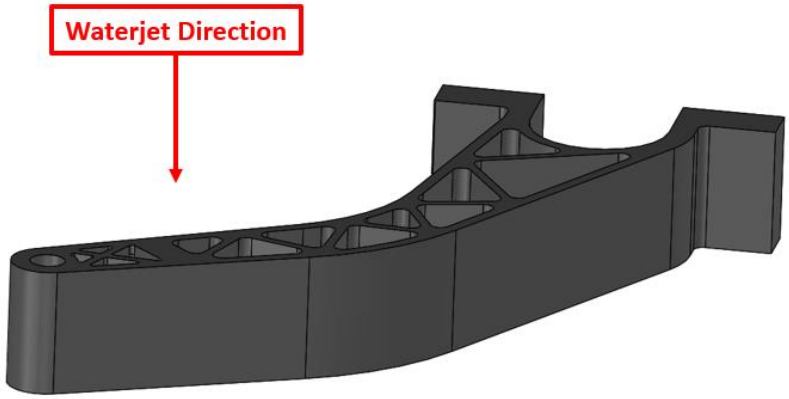

Figure 97: Waterjet direction for front-rear member blank

After, the width of the front of the member needs to be machined down, such that it snugly fits within the square tube to which it mounts. Table clamps, such as those found in Figure 99, could simply be used and the faces on the ends milled. Lastly, the two mounting holes for bolts to the ARB mount need to be drilled. The machined areas of the front-rear member are shown in Figure 98.

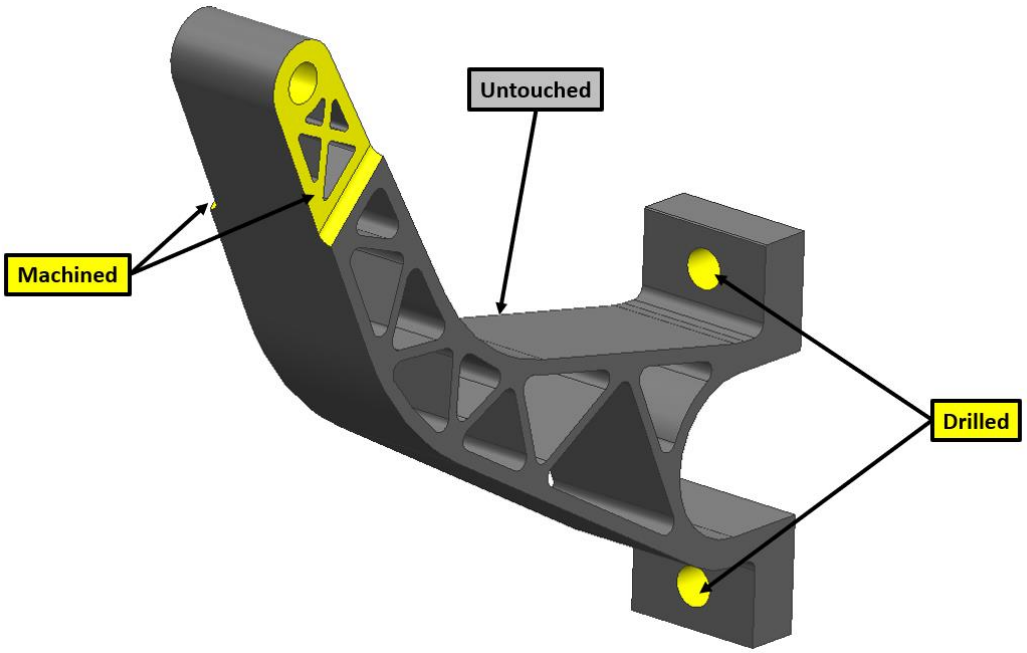

Figure 98: Front-rear member after post-machining, with machined areas in yellow

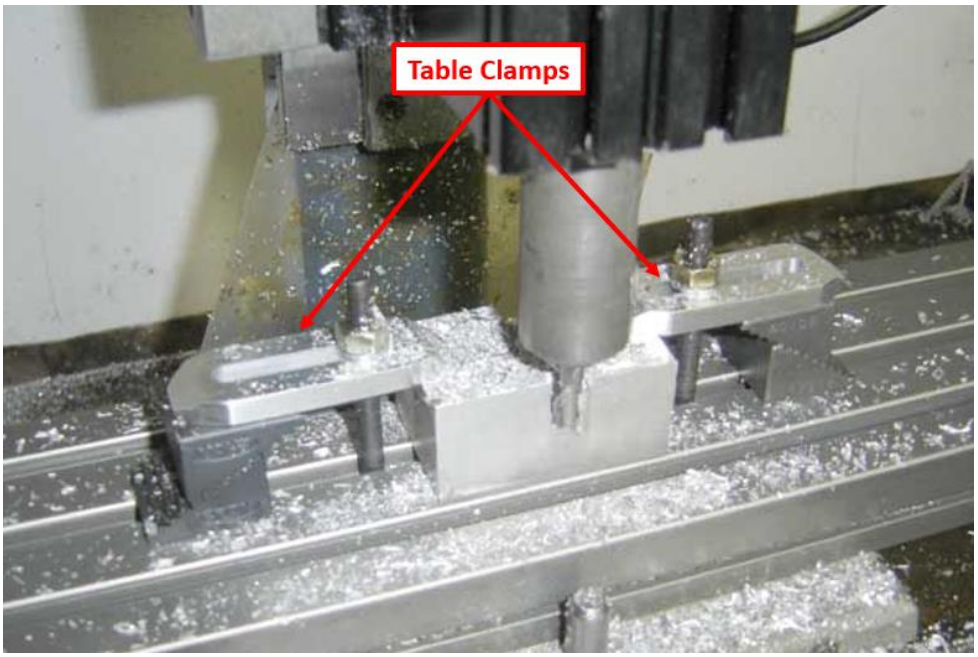

Figure 99: Example of milling table clamps [142]

The second item to be machined were the bushing mounts for the body and e-axle, as shown in Figure 100. These mounts were basically thick-walled tubes, but the inside has a specific diameter, pertaining to the bushings used. As such, thick-walled tubes could simply be purchased and the inside machined to a larger diameter until it was at the final size, as shown in Figure 101.

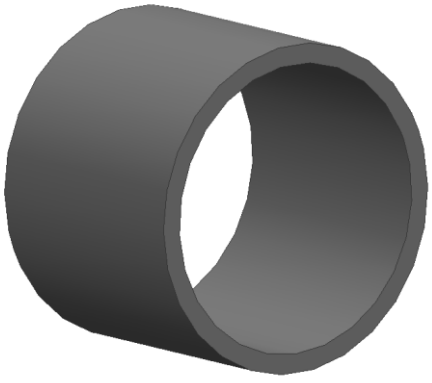

Figure 100: Isometric view of a bushing mount

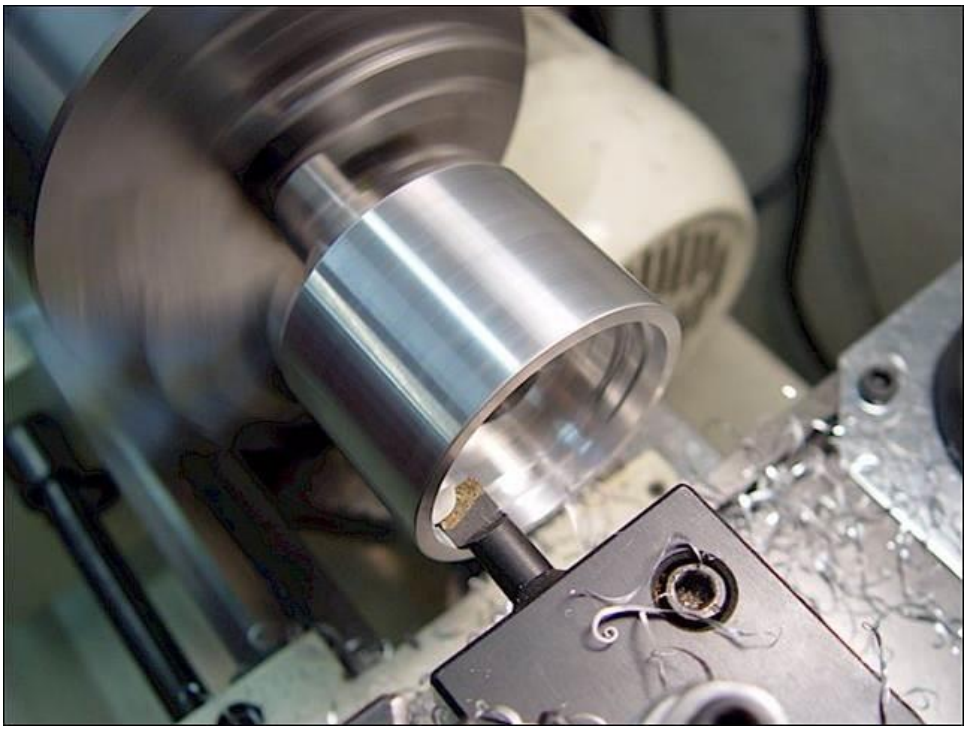

Figure 101: Example of machining inside diameter [143]

With all the individual parts made, everything would then be welded together to form the cradle. However, as alluded to in Chapter 6, jigs such as those shown in Figure 102 would be required to maintain dimensional accuracy. There are two reasons for this – first, fitment of the cradle with supporting components may not be possible. For example, if the relative position of the bushing mounts for the body are not maintained, there may be a situation where the cradle cannot physically assemble to the body of the vehicle. Secondly, dimensional inaccuracies with the cradle itself could affect the drivability of the vehicle if the suspension mounting points are not in the correct position. It is important to note that jig design is out of the scope of this thesis, though as the requirements for weight as not critical, it is objectively an easier design task than the cradle, with no structural analysis required.

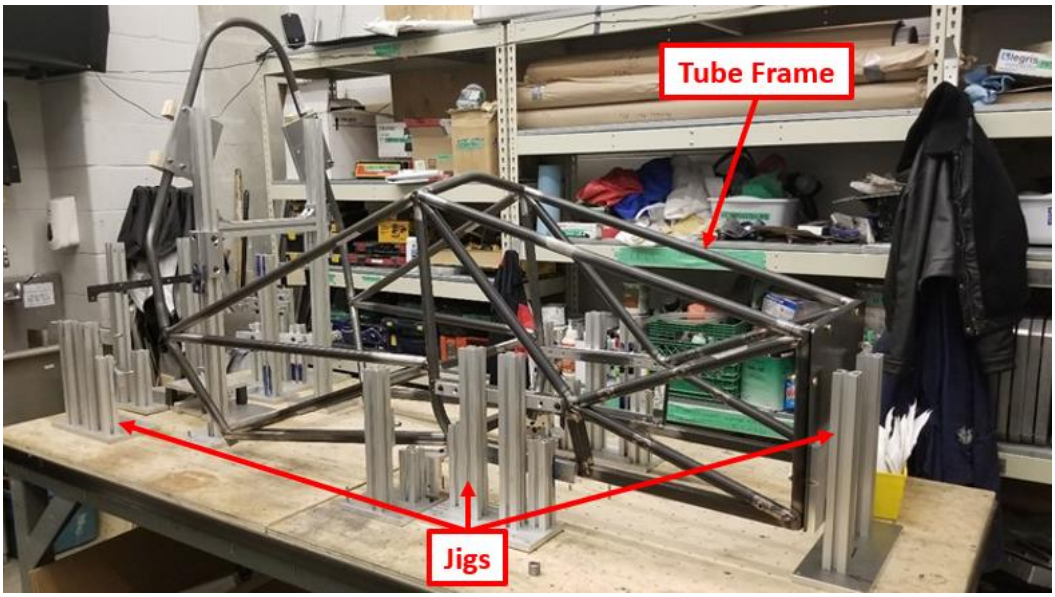

Figure 102: Example of tubular spaceframe with jig

7.3.3 Cost

With the construction methods and materials identified, it was possible to perform a cost analysis to generate an estimate for the project. The two categories for cost were materials and labour. Material costs were calculated by summing the total amount of material to be used. For example, the total length for each type of tube used were known, so it was just a matter of researching the price of tubes for the length needed. Labour costs were estimated by summing up the number of manufacturing steps needed along with estimated length of time taken for each step.

The resultant total cost was estimated to be $2,131 Canadian, with $1,732 of that as material and $398 of that as labour. It is important to note that this is using the $15 per hour school shop labour rate for student teams, which is significantly lower than the $60-80 per hour industry average, however the initial budget set accounted for this factor [144]. This final sum was significantly lower than the budget of $3,000 Canadian, and thus this requirement was met. Detailed calculations can be found in Appendix B.

7.4 Structural Verification

Although an ideal structural form factor as well as tube layout were determined through topology optimization and 1D beam structural analysis, adequately modelling the CAD geometry in detail was needed to finally determine if the design met GM requirements. As all the geometry of the cradle were flat sheet or tube with constant wall thickness, 2D shell elements were sufficient in capturing resultant stresses and displacements [129]. The final design had relatively minor changes compared to what the 1D studies showed with only slight increases in tube wall thickness for a few members. The final layout of the cradle is shown in Figure 103.

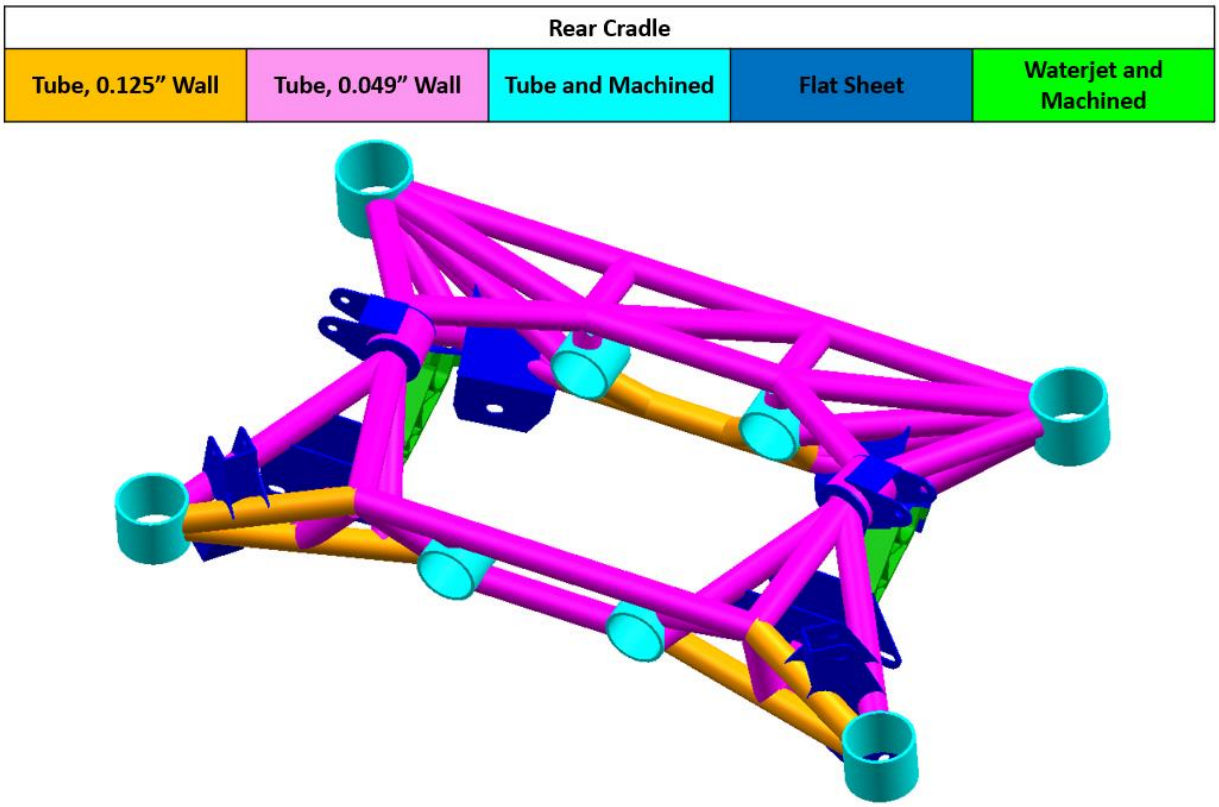

Figure 103: Final layout of the cradle, showing all the different material stock used

7.4.1 Strength

The first point to address is how welding has affected the strength of the cradle and whether the HAZ should be accounted for in the requirements. As mentioned in Chapter 3, welding aluminum results in reduced strength in areas adjacent to the weld. With respect to 6061-T6 specifically, as this specific grade of aluminum is precipitation hardened, the high heating and cooling result in annealing, which has a much lower yield strength [145]. If the cradle were left in this state, the reduced stresses in the HAZ would have to be accounted for. However, pre-weld strength can be re-attained if the material is heat treated [106]. Given this process, the cradle can be made lighter, and strength requirements being uniform across the component greatly simplify fatigue calculations. As such, the design of this cradle relies on heat treatment after welding to take advantage of the benefits of this process.

The final design of the cradle met stress requirements for all GM loadcases, which meant waiver requirements were satisfied. However, during the FEA process it was observed that stresses in some of the members exceeded the requirement, so tube wall thickness had to be increased. Initially, all the tubes were 1.5" outer diameter (OD) x 0.049" thick, but thickness had to be increased to the next available, which was 0.125". As a result, there was a slight increase in weight, but this change was necessary to pass requirements. Figure 104 shows the effects of changing the lowermost rear member, as there were high stresses as a result of significant bending in that member.

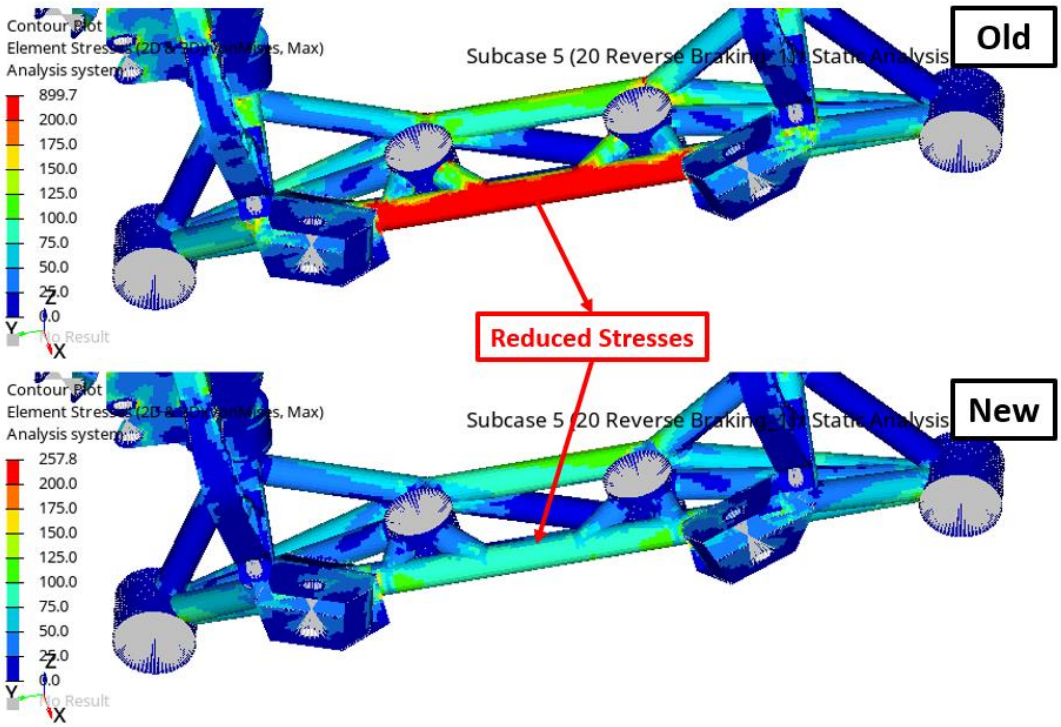

Figure 104: Lower stresses with increasing tube wall thickness in the rear lower member

Another important discussion point are the effects of adding the front-rear member. As previously mentioned, the front-rear member was added primarily to increase the overall stiffness of the cradle. However, as observed in Figure 105, predicted peak stresses were reduced, as stress concentrations were eliminated. Stress concentrations are small, isolated areas of the cradle that have exceedingly high stresses, which could cause an otherwise structurally sound cradle to exceed stress limits. Without this member, there was significant bending in the centre of the cradle, at its narrowest point. As depicted in Figure 106, adding the front-rear member significantly reduced this bending, which eliminated this stress hot spot.

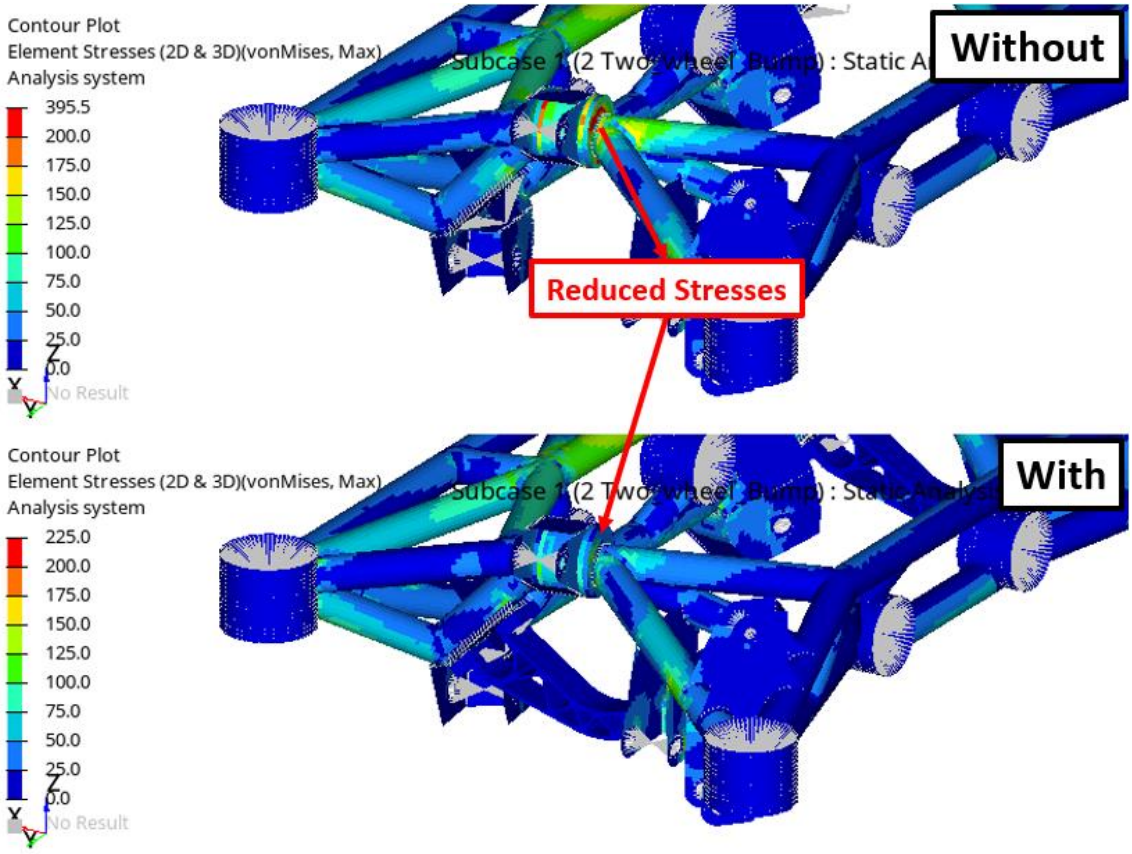

Figure 105: Eliminated stress concentrations in the side member with the addition of the front-rear member

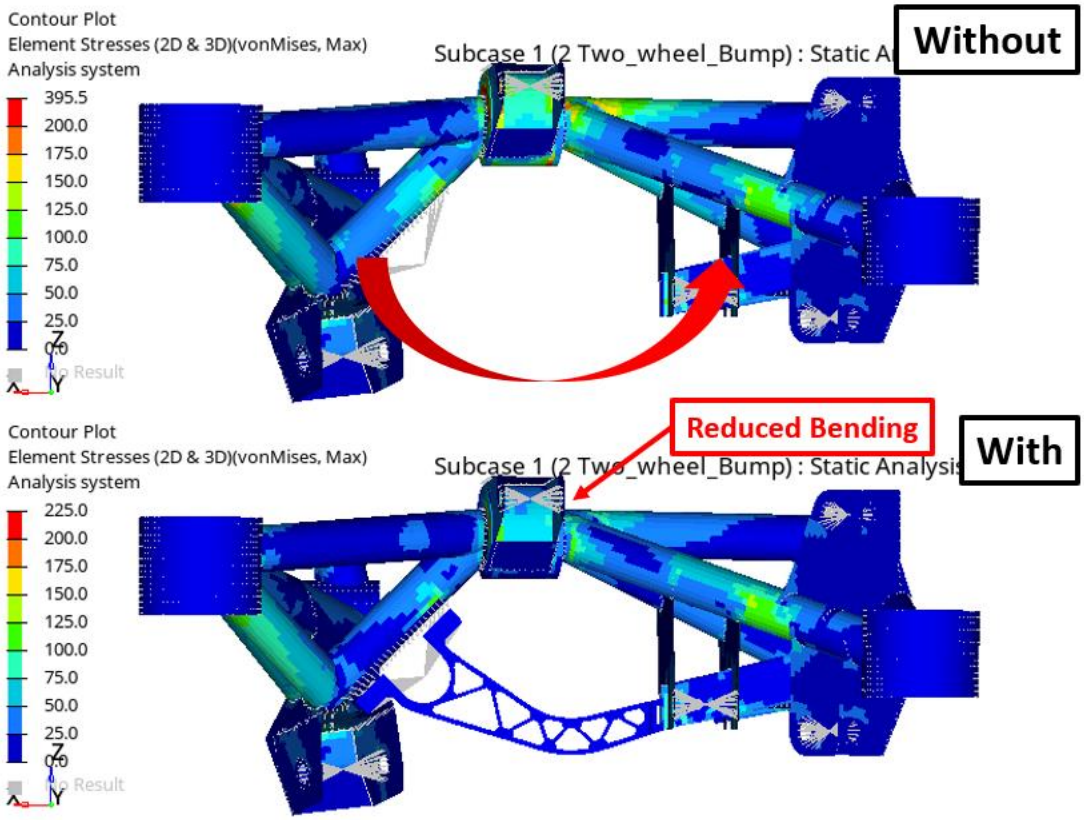

Figure 106: Diagram of reduced bending in the side member with the addition of the front-rear member

Figure 107 shows the resultant stresses in terms of percentage of the requirement. As such, any values over 100 would mean the requirement was exceed, and values under 100% would result in a pass. As shown, all the values were lower than 100%, showing that GM stress requirements were met.

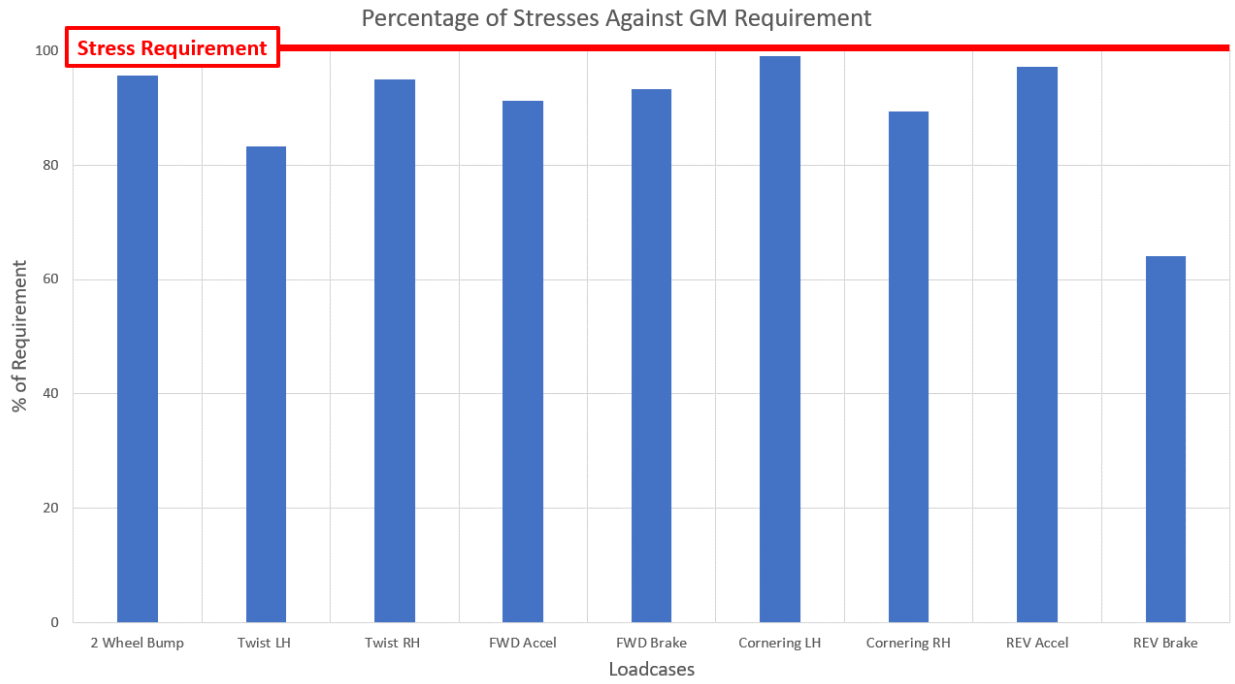

Figure 107: Resultant stresses in terms of percentage of requirement, with the maximum allowable stress percentage in red

Lastly as mentioned in Chapter 4, stresses must not exceed 184 MPa, under 8g and 20g loading conditions. Resultant stresses were 73.0, 123.5, and 29.3 MPa for 8g vertical, 20g longitudinal, and 20g lateral respectively. As shown in Figure 108, these were significantly lower than the requirement, and thus an easy pass.

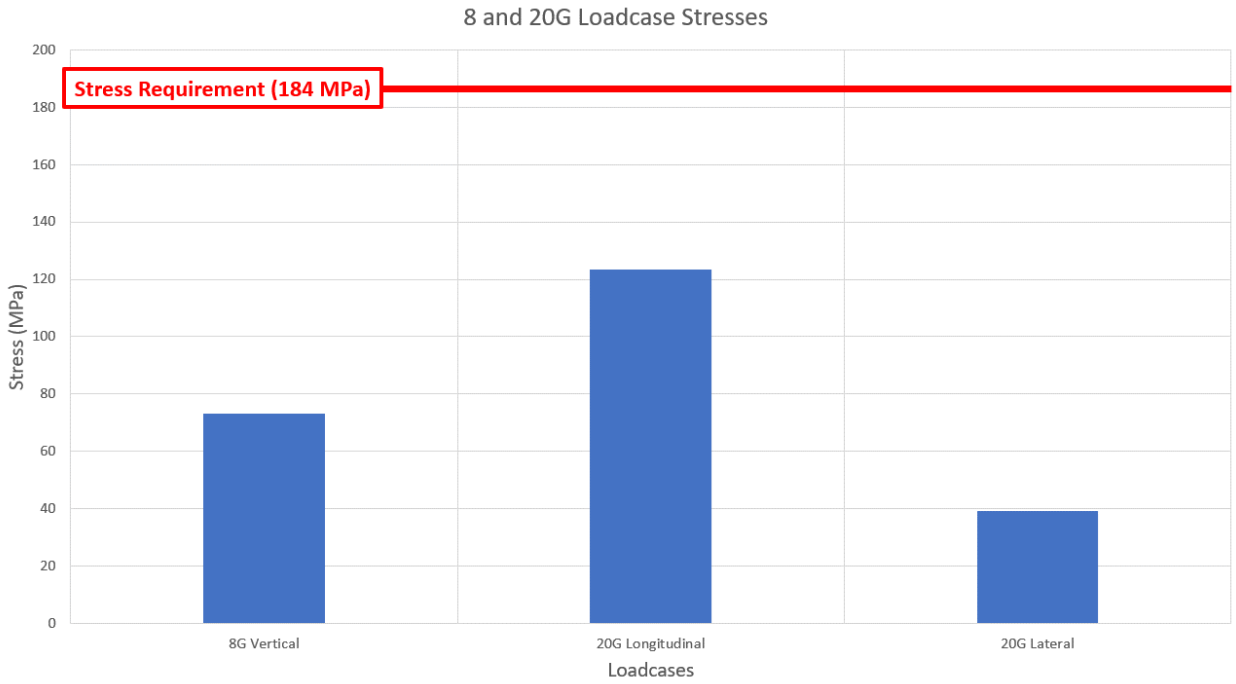

Figure 108: 8g and 20g stress results, with the maximum allowable stress in red

Stress contours of the final design for all loadcases are detailed in Appendix C.

7.4.2 Stiffness

Although stresses were just barely meeting requirements, stiffness was not as critical. Even with all tubes set to 0.049" wall thickness, displacements were well within the requirements set by GM. However, adding the 0.125" thick tubes to lower stresses did increase the stiffness of the cradle, as shown in Figure 109.

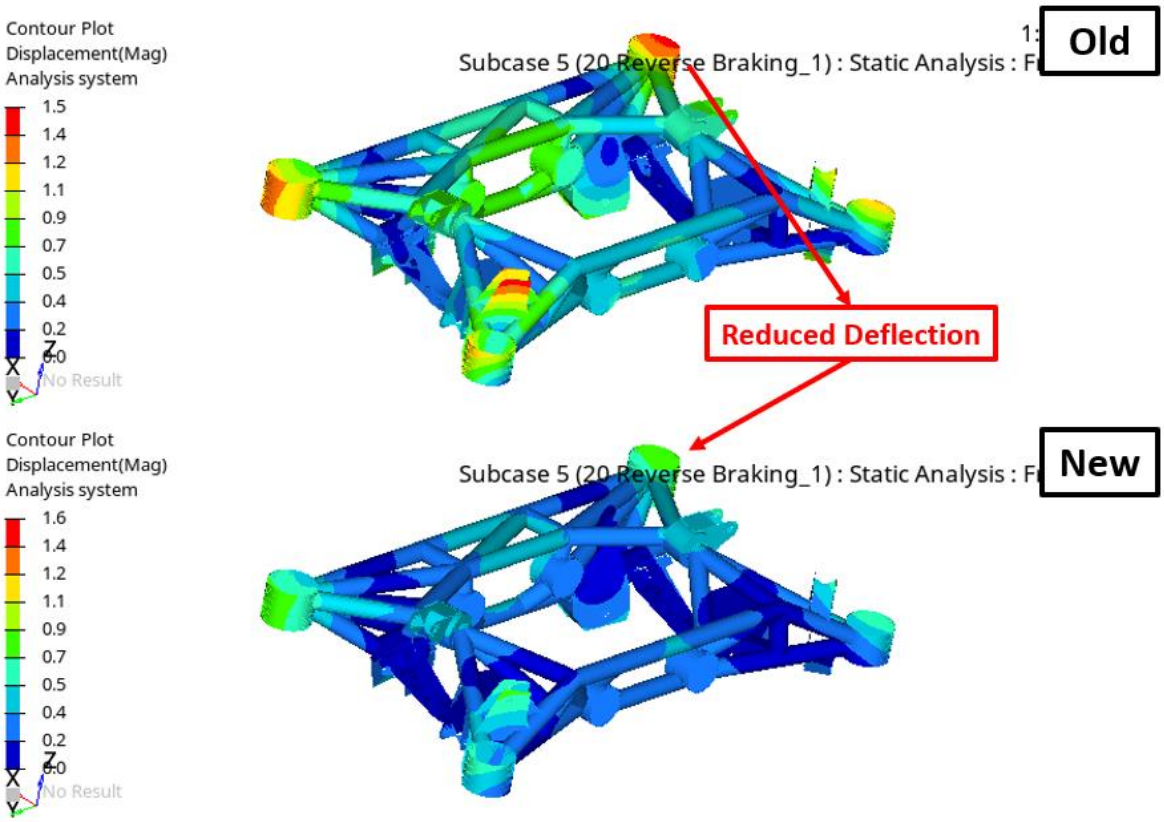

Figure 109: Reduced deflections due to thicker tube walls

As a matter of fact, what was critical in lowering displacements to within requirements was the inclusion of the front-rear member, which follows the earlier 1D beam studies mentioned in Chapter 6. Without this member, displacements would exceed requirements. The effect of adding this member to connect the front and rear halves of the cradle is illustrated in Figure 110, where certain loadcases would cause bending at the centre of the cradle.

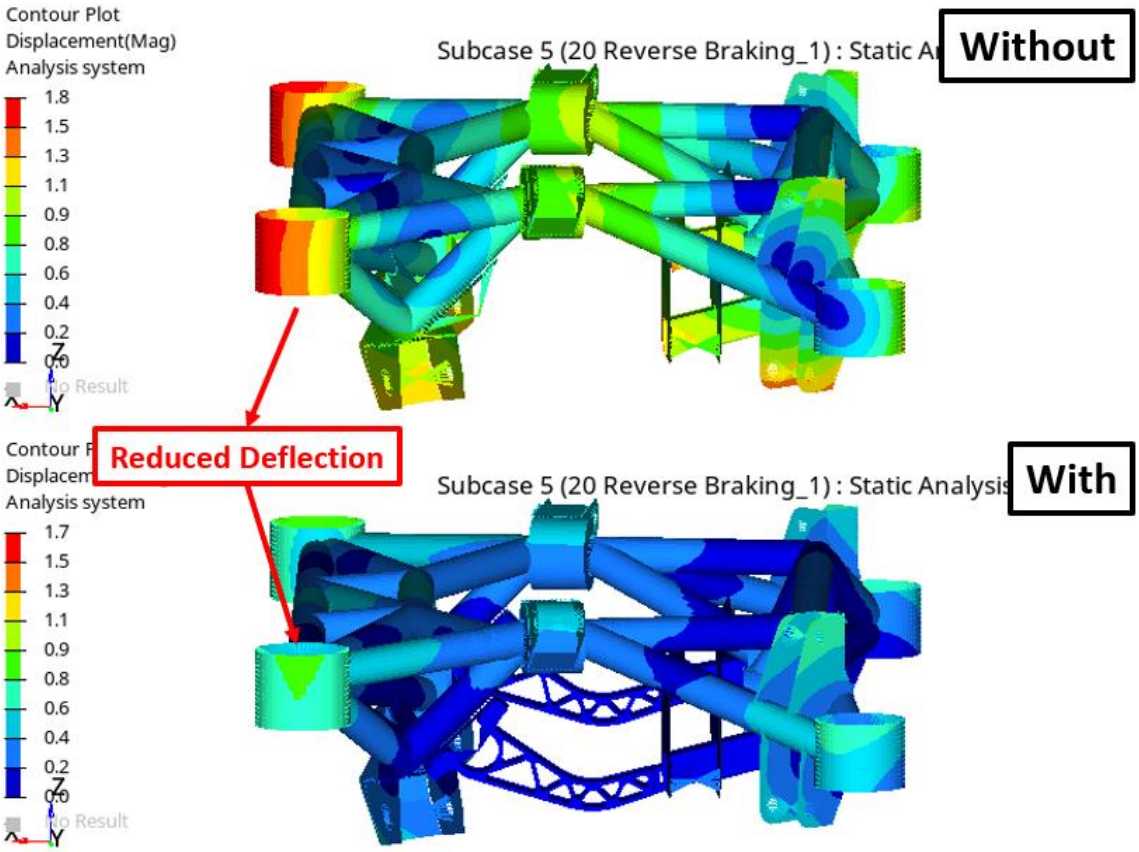

Figure 110: Reduced deflections due to front-rear member

As recalled from Chapter 4, the stiffness requirements of the cradle were defined such that deflection of any suspension hardpoint could not exceed 1 mm greater than those of the original GM analysis. There were a total of 14 hardpoints on the cradle coupled with 9 loadcases. As such, the displacement of each hardpoint for each loadcase was output and compared against the results of the original analysis. Due to NDA, absolute values could not be shown. As such, Figure 111 shows the relative displacements of the final analysis to the original – positive values indicate that the displacements exceeded that of the original, and negative values indicate the displacements were reduced. As depicted, none of the displacements exceed the +1 mm mark on the graph, which means that all stiffness requirements were satisfied.

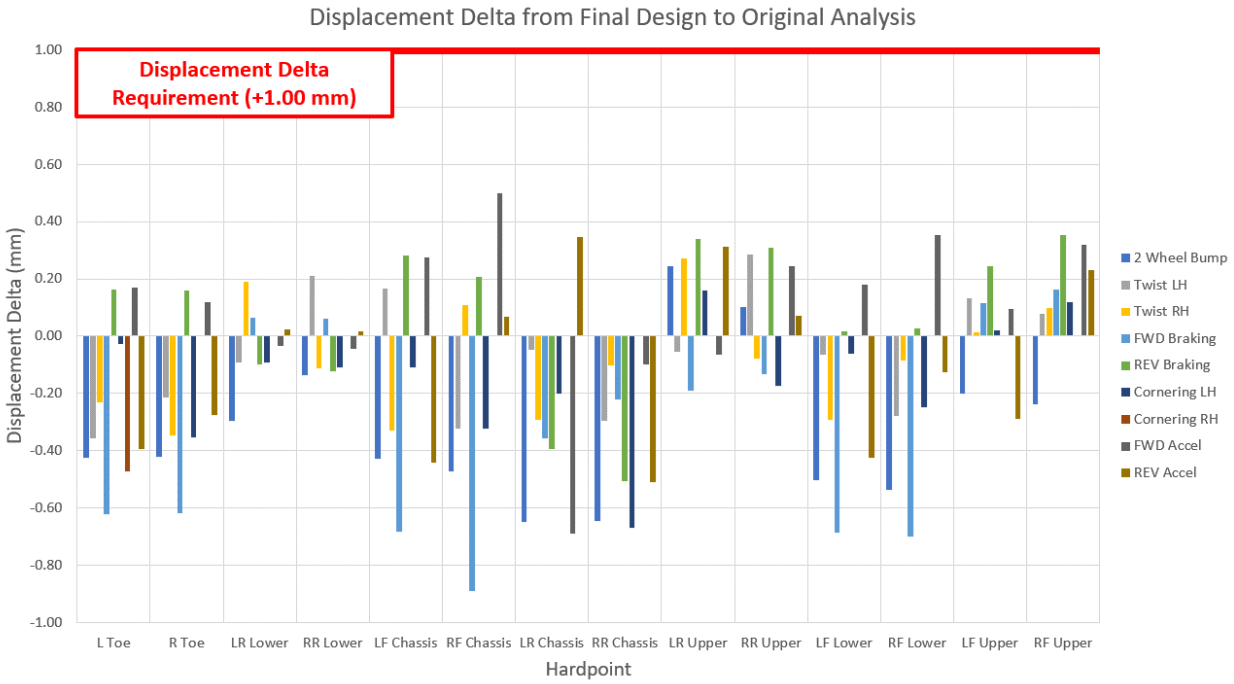

Figure 111: Displacement delta from final design to original analysis, showing the maximum allowable displacement in red

Stiffness contours of the final design for all loadcases are detailed in Appendix D.

Chapter 8
Summary

As a summary of all previous chapters, this section provides the reader with a flow chart outlining the procedure for developing a major structural component for a vehicle, with the constraints that a small shop or research group would have for prototyping. This chart can be used as a quick-reference guide during the design process, so the reader knows the immediate steps necessary to obtain a component that is lightweight while maintaining the structural integrity of the vehicle. Figure 112 shows the flow chart, with each of the steps segregated by thesis chapter.

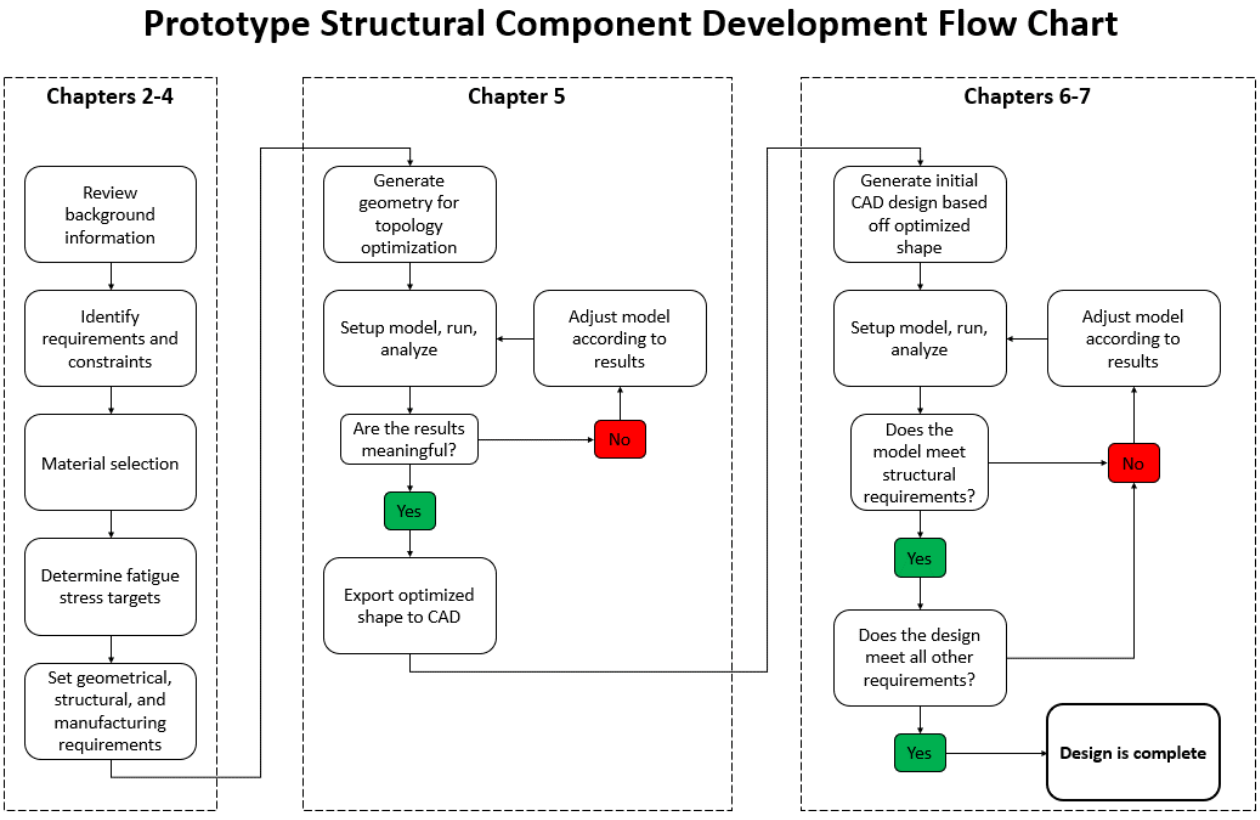

Figure 112: Flow chart depicting the full development process for a prototype structural component of a vehicle

Chapter 9
Conclusions

This thesis outlined the development for a major structural component of a vehicle within the limitations of small shops or groups producing one-off or a handful of components. The custom rear cradle for the UWAFT vehicle was used as an example. Various software tools were used, which resulted in a cradle that met all structural and manufacturability requirements while weighing only 43% of the cradle that was original to the stock vehicle.

Early in the development process, it was determined that 6061-T6 aluminum would be the most suitable material due to multiple factors such as availability, manufacturability, weight, and cost. This new material inherently needed new strength requirements to be set, given the material change from steel. As such, extensive fatigue calculations were performed to obtain resultant stress limits derived from cycle counts due to accumulated mileage. Stiffness requirements were set as well, with a maximum delta of 1 mm set from the original analysis. Material selection and setting stress targets are one of the most critical steps in development of a structural component, as it is critical to vehicle safety and has a major impact on resultant weight.

Next, other design requirements such as geometrical and manufacturing were defined. Given the numerous components that interact with the cradle, it was crucial to consider the needs of all components. For example, as the suspension links swing with suspension articulation, it was critical to ensure that unwanted contact between the links and cradle were prevented. Practicality was another factor as well – given the size of the e-axle, it was vital to ensure it could be installed and remove from the cradle with relative ease. This process would apply to any major component for a vehicle and is important to consider for serviceability and manufacturability.

As the cradle is a critical structural component of the vehicle, extensive analysis was needed to ensure the safety of the vehicle and minimize the weight of the component. Topology optimization was used to obtain a rough ideal structure shape and layout. With respect to the limitations in manufacturing, two primary construction methods were possible, which was to

fabricate the cradle from sheet metal or weld tubes to create a spaceframe. Preliminary studies were conducted to assess both methods, with the tubular spaceframe being the more optimal solution. Additionally, it was easier to replicate the optimized geometry by building a spaceframe, which followed the results of the study.

To minimize time between iterations, 1D beam analysis was used. Tube diameters and wall thicknesses were iterated until strength and stiffness requirements were met. The result of this analysis was used as reference for the final design, which was then analyzed with traditional FEA methods. In this analysis, there were still a few areas of high stress which necessitated increases in wall thickness for a few tubes. However, not many iterations were required due to the 1D study. With any structural component, similar analysis methods could be employed to reduce iteration time while still obtaining meaningful analysis results.

In the end, the completed design was projected at 9.4 kg, which was 43% of the cradle original to the vehicle at 21.8 kg and 40% of the 2019 cradle at 23.5 kg. Thus, all requirements were met, while achieving a significant reduction in weight. All the considerations and processes with respect to development of a rear cradle were effectively outlined in this thesis such that it may serve as a guide for the development of similar structural components that play a crucial part of a vehicle.

Chapter 10
Recommendations

1. **Further weight reduction with selective removal of material**

   In general, with any structural component stresses that are far lower than the requirement means there is room to safety reduce material, and thus weight. With the cradle, much iteration was done on tube diameter and wall thickness, however time constraints toward the latter half of the project meant the design of the suspension brackets and front-rear member were not as much of a focus. In reviewing the strength and stiffness results, there was some room to further reduce weight of these parts, while still meeting structural requirements.

   Increased fidelity of fatigue analysis

   Fatigue analysis was conducted solely on the basis of cycle counts coupled with a S-N curve for 6061-T6 aluminum. This was a conservative approach, as it assumes fully reversed cyclic stress accumulated through all 9 loadcases. However, this is not the case given differing stress levels throughout the part with each loadcase. There are software tools available that can do such detailed fatigue analysis, accounting for various stress levels throughout the component. As such, there is the potential for stress requirements to increase, which could lead to further reduction in weight.

2. **Investigate other materials**

   The entire cradle was set to use 6061-T6, which is an excellent grade of aluminum for this application. However, this specific material is prone to cracking with high bend angles; therefore, some of the suspension brackets had to be composed of multiple flat sections welded together. There are other grades of aluminum that are suitable for bending, such as 5052-H34 [146]. Using this grade of aluminum would reduce part complexity; however, it ties into the above point, where more extensive fatigue analysis would be required.

References

[1] B. Leard, J. Linn and Y. Zhou, "The Effect of Standards for New Vehicle Fuel Economy and GHG Emissions on US Consumers," Resources, 28 September 2017. [Online]. Available: https://www.resourcesmag.org/archives/the-effect-of-standards-for-new-vehicle-fuel-economy-and-ghg-emissions-on-us-consumers/. [Accessed 22 January 2021].

[2] U.S. Department of Energy Office of Energy Efficiency and Renewable Energy, "Energy Efficient Technologies," Oak Ridge National Laboratory, [Online]. Available: https://www.fueleconomy.gov/feg/tech_adv.shtml. [Accessed 22 January 2021].

[3] U.S. Department of Energy Office of Energy Efficiency and Renewable Energy, "Hybrid and Plug-In Electric Vehicle Conversions," Alternative Fuels Data Center, [Online]. Available: https://afdc.energy.gov/vehicles/electric_conversions.html. [Accessed 22 January 2021].

[4] N. Walji, "This Toronto businessman retrofits classic cars with electric motors," CBC, 3 October 2019. [Online]. Available: https://www.cbc.ca/news/technology/what-on-earth-newsletter-converting-electric-cars-1.5307221. [Accessed 22 January 2021].

[5] S. Stadler, K. Thum, M. Hirz and P. Rossbacher, "Conceptual Full-Vehicle Development supported by Integrated Computer-Aided Design Methods," *Computer-Aided Design and Applications,* pp. 159-172, August 2013.

[6] Argonne National Laboratory, "EcoCAR Mobility Challenge," Argonne National Laboratory, [Online]. Available: https://avtcseries.org/ecocar-mobility-challenge/. [Accessed 20 January 2021].

[7] Manufacturing.net, "Comparing Metal Parts Manufacturing Methods," Manufacturing.net, 30 July 2018. [Online]. Available: https://www.manufacturing.net/operations/article/13196732/comparing-metal-parts-manufacturing-methods. [Accessed 22 January 2021].

[8] S. Wells, "Space Frame Chassis," Motoring Weekly, 17 August 2017. [Online]. Available: https://www.motoringweekly.com.au/2017/08/17/space-frame-chassis/. [Accessed 6 February 2021].

[9] R. Bowen, "Atom Imposter: Building an Ariel Atom Replica From Scratch," Grassroots Motorsports, 17 July 2018. [Online]. Available: https://grassrootsmotorsports.com/articles/atom-imposter-building-ariel-atom-replica-scratch/. [Accessed 6 February 2021].

[10] A. Chesterton, "How many cars are there in the world?," carsguide, 6 August 2018. [Online]. Available: https://www.carsguide.com.au/car-advice/how-many-cars-are-there-in-the-world-70629#:~:text=There%20is%20an%20estimated%201.4,at%20around%2018%20per%20cent.. [Accessed 12 February 2021].

[11] J. Brandon, "How computers have revolutionised our cars," techradar, 4 July 2013. [Online]. Available: https://www.techradar.com/news/car-tech/how-computers-have-revolutionised-car-design-1160141. [Accessed 12 February 2021].

[12] International Energy Agency, "Global EV Outlook 2019," International Energy Agency, May 2019. [Online]. Available: https://www.iea.org/reports/global-ev-outlook-2019. [Accessed 12 February 2021].

[13] A. Weber, "Lightweighting Is Top Priority for Automotive Industry," Assembly Magazine, 7 June 2018. [Online]. Available: https://www.assemblymag.com/articles/94341-lightweighting-is-top-priority-for-automotive-industry. [Accessed 12 February 2021].

[14] B. Beckert, "Why Lightweighting is a Game Changer in Automotive Design," Altair, [Online]. Available: https://www.altair.com/c2r/sf2016/why-lightweighting-is-game-changer-automotive-design. [Accessed 12 February 2021].

[15] J. Lipshaw, "What is Lightweighting and How Does it Improve Fuel Economy in Vehicles?," Union of Concerned Scientists, 24 August 2020. [Online]. Available: https://blog.ucsusa.org/science-blogger/lightweighting-and-fuel-economy-in-vehicles. [Accessed 12 February 2021].

[16] D. Schmueser, "Vehicle Structural Analysis for Automotive Systems:," American Society for Engineering Education, 26-29 June 2016. [Online]. Available: https://pdfs.semanticscholar.org/30b3/b39eee08a8ac6e9eaeb2efb26bde04d6357b.pdf. [Accessed 12 February 2021].

[17] Toyota Motor Corporation, "How many parts is each car made of?," Toyota Motor Corporation, [Online]. Available: https://www.toyota.co.jp/en/kids/faq/d/01/04/. [Accessed 6 February 2021].

[18] A. Binder, "Automotive industry," Britannica, [Online]. Available: https://www.britannica.com/technology/automotive-industry/Ford-and-the-assembly-line. [Accessed 6 February 2021].

[19] European Aluminium, "The Aluminium Automotive Manual," European Aluminium, [Online]. Available: https://www.european-aluminium.eu/media/1558/aam-applications-chassis-suspension-1-subframes.pdf. [Accessed 6 February 2021].

[20] newsroom, "Marriages at Porsche," Porsche AG, 20 June 2014. [Online]. Available: https://newsroom.porsche.com/en/company/marriage-10780.html. [Accessed 7 February 2021].

[21] B. Davis, "E92 BMW M3 Coupe production ends, making way for F30," Performance Drive, 6 July 2013. [Online]. Available: https://performancedrive.com.au/e92-bmw-m3-coupe-production-ends-making-way-for-f30-0621/. [Accessed 6 February 2021].

[22] S. Corby, "What is NVH?," carsguide, 20 October 2015. [Online]. Available: https://www.carsguide.com.au/car-advice/what-is-nvh-36403. [Accessed 8 February 2021].

[23] M. Hirz, P. Rossbacher and J. Gulanova, "Future trends in CAD - from the perspective of automotive industry," *Computer-Aided Design and Applicatons,* vol. 14, no. 6, pp. 1-8, 2017.

[24] M. Vielhaber, H. Burr, T. Deubel, C. Weber and S. Haasis, "Assembly-oriented Design in Automotive Engineering," in *International Design Conference - Design 2004*, Dubrovnik, 2004.

[25] Bitchin'57, "Anyone using these tubular upper & lower control arms?," Chevy Tri Five Forum, 27 July 2016. [Online]. Available: https://www.trifive.com/threads/anyone-using-these-tubular-upper-lower-control-arms.159263/. [Accessed 15 February 2021].

[26] C.-H. Lee and A. Polycarpou, "Development of an Apparatus to Investigate Friction," *Tribology Transactions,* vol. 48, no. 4, pp. 505-514, 2005.

[27] 4x4Dustin, "Cv axle angles??," Ford F150 Forum, 13 December 2012. [Online]. Available: https://www.f150forum.com/f6/cv-axle-angles-184898/. [Accessed 10 February 2021].

[28] S. Park, Y. Jeon, D.-o. Kang, M.-s. Hyun and S.-j. Heo, "Predicting the Vehicle Performance at an Early Stage of Development Process via Suspension Bushing Design Tool," in *International Modelica Conference*, Regensburg, 2019.

[29] V. Kljaic, "How EVs Challenge Bushing Suppliers To Keep Things Quiet," suspension.com, 4 November 2015. [Online]. Available: https://www.suspension.com/blog/rubber-v-polyurethane-suspension-bushings/. [Accessed 16 February 2021].

[30] J. Lebowsky, "Drivetrain Design for the 2016 Global Formula Racing Combustion Car," Oregon State University, Corvallis, 2016.

[31] L. T. Borg, "An Approach to Using Finite Element Models to Predict Suspension Member Loads in a Formula SAE Vehicle," Virginia Polytechnic Institute, Blacksburg, 2009.

[32] H. Nguyen, Interviewee, *UWAFT Rear Cradle Development.* [Interview]. 23 July 2020.

[33] N. Dowling, "Mechanical Behavior of Materials," in *Mechanical Behavior of Materials - Engineering Methods for Deformation, Fracture, and Fatigue*, Upper Saddle River, Pearson Education Inc., 2012, pp. 416-417.

[34] YourMechanic, "Symptoms of a Bad or Failing Engine Mount," autoblog, 7 January 2016. [Online]. Available: https://www.autoblog.com/2016/01/07/symptoms-of-a-bad-or-failing-engine-mount/. [Accessed 15 February 2021].

[35] L. Jing, L. Wu, X. Li and Y. Zhang, "Study on kinematic and compliance test of suspension," in *IOP Conference Series: Materials Science and Engineering*, Singapore, 2017.

[36] P. Clarke, "Some of the Issues a Team Faces When Designing for FSG.," Formula Student Germany, 16 July 2014. [Online]. Available: https://www.formulastudent.de/pr/news/details/article/some-of-the-issues-a-team-faces-when-designing-for-fsg/#:~:text=The%20usual%20cause%20of%20toe,for%20a%20toe%20compliance%20link!. [Accessed 10 February 2021].

[37] H. Nguyen, Interviewee, *Rear Cradle Loading/Cycle Questions.* [Interview]. 4 February 2021.

[38] M. A. Fentahun and M. A. Savas, "Materials Used in Automotive Manufacture and Material Selection Using Ashby Charts," *International Journal of Materials Engineering,* vol. 8, no. 3, pp. 40-54, 2018.

[39] AZO Materials, "The Discovery of Metals," AZO Materials, 21 June 2012. [Online]. Available: https://www.azom.com/article.aspx?ArticleID=6101. [Accessed 16 February 2021].

[40] D. Brasher, "PR Guru," Automotive Steel – A History of Steel Within the Automotive Industry, 30 July 2018. [Online]. Available: http://www.prguru.com.au/automotive-steel-history-steel-within-automotive-industry/. [Accessed 16 February 2021].

[41] T. James, "Why Is Steel Used for Car Bodies?," Leaf Group Ltd., [Online]. Available: https://itstillruns.com/steel-used-car-bodies-7592134.html. [Accessed 16 February 2021].

[42] M. Tisza and I. Czinege, "Comparative study of the application of steels and aluminium in lightweight production of automotive parts," *International Journal of Lightweight Materials and Manufacture,* vol. 1, no. 4, pp. 229-238, 2018.

[43] Total Materia, "Automotive Uses of Magnesium Alloys: Part One," Keys to Metals AG, July 2010. [Online]. Available: https://www.totalmateria.com/page.aspx?ID=CheckArticle&site=ktn&NM=246. [Accessed 16 February 2021].

[44] Total Materia, "Automotive Uses of Magnesium Alloys: Part Two," Keys to Metals AG, August 2010. [Online]. Available:

https://www.totalmateria.com/page.aspx?ID=CheckArticle&site=ktn&NM=248. [Accessed 16 February 2021].

[45] G. Kardys, "Magnesium Car Parts: Cost Factors (Part 2)," Engineering360, 5 December 2017. [Online]. Available: https://insights.globalspec.com/article/7250/magnesium-car-parts-cost-factors-part-2. [Accessed 16 February 2021].

[46] C. Cavallo, "Steel vs. Titanium - Strength, Properties, and Uses," Thomas, [Online]. Available: https://www.thomasnet.com/articles/metals-metal-products/steel-vs-titanium-strength-properties-and-uses/. [Accessed 16 February 2021].

[47] G. Mathers, "Welding of Titanium and its Alloys - Part 1," TWI Ltd., [Online]. Available: https://www.twi-global.com/technical-knowledge/job-knowledge/welding-of-titanium-and-its-alloys-part-1-109. [Accessed 16 February 2021].

[48] AZO Materials, "Titanium for Automotive Applications," AZO Materials, 20 June 2001. [Online]. Available: https://www.azom.com/article.aspx?ArticleID=553. [Accessed 16 February 2021].

[49] B. Smith, "The Plastics Used in Automotives," AZO Materials, 23 October 2018. [Online]. Available: https://www.azom.com/article.aspx?ArticleID=17014. [Accessed 17 February 2021].

[50] SMLease Design, "Advantages and Disadvantages of Plastic Compared to Metal," SMLease Design, [Online]. Available: https://www.smlease.com/entries/plastic-design/advantages-and-limitations-of-plastics-over-metal/. [Accessed 17 February 2021].

[51] A. Pearson, "10 Disadvantages of 3D Printing Technology," 3D Insider, 24 January 2018. [Online]. Available: https://3dinsider.com/3d-printing-disadvantages/. [Accessed 17 February 2021].

[52] CompositesLab, "What Are Composites?," American Composites Manufacturers Association, [Online]. Available: http://compositeslab.com/composites-101/what-are-composites/. [Accessed 17 February 2021].

[53] I. Mackenzie, "Carbon fibre's journey from racetrack to hatchback," British Broadcasting Corporation, 10 March 2011. [Online]. Available: https://www.bbc.com/news/technology-12691062. [Accessed 17 February 2021].

[54] C. Latorre, "BMW i3: carbon fiber body," Plastix World, 10 October 2013. [Online]. Available: https://www.plastix-world.com/bmw-i3-carbon-fiber-body/. [Accessed 17 February 2021].

[55] Rock West Composites, "Yes – DIY Carbon Fiber Fabrication Is Possible," Rock West Composites, 5 November 2018. [Online]. Available: https://www.rockwestcomposites.com/blog/yes-diy-carbon-fiber-fabrication-is-possible/. [Accessed 17 February 2021].

[56] R. Lofland and C. Grant, "Composites 101 Workshop," Aerodef Manufacturing, 7-8 March 2017. [Online]. Available: https://www.aerodefevent.com/wp-content/uploads/2017/03/AeroDef-2017-Composites-101-Workshop.pdf. [Accessed 17 February 2021].

[57] A. Aronsson, "Design, Modeling and Drafting of Composite Structures," Luleå University of Technology, Luleå, 2005.

[58] Tuckey, "Most Common Metal Fabrication Processes and Applications," Tuckey, 24 April 2017. [Online]. Available: https://www.tuckey.com/blog/common-metal-fabrication-processes-applications/. [Accessed 17 February 2021].

[59] East West Manufacturing, "What is Design for Manufacturing or DFM?," East West Manufacturing, 24 March 2020. [Online]. Available: https://news.ewmfg.com/blog/manufacturing/dfm-design-for-manufacturing. [Accessed 17 February 2021].

[60] GearSolutions, "Forging Foundations," GearSolutions, [Online]. Available: https://gearsolutions.com/features/forging-foundations/. [Accessed 18 February 2021].

[61] Reliance Foundry, "Make it Snappy: Rapid Prototyping for Metalwork," Reliance Foundry, [Online]. Available: https://www.reliance-foundry.com/blog/rapid-prototyping. [Accessed 18 February 2021].

[62] formlabs, "3D Printing Technology Comparison: FDM vs. SLA vs. SLS," formlabs, [Online]. Available: https://formlabs.com/blog/fdm-vs-sla-vs-sls-how-to-choose-the-right-3d-printing-technology/. [Accessed 18 February 2021].

[63] CompositesWorld, "Materials & Processes: Fabrication methods," CompositesWorld, 23 March 2016. [Online]. Available: https://www.compositesworld.com/articles/fabrication-methods. [Accessed 18 February 2021].

[64] Easy Composites Ltd., "Trimming and Assembling a Carbon Fibre Bonnet (or Similar Panel)," Easy Composites Ltd., 22 April 2012. [Online]. Available: https://www.easycomposites.co.uk/learning/how-to-trim-finish-and-assemble-a-carbon-fibre-bonnet. [Accessed 18 February 2021].

[65] R. Evans, "What methods are used to join materials?," Medical Design & Outsourcing, 8 August 2016. [Online]. Available: https://www.medicaldesignandoutsourcing.com/methods-used-join-materials/. [Accessed 18 February 2021].

[66] R. N. Waje, "Advantages and disadvantages of bolted joints," Mechstudy, 2 September 2020. [Online]. Available: https://www.mechstudy.com/2020/09/advantages-and-disadvantages-of-bolted.html. [Accessed 18 February 2021].

[67] K. Vyas, "Types Of Welding: Applications, Advantages, and Disadvantages," Interesting Engineering, 6 February 2021. [Online]. Available: https://interestingengineering.com/types-of-welding-their-applications-advantages-and-disadvantages. [Accessed 18 February 2021].

[68] B. Kinsey and X. Wu, Tailor Welded Blanks for Advanced Manufacturing, Cambridge: Woodhead Publishing, 2011.

[69] TWI Ltd., "What is the Heat Affected Zone (HAZ)?," TWI Ltd., [Online]. Available: https://www.twi-global.com/technical-knowledge/faqs/what-is-the-heat-affected-zone. [Accessed 18 February 2021].

[70] TWI Ltd., "What is Friction Stir Welding (FSW)? - Process and Applications," TWI Ltd., [Online]. Available: https://www.twi-global.com/technical-knowledge/faqs/faq-what-is-friction-stir-welding. [Accessed 18 February 2021].

[71] Kaempf & Harris, "Is There A Difference Between Welding And Soldering?," Kaempf & Harris, [Online]. Available: https://www.kaempfandharris.com/industry-news/difference-between-welding-and-soldering. [Accessed 18 February 2021].

[72] J. Sprovieri, "Adhesives and Automobiles," Assembly Magazine, 17 December 2007. [Online]. Available: https://www.assemblymag.com/articles/85099-adhesives-and-automobiles. [Accessed 18 February 2021].

[73] D. Kopeliovich, "Adhesive bonding (introduction)," SubsTech, [Online]. Available: https://www.substech.com/dokuwiki/doku.php?id=adhesive_bonding_introduction. [Accessed 18 February 2021].

[74] AdhesivesToolKit, "Cleavage Tests," AdhesivesToolKit, [Online]. Available: http://www.adhesivestoolkit.com/Docs/test/MECHANICAL%20TEST%20METHOD%201%20-%20Cleavage%20Tests.xtp. [Accessed 18 February 2021].

[75] Permabond, "The Importance of Surface Preparation," Permabond, [Online]. Available: https://www.permabond.com/resource-center/the-importance-of-surface-preparation-2/. [Accessed 19 February 2021].

[76] Adhesive Design Toolkit, "Mechanical Test Methods," Adhesive Design Toolkit, [Online]. Available: http://www.adhesivestoolkit.com/Docs/test/MECHANICAL%20TEST%20METHOD%201.xtp. [Accessed 19 February 2021].

[77] M. Bedworth, "MODIFYING CARS, WHY DO YOU DO IT?," Drivetribe, [Online]. Available: https://drivetribe.com/p/modifying-cars-why-do-you-do-it-UXUMVOg7SuCzVWJqzn_qHw?iid=d7bimnrfQvGT8gVOW3J2SA. [Accessed 3 February 2021].

[78] Verus Engineering, "7000 Series Rear LCA Kit - Subaru WRX/STI (08-Current), BRZ/FRS/GT86 (2013-Current)," Verus Engineering, [Online]. Available: https://www.verus-engineering.com/shop/product/7000-series-rear-lca-kit-subaru-wrx-sti-08-current-brz-frs-gt86-2013-current-346. [Accessed 22 February 2021].

[79] Turkish, "Best LCA's?," ft86club, 29 January 2015. [Online]. Available: https://www.ft86club.com/forums/showthread.php?p=2112222. [Accessed 22 February 2021].

[80] Treasure Coast Miata & Jeeps, "Browse Suspension, Chassis, Steering, Brakes Products," Treasure Coast Miata & Jeeps, [Online]. Available: https://treasurecoastmiata.com/c-370447-used-miata-parts-miata-99-05-suspension-chassis-steering-brakes.html. [Accessed 22 February 2021].

[81] 5. Miata, "DIY 306 Miata Swap," StangNet, 11 January 2010. [Online]. Available: https://www.stangnet.com/mustang-forums/threads/diy-306-miata-swap.804656/. [Accessed 22 February 2021].

[82] Grannas Racing, "Ultimate IRS - Supra Tubular Subframe Cradle," Grannas Racing, [Online]. Available: https://www.grannasracing.com/products/grannas-racing-ultimate-irs?variant=621566492688. [Accessed 24 February 2021].

[83] D. Triantos and M. Michaels, "Design and Fabrication of an Aluminum Engine Cradle for a General Motors Vehicle," Society of Automotive Engineers, Detroit, 1999.

[84] Verus Engineering, "About Us," Verus Engineering, [Online]. Available: https://www.verus-engineering.com/aboutus. [Accessed 24 February 2021].

[85] J. Sasseen, "Mechanics warn about poor quality parts," HeraldNet, 30 December 2016. [Online]. Available: https://www.heraldnet.com/business/mechanics-warn-about-poor-quality-parts/. [Accessed 24 February 2021].

[86] chezzy79, "RACER X FRONT LOWER CONTROL ARM FAILURE WHILE DRIVING ON HIGHWAY: UPDATE WITH MORE D," ft86club, 4 March 2017. [Online]. Available: https://www.ft86club.com/forums/showthread.php?p=2865556. [Accessed 24 February 2021].

[87] Argonne National Laboratory, "University of Waterloo - About Us," U.S. Department of Energy, [Online]. Available: https://avtcseries.org/ecocar-mobility-challenge/teams/university-of-waterloo/about-us/. [Accessed 3 August 2021].

[88] Argonne National Laboratory, "AVTC History," Argonne National Laboratory, [Online]. Available: https://avtcseries.org/avtc-history/. [Accessed 24 February 2021].

[89] Argonne National Laboratory, "EcoCAR Mobility Challenge," Argonne National Laboratory, [Online]. Available: https://avtcseries.org/ecocar-mobility-challenge/. [Accessed 24 February 2021].

[90] MAHLE GmbH, "Through the Road Parallel Hybrid," MAHLE GmbH, [Online]. Available: https://www.mahle-powertrain.com/en/experience/through-the-road-parallel-hybrid/. [Accessed 24 February 2021].

[91] P. Janssen, "Highly Integrated Electric Drive Unit For Passenger Cars," Auto Tech Review, 13 December 2018. [Online]. Available: https://autotechreview.com/technology/highly-integrated-electric-drive-unit-for-passenger-cars. [Accessed 24 February 2021].

[92] American Axle & Manufacturing, Inc., "Who We Are," American Axle & Manufacturing, Inc., [Online]. Available: https://www.aam.com/who-we-are. [Accessed 24 February 2021].

[93] American Axle & Manufacturing Inc., "AAM's Electric Drive System Powers New Jaguar I-PACE," American Axle & Manufacturing Inc., 8 August 2019. [Online]. Available: https://www.aam.com/media/story/aam-s-electric-drive-system-powers-new-jaguar-i-pace. [Accessed 24 February 2021].

[94] University of Waterloo EcoCAR Team, "Architecture Selection Report," University of Waterloo EcoCAR Team, Waterloo, 2019.

[95] Argonne National Laboratory, "Non-Year Specific Rules," Argonne National Laboratory, Chicago, 2021.

[96] General Motors, "ECOCAR REAR CRADLE WAIVER ANALYSIS PROCESS," General Motors, Detroit, 2019.

[97] D. Askeland, P. Fulay and W. Wright, The Science and Engineering of Materials, Stamford: Global Engineering, 2010.

[98] Chicago Metal Rolled Products, "Exploring the Stress / Strain Curve for Mild Steel," Chicago Metal Rolled Products, [Online]. Available: https://www.cmrp.com/blog/faq/analysis-design/exploring-stress-strain-curve-mild-steel.html. [Accessed 18 June 2021].

[99] S. Davis and R. Boundy, Transportation Energy Data Book, Oak Ridge: Oak Ridge National Laboratory, 2021.

[100] J. C. Ahlbrandt, "Mechanical Properties of Rapid Manufacturing and Plastic Injection," University of Missouri - Columbia, Columbia, 2014.

[101] Formlabs, "Validating Isotropy in SLA 3D Printing," Formlabs, [Online]. Available: https://formlabs.com/blog/isotropy-in-SLA-3D-printing/. [Accessed 23 June 2021].

[102] M. Brain, "How Stereolithography 3-D Layering Works," howstuffworks, [Online]. Available: https://computer.howstuffworks.com/stereolith.htm. [Accessed 23 June 2021].

[103] Cote's Auto Body Inc., "https://cotesautobody.com/top-5-common-types-of-metal-used-in-car-manufacturing/," Cote's Auto Body Inc., 15 September 2018. [Online]. Available: https://cotesautobody.com/top-5-common-types-of-metal-used-in-car-manufacturing/#. [Accessed 23 June 2021].

[104] Keronite, "Selecting the right lightweight metal," Keronite, 21 April 2020. [Online]. Available: https://blog.keronite.com/selecting-the-right-lightweight-metal. [Accessed 23 June 2021].

[105] Alro Steel, "Aluminum Plate," Alro Steel, [Online]. Available: https://www.alro.com/divsteel/metals_comp_type.aspx?Mat=ALUMINUM&Type=Plate&mc=AL. [Accessed 23 June 2021].

[106] F. Armao, "Aluminum Workshop: Achieving T6 designation for 6061," The Welder, 14 March 2011. [Online]. Available: https://www.thefabricator.com/thewelder/article/aluminumwelding/achieving-t6-designation-for-6061. [Accessed 23 June 2021].

[107] D. Menzies, "Speed humps: effective speed control or just political meddling?," The Globe and Mail, 4 September 2014. [Online]. Available: https://www.theglobeandmail.com/globe-drive/culture/commuting/toronto-get-ready-for-even-more-speed-humps/article20332471/. [Accessed 19 June 2021].

[108] V. Stevanovic-Briatico, "City of Toronto Road Classification System," City of Toronto, Toronto, 2013.

[109] Transport Canada, "Grade Crossings Inventory," Transport Canada, Toronto, 2020.

[110] Harper's Magazine, "Harper's Index," Harper's Magazine, [Online]. Available: https://harpers.org/harpers-index/2012/10/potholes-in-the-united-states/. [Accessed 19 June 2021].

[111] American Road & Transportation Builders Association, "Frequently Asked Questions," American Road & Transportation Builders Association, [Online]. Available: https://www.artba.org/about/faq/#:~:text=In%202017%2C%20there%20were%204.18,to%20the%20Federal%20Highway%20Administration.. [Accessed 19 June 2020].

[112] City of Toronto, "Traffic Lights," City of Toronto, [Online]. Available: https://www.toronto.ca/services-payments/streets-parking-transportation/traffic-management/traffic-signals-street-signs/types-of-traffic-signals/traffic-lights/. [Accessed 19 June 2021].

[113] R. Johnson, "Solo Course Design," Sports Car Club of America, Houston, 2014.

[114] General Motors, "Load Case and Related Cycle Count," General Motors, Detroit, 2020.

[115] C. Doug, "EDU4 Assembly Interface Document," American Axle & Manufacturing Inc., Detroit, 2020.

[116] C. Tragakis, "What is Torque Steer?," CJ Pony Parts, 2020 30 June. [Online]. Available: https://www.cjponyparts.com/resources/what-is-torque-steer#:~:text=Torque%20steer%20is%20most%20often,t%20prone%20to%20torque%20steer.. [Accessed 2021 24 June].

[117] X-Engineer, "Drivetrain losses (efficiency)," X-Engineer, [Online]. Available: https://x-engineer.org/automotive-engineering/drivetrain/transmissions/drivetrain-losses-efficiency/. [Accessed 24 June 2021].

[118] iCrank, "Suggested Wrench Clearances," iCrank, [Online]. Available: http://icrank.com/cgi-bin/pageman/pageout.cgi?path=/data/wrench/wrench.html&t=2. [Accessed 24 June 2021].

[119] J. Bi, S. Eyl and G. Dimitrova, "Rubber bushing design and shape optimization based on fatigue life prediction," Dassault Systemes Simulia Corp., Johnston, 2015.

[120] Aerospace Specification Metals Inc., "Aluminum 6061-T6; 6061-T651," Aerospace Specification Metals Inc., [Online]. Available: http://asm.matweb.com/search/SpecificMaterial.asp?bassnum=MA6061T6. [Accessed 25 June 2021].

[121] T. Best, S. Neads, J. Whitehead and I. Willows, "Design and Operation of a New Vehicle Suspension Kinematics and Compliance Facility," *Journal of Passenger Cars: Part 1,* vol. 106, no. 6, pp. 34-44, 1997.

[122] M. Tunc, "Computerized Cost Estimation for Forging Industry," The Middle East Technical University, Ankara, 2003.

[123] "Comparing Metal Parts Manufacturing Methods," Manufacturing.net, 30 July 2018. [Online]. Available: https://www.manufacturing.net/operations/article/13196732/comparing-metal-parts-manufacturing-methods. [Accessed 25 June 2021].

[124] University of Waterloo, "Engineering Machine Shop Equipment," University of Waterloo, [Online]. Available: https://uwaterloo.ca/engineering-machine-shop/equipment. [Accessed 25 June 2021].

[125] A. B. Varotsis, "Introduction to metal 3D printing," Hubs, [Online]. Available: https://www.hubs.com/knowledge-base/introduction-metal-3d-printing/. [Accessed 25 June 2021].

[126] Protech Asia, "How Much Does CNC Machining Cost: The Important Things to Know," Protech Asia, 26 December 2020. [Online]. Available: https://prototechasia.com/en/how-much-does-cnc-machining-cost. [Accessed 25 June 2021].

[127] L. Langnau, "What is topology optimization?," Make Parts Fast, 14 August 2019. [Online]. Available: https://www.makepartsfast.com/what-is-topology-optimization/. [Accessed 26 June 2021].

[128] enlyft, "Companies using Altair Hyperworks," enlyft, [Online]. Available: https://enlyft.com/tech/products/altair-hyperworks. [Accessed 27 June 2021].

[129] F. Burger, "General Modeling Guidelines for Stamped Steel Welded Fabrications Used in Chassis Structures & Suspensions," General Motors, Detroit, 2013.

[130] M. Sanew, Director, *2021 Chevy Blazer | The Art of Phoning It In.* [Film]. United States of America: savagegeese, 2021.

[131] R. Janczur, "Vertical Accelerations of the Body of a Motor Vehicle when Crossing a Speed Bump," Cacow University of Technology, Cacow, 2015.

[132] CopRadar.com, "Acceleration Parameters," CopRadar.com, [Online]. Available: https://copradar.com/chapts/references/acceleration.html. [Accessed 27 June 2021].

[133] R. Dienemann, A. Schumacher and S. Fiebig, "An Element Deactivation and Reactivation Scheme for the Topology Optimization Based on the Density Method," Chair for Optimization of Mechanical Structures, Braunschweig, 2017.

[134] Altair Engineering Inc., "Optistruct Verification Manual," Altair Engineering Inc., Troy, 2017.

[135] Protech Asia, "3 Key questions about CNC machining," Protech Asia, [Online]. Available: https://prototechasia.com/en/plastic-cnc-machining/questions-cnc-machining. [Accessed 27 June 2021].

[136] L. Zhang, "Implementation of a beam element in finite element analysis," Brown University, Providence, 2013.

[137] R. Hibbeler, Mechanics of Materials, Hoboken: Pearson, 2011.

[138] T. S. Chawla and E. Leonhardt, "Two Approaches to Optimize Formula SAE Chassis Design Using Finite Element Analysis," Western Washington University, Bellingham, 2018.

[139] Centurial Inc., "The perfect tube coping or pipe notching tool! You need this tool!!," YouTube, 19 January 2020. [Online]. Available: https://www.youtube.com/watch?v=SYvkx5JlWCs. [Accessed 12 July 2021].

[140] VR3 Engineering, "Our Process, Your Project Incredibly accurate tube structures," VR3 Engineering, [Online]. Available: https://vr3.ca/our-process/. [Accessed 12 July 2021].

[141] Miller Mechanical Services, Inc., "Nesting on a Waterjet," Miller Mechanical Services, Inc., 4 December 2015. [Online]. Available: https://www.millermech.com/2015/water-jet/nesting-on-a-waterjet/. [Accessed 12 July 2021].

[142] N. Carter, "Review of the Robitek clamp set for the Taig milling machine," [Online]. Available: http://www.cartertools.com/robitek.html. [Accessed 12 July 2021].

[143] University of Florida, "Boring on the Lathe," University of Florida, [Online]. Available: https://mae.ufl.edu/designlab/Advanced%20Manufacturing/Lathe%20Boring/Boring%20on%20Lathe.htm. [Accessed 12 July 2021].

[144] CNC Machinist Training, "Machine Shop Rates – What's the Average Hourly Rate," CNC Machinist Training, [Online]. Available: https://cncmachinisttraining.com/2013/08/16/machine-shop-rates-whats-the-average-hourly-rate/. [Accessed 16 July 2021].

[145] ESAB, "The HAZ In Aluminum Welds," ESAB KNOWLEDGE CENTER, [Online]. Available: https://www.esabna.com/us/en/education/blog/the-haz-in-aluminum-welds.cfm. [Accessed 15 July 2021].

[146] Industrial Metal Supply Co., "Differences between 6061 Aluminum and 5052 Aluminum," Industrial Metal Supply Co., 9 October 2020. [Online]. Available: https://www.industrialmetalsupply.com/blog/6061-vs-5052-aluminum. [Accessed 15 July 2021].

[147] W. Pemberton, "Custom Motor Mounts - Mount any Motor/Tranny in any Frame," how-to-build-hotorods.com, [Online]. Available: http://www.how-to-build-hotrods.com/custom-motor-mounts.html. [Accessed 16 February 2021].

[148] actually_iceman, "reddit," reddit, 10 January 2020. [Online]. Available: https://www.reddit.com/r/AwesomeCarMods/comments/emxdhh/rob_dahms_awd_billet_turbo_4_rotor_rx7_capable_of/. [Accessed 22 February 2021].

[149] D. D. Carbonare, "Speedhunters," An AWD, Turbo, 4-Rotor RX-7. What?!, 2 November 2016. [Online]. Available: http://www.speedhunters.com/2016/11/awd-4-rotor-fd3s-sema/. [Accessed 22 February 2021].

[150] D. Wegener, "Kinematic and Compliance Test Rig (K&C)," fka, [Online]. Available: https://www.fka.de/en/testing/chassis/110-kinematic-and-compliance-test-rig.html. [Accessed 25 June 2021].

[151] H. Nguyen, Interviewee, *UWAFT Rear Cradle Development.* [Interview]. 29 July 2020.

[152] FEA Training Consultants Inc., "Using Weldments and its features," Dassault Systemes, 25 January 2016. [Online]. Available: https://blogs.solidworks.com/tech/2016/01/using-weldments-features.html. [Accessed 30 June 2021].

Appendix A

Added Loads from E-Axle

	A	B
1	**Loads from Motor Torque**	
2	Horizontal distance from axle to centre of front bushing (mm)	182.700
3	Vertical distance from axle to centre of front bushing (mm)	10.045
4	Horizontal distance from axle to centre of rear bushing (mm)	183.250
5	Vertical distance from axle to centre of rear bushing (mm)	9.500
6	Max motor torque (Nm)	351.000
7		
8	Resultant angle to horizontal for front (rad)	0.055
9	Resultant angle to horizontal for rear (rad)	0.052
10	Resultant distance for axle to centre of front bushing (mm)	182.976
11	Resultant distance for axle to centre of rear bushing (mm)	183.496
12		
13	Resultant force at front bushing (N)	479.571
14	Resultant force at rear bushing (N)	478.212
15		
16	Resultant vertical force at front bushing (N)	478.848
17	Resultant horizontal force at front bushing (N)	26.327
18	Resultant vertical force at rear bushing (N)	477.571
19	Resultant horizontal force at rear bushing (N)	24.758
20		
21	**Loads from Gravity**	
22	Motor Weight (kg)	74
23	Force from Motor for 1G per bushing (N)	181.485

	C	D	E	F	G	H	I	J	K	L	M	N	O	P	Q
		Loadcase		**FL**			**FR**			**RL**			**RR**		
		Direction	**X**	**Y**	**Z**	**X**	**Y**	**Z**	**X**	**Y**	**Z**	**X**	**Y**	**Z**	**Notes**
		2 Wheel Bump	0.000	0.000	-362.970	0.000	0.000	-362.970	0.000	0.000	-362.970	0.000	0.000	-362.970	2G vertical bump
		Twist LH	0.000	0.000	-181.485	0.000	0.000	-181.485	0.000	0.000	-181.485	0.000	0.000	-181.485	1G gravity
		Twist RH	0.000	0.000	-181.485	0.000	0.000	-181.485	0.000	0.000	-181.485	0.000	0.000	-181.485	1G gravity
		FWD Braking	-155.158	0.000	-660.333	-155.158	0.000	-660.333	-206.243	0.000	296.086	-206.243	0.000	296.086	1G gravity + 1G decel + 351 Nm rev torque loading
		REV Braking	155.158	0.000	297.363	155.158	0.000	297.363	206.243	0.000	-659.056	206.243	0.000	-659.056	1G gravity + 1G accel + 351 Nm fwd torque loading
		Cornering LH	0.000	181.485	-181.485	0.000	181.485	-181.485	0.000	181.485	-181.485	0.000	181.485	-181.485	1G gravity + 1G cornering
		Cornering RH	0.000	-181.485	-181.485	0.000	-181.485	-181.485	0.000	-181.485	-181.485	0.000	-181.485	-181.485	1G gravity + 1G cornering
		FWD Accel	155.158	0.000	297.363	155.158	0.000	297.363	206.243	0.000	-659.056	206.243	0.000	-659.056	1G gravity + 1G accel + 351 Nm fwd torque loading
		Rev Accel	-155.158	0.000	-660.333	-155.158	0.000	-660.333	-206.243	0.000	296.086	-206.243	0.000	296.086	1G gravity + 1G decel + 351 Nm rev torque loading

	A	B
1	**Loads from Motor Torque**	
2	Horizontal distance from axle to centre of front bushing (mm)	182.7
3	Vertical distance from axle to centre of front bushing (mm)	10.045
4	Horizontal distance from axle to centre of rear bushing (mm)	183.25
5	Vertical distance from axle to centre of rear bushing (mm)	9.5
6	Max motor torque (Nm)	351
7		
8	Resultant angle to horizontal for front (rad)	=ATAN(B3/B2)
9	Resultant angle to horizontal for rear (rad)	=ATAN(B5/B4)
10	Resultant distance for axle to centre of front bushing (mm)	=SQRT(B2^B2+B3^B3)
11	Resultant distance for axle to centre of rear bushing (mm)	=SQRT(B5^B5+B4^B4)
12		
13	Resultant force at front bushing (N)	=(B6/4)/(B10/1000)
14	Resultant force at rear bushing (N)	=(B6/4)/(B11/1000)
15		
16	Resultant vertical force at front bushing (N)	=B13*COS(B8)
17	Resultant horizontal force at front bushing (N)	=B13*SIN(B8)
18	Resultant vertical force at rear bushing (N)	=B14*COS(B9)
19	Resultant horizontal force at rear bushing (N)	=B14*SIN(B9)
20		
21	**Loads from Gravity**	
22	Motor Weight (kg)	74
23	Force from Motor for 1G per bushing (N)	=B22/4*9.81

	C	D	E	F	G	H	I	J	K	L	M	N	O	P	Q
		Loadcase		**FL**			**FR**			**RL**			**RR**		
		Direction	**X**	**Y**	**Z**	**X**	**Y**	**Z**	**X**	**Y**	**Z**	**X**	**Y**	**Z**	**Notes**
		2 Wheel Bump	0	0	=-B23*2	0	0	=-B23*2	0	0	=-B23*2	0	0	=-B23*2	2G vertical bump
		Twist LH	0	0	=-B23	0	0	=-B23	0	0	=-B23	0	0	=-B23	1G gravity
		Twist RH	0	0	=-B23	0	0	=-B23	0	0	=-B23	0	0	=-B23	1G gravity
		FWD Braking	=-B23+B17	0	=-B23+B16	=-B23+B17	0	=-B23+B16	=-B23+B19	0	=-B23+B18	=-B23+B19	0	=-B23+B18	1G gravity + 1G decel + 351 Nm rev torque loading
		REV Braking	=B23+B17	0	=-B23+B16	=B23+B17	0	=-B23+B16	=B23+B19	0	=-B23+B18	=B23+B19	0	=-B23+B18	1G gravity + 1G accel + 351 Nm fwd torque loading
		Cornering LH	0	=B23	=-B23	0	=B23	=-B23	0	=B23	=-B23	0	=B23	=-B23	1G gravity + 1G cornering
		Cornering RH	0	=-B23	=-B23	0	=-B23	=-B23	0	=-B23	=-B23	0	=-B23	=-B23	1G gravity + 1G cornering
		FWD Accel	=E7	=F7	=G7	=H7	=I7	=J7	=K7	=L7	=M7	=N7	=O7	=P7	1G gravity + 1G accel + 351 Nm fwd torque loading
		Rev Accel	=E6	=F6	=G6	=H6	=I6	=J6	=K6	=L6	=M6	=N6	=O6	=P6	1G gravity + 1G decel + 351 Nm rev torque loading

Appendix B

Project Cost

	A	B	C	D	E	F	G	H	I	J	K	L	M	N	O	P	Q	R	S
1	**Main Structure**				**Suspension Brackets**				**Front-Rear Member**				**Bushing Mounts**				**Jig**		
2																			
3	Length from Cradle				2'x2'x1/8" Aluminum Sheet	92.11	$		12"x12"x1-1/2" Aluminum	142.36	$		4"x3.5"x6" Round Aluminum Tube	38.63	$		Estimate*	1000	$
4	1.5"x0.049" Aluminum Round Tube	9046	mm										3-1/4"x3"x6" Aluminum Tube	68.09	$		Conservative		
5		356.141732	in																
6	1.5"x0.125" Aluminum Round Tube	1273	mm																
7		50.1181102	in																
8	1.5"x0.049" Aluminum Square Tube	809	mm																
9		31.8503937	in																
10	3"x0.125" Aluminum Round Tube	120	mm																
11		4.72440945	in																
12																			
13	Raw Material Cost																		
14	1.5"x0.049" Aluminum Round Tube	64.52	72	in															
15	1.5"x0.125" Aluminum Round Tube	63.38	72	in															
16	1.5"x0.049" Aluminum Square Tube	14.36	36	in															
17	3"x0.125" Aluminum Round Tube	37.9	12	in															
18																			
19	Total Cost																		
20	1.5"x0.049" Aluminum Round Tube	319.142563	$																
21	1.5"x0.125" Aluminum Round Tube	44.1178587	$																
22	1.5"x0.049" Aluminum Square Tube	12.7047682	$																
23	3"x0.125" Aluminum Round Tube	14.9212598	$																
24																			
25	**SUMMARY**																		
26	Total Cost	1732.07645	$																
27																			
28																			
29																			

Total Cost | Material | Manufacturing | Susp Brackets Waterjet Cut Lgth

	A	B	C	D	E	F	G	H	I	J	K	L	M	N	O	P	Q	R	S
1	**Main Structure**				**Suspension Brackets**				**Front-Rear Member**				**Bushing Mounts**				**Jig**		
2																			
3	Num of Tubes	43			Waterjet Cut Length Total	12354	mm		Waterjet Cut Length Total	2820	mm		Num of Cuts	8			Estimate*	20	hr
4																	Conservative		
5	Num of Cuts	43			Waterjet Cut Speed*	40.6	in/min		Waterjet Cut Speed*	2.56	in/min		Cut Time (per cut)	0.033333333	hr				
6	Num of Joints	86			*Note conservative value	1031.24	mm/min		*Note conservative value	65.024	mm/min								
7													Total Cut Time	0.266666667	hr				
8					Waterjet Cut Time	0.199662542	hr		Waterjet Cut Time	0.722810039	hr								
9	Cut Time (per cut)	0.016666667	hr										Machining Time	2	hr				
10	Notch Time (per notch)	0.25	hr		Num of Joints	68			Machining Time	5	hr								
11	Weld Time (per joint)	0.166666667	hr																
12					Weld Time (per joint)	0.166666667	hr												
13	Total Cut Time	0.716666667	hr																
14	Total Notch Time	21.5	hr		Total Weld Time	11.33333333	hr												
15	Total Weld Time	14.33333333	hr																
16																			
17	**SUMMARY**																		
18	Shop Staff Hours	26.58913925	hr																
19	Student Hours	49.48333333	hr																
20																			
21	Shop Hourly Rate	15	$/hr																
22																			
23	**Total Labour Cost**	398.8370887	$																
24																			

Total Cost | Material | Manufacturing | Susp Brackets Waterjet Cut Lgth

Appendix C

Final Analysis – Stress

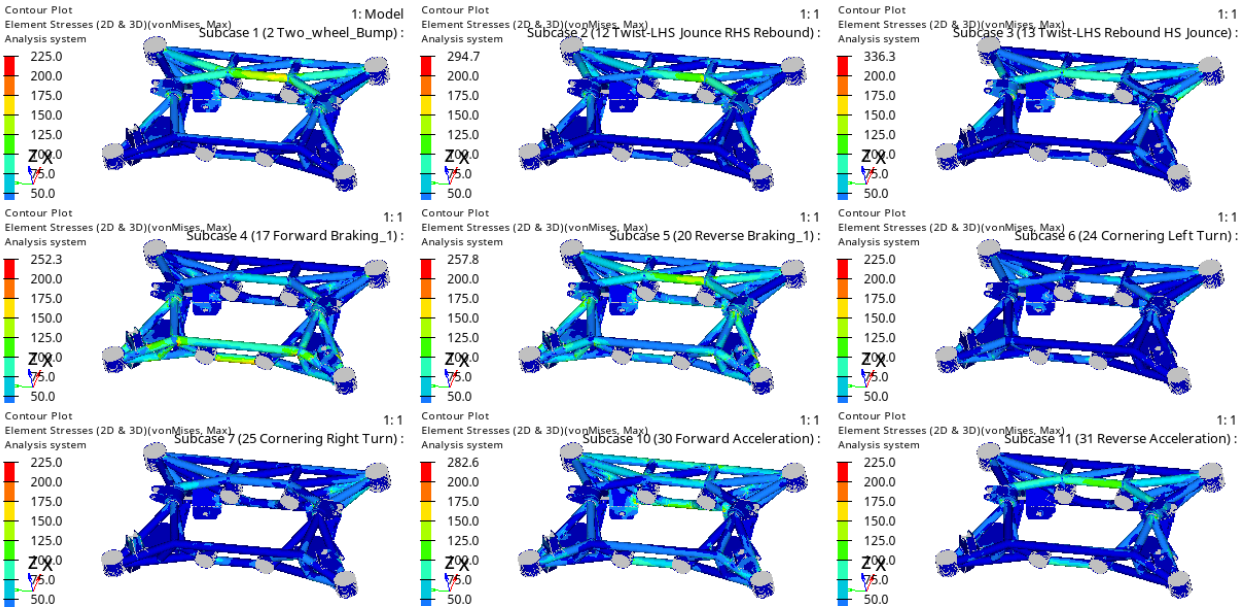

Appendix D

Final Analysis – Stiffness